AN ABSTRACT OF THE THESIS OF

Ok-Hee Kim for the degree of Doctor of Philosophy in Chemistry presented on November 12, 1996. Title: Mass Spectrometric Studies of Peptides and Proteins: Probing Structural Elements and Structural Fluctuations in Melittin and Bovine Pancreatic Trypsin Inhibitor (BPTI) Using Amide H/D Exchange and HPLC-Electrospray Ionization Mass Spectrometry.

Abstract approved: _____

Max L. Deinzer

Hydrogen/deuterium (H/D) exchange reactions followed by electrospray ionization mass spectrometry (ESIMS) with or without microbore HPLC coupling to the mass spectrometer, was applied to melittin for probing global structural domains. A variety of exchange conditions were used, including changes in pH (pD 3.2 vs. pD 4.3), temperature (0°C vs. 20°C vs. 60°C) and solvent composition [D_2O vs. 0.1%CD_3CO_2D/D_2O vs. $CD_3COD/D_2O/CD_3CO_2D$ (=80:20:2)]. The mass spectrometric analysis of the deuterium content was dependent on the same experimental parameters (pH, temperature, solvent composition) as those used in NMR spectroscopic studies. Amide H/D exchange experiments, followed by analysis of the deuterium content in each amino acid residue by ESI tandem mass spectrometric analyses (ESIMS/MS) was used to locate two α-helical regions in melittin (Gly3-Leu13 and Ala15-Gln26).

Amide H/D exchange, followed by ESIMS analysis was also used to probe the tertiary structural changes in bovine pancreatic trypsin inhibitor (BPTI). Both native BPTI and modified BPTIs were examined. The H/D exchange results obtained for these molecules provided structural information very similar to those obtained by CD spectroscopic measurements.

In an effort to locate structural regions in BPTI, pepsin-digestion was carried out on deuterated oxidized BPTI and the peptic peptides obtained were analyzed by microbore HPLC-ESIMS under slow exchange conditions (pH 2-3, 0°C). Fully deuterated BPTI was oxidized with performic acid in a HCO_2H-NH_4OH/8.5% MeOH buffer (pH 2.8, -20°C, 2 hr). BPTI retained only 3.2 peptide amide deuteriums (10%) after oxidation of the fully deuterated BPTI. Pepsin-digestion of this product yielded eight peptic peptides but no deuterium labels. However, an oxidation intermediate which corresponded to BPTI+O_4 retained 17.8 deuteriums (60%) after oxidation and 15.5 (49%) after pepsin-digestion. It is reasoned that the product (BPTI+O_4) likely had a native-like structure with intact disulfide bonds and thus, the deuteriums buried in the structural regions of the molecule were not available to the exchange medium.

Mass Spectrometric Studies of Peptides and Proteins: Probing Structural Elements and Structural Fluctuations in Melittin and Bovine Pancreatic Trypsin Inhibitor (BPTI) Using Amide H/D Exchange and HPLC-Electrospray Ionization Mass Spectrometry

by

Ok-Hee Kim

A THESIS

submitted to

Oregon State University

in partial fulfillment of

the requirements for the

degree of

Doctor of Philosophy

Completed November 12, 1996

Commencement June 1997

Doctor of Philosophy thesis of Ok-Hee Kim presented on November 12, 1996

APPROVED:

Redacted for Privacy

Major Professor, Representing Chemistry

Redacted for Privacy

Chair of Department of Chemistry

Redacted for Privacy

Dean of Graduate School

I understand that my thesis will become part of the permanent collection of Oregon State University libraries. My signature below authorizes the release of my thesis to any reader upon request.

Redacted for Privacy

Ok-Hee Kim, Author

Acknowledgments

I would like to thank my advisor Professor Max L. Deinzer for all of his support and encouragement. I would like to thank Professor Douglas F. Barofsky for critical guidance. I also would like to thank Dr. Claudia Maier for intense discussion and patient instruction in my research work. I especially thank Don Griffin for his kind instruction and patience. I also thank Lilo Barofsky for MALDI-TOFMS analysis and Brian Arbogast for FABMS analysis. I would like to thank Professor W. C. Johnson for generous guidance in CD spectroscopic analysis. And I also thank Jeannine Lawrence and C. Krittanai (Chai) for CD and OD experiments. I thank my mass spec. group members, Paul Mazurkiewicz, Dr. James Laramée, Dr. Susan Chen, Dr. Jan Stevens (Fred), Dr. Ann Westman, Dr. Gunnar Brinkmalm, Phil Gafken for their help at the right time.

With all my heart, I would like to thank my parents for their endless love and sacrifices. And I would like to thank all my family members living in Korea and in L. A. Finally, I thank my husband Tae-Seong and my son Sang-Min for their love and patience.

This thesis is dedicated to my father and my mother.

Table of Contents

Table of Contents (Continued)

List of Figures

List of Figures (Continued)

List of Figures (Continued)

List of Figures (Continued)

List of Figures (Continued)

List of Tables

List of Tables (Continued)

List of Tables (Continued)

List of Tables (Continued)

List of Equations

List of Schemes

Mass Spectrometric Studies of Peptides and Proteins:

Probing Structural Elements and Structural Fluctuations in Melittin and Bovine Pancreatic Trypsin Inhibitor (BPTI) Using Amide H/D Exchange and HPLC-Electrospray Ionization Mass Spectrometry

I. Background

I.1 Introduction

Proteins are among the most abundant and most important of biopolymers. They are responsible for catalyzing a large number of chemical reactions in living organisms as well as providing the structural integrity. For proteins to function properly, they must be correctly folded into a well-defined three-dimensional structure. Due to their complexity, the structure determination of proteins requires considerable experimental data. The most detailed information on structures is obtained from X-ray crystallography,[1] but multidimensional NMR spectroscopy[1,2] can be used to generate data for elucidating the structures that are only slightly less detailed. Other simpler techniques, notably CD spectroscopy[1,2a,3] provides a more qualitative measure of average structural elements, especially α-helices, β-sheets and β-turns. More recently, mass spectrometry (MS), especially liquid chromatography-fast atom bombardment mass spectrometry (LC-FABMS)[4] and electrospray ionization mass spectrometry (ESIMS),[5] has emerged as one of the most exciting new techniques applicable for the study of protein conformations and their folding processes.

As was suggest by Linderstrøm-Lang (1955),[6] the hydrogen/deuterium (H/D) exchange of peptide amide hydrogens (NHs), mainly in conjunction with NMR spectroscopy, has turned out to be a very powerful tool for studying protein conformations[7] in solution, structural fluctuations in folding processes,[8] folding intermediates[9] and the effects of ligands, inhibitors, and substrates on enzymes.[10] This is because the exchange rates of peptide amide hydrogens depend on the three-dimensional structures of the proteins as well as on experimental variables[11] such as pH, temperature, and the chemical environments.

NMR spectroscopy has been particularly useful for following H/D exchange at nearly all amino acid residues in proteins.[12] However, its use is limited to smaller (up to 15 kDa) and more highly soluble proteins. This technique also needs a large amount of sample material (mM concentration) and assignments of all NH resonances must be made in advance.

Mass spectrometry has also been used to measure H/D exchange rates on amide groups of proteins and peptides. These analyses have provided global information about solution conformations,[5] gas phase conformations[13] and transient folding intermediates[14]. To obtain H/D exchange rates of specific regions within proteins, a medium resolution method such as " protein fragmentation-separation method ", has been described by Rosa and Richards (1979)[8a,15]. This method has been extended to mass spectrometric application by Zhang and Smith (1993)[4]. This technique employs proteolytic digestion of the protein with pepsin under minimum hydrogen exchange conditions (pH 2.4, 0°C) followed by HPLC separation of the peptides and determination of the deuterium incorporation levels of the peptides using on-line HPLC-continuous flow fast atom bombardment mass spectrometry (HPLC-CF-FABMS). More recently, electrospray ionization mass spectrometry (ESIMS) was used in combination with

H/D exchange to observe different populations of transient folding intermediates of lysozyme[14] and to detect conformational changes in cytochrome c[16] and myoglobin.[17] More regional resolution of hydrogen exchange has been obtained by using tandem mass spectrometry (MS/MS),[18] which could be used to determine the location and the stability of secondary structures of peptides.

To evaluate the H/D exchange protocols using on-line microbore HPLC-ESIMS and -MS/MS techniques, melittin was studied as a simple model peptide and bovine pancreatic trypsin inhibitor (BPTI) as a complex model protein. Commercially available melittin (2846 Da, 26 residues) was tested because of its small size and exclusive α-helical conformation (**Figure I.1-1**).[18,19] H/D exchange data obtained by on-line microbore HPLC-ESIMS and HPLC-ESIMS/MS were compared to those obtained by a previously reported method using continuous flow infusion ESIMS (CF-ESIMS) and CF-ESIMS/MS[18]. Commercially available BPTI (6510 Da, 58 residues) was chosen because of the complexity of its structure (**Figure I.1-2**)[20] which includes three disulfide bonds (Cys5-Cys55, Cys14-Cys38, and Cys30-Cys51), two α-helical regions (N- and C-terminal regions) and three β-strands. Its folding pathways[21] have been extensively studied by NMR spectroscopy and are, thus, well established. Chemical modifications (reductions[22] and oxidations[23]) of the three disulfide bonds of BPTI are essential because of the complete resistance of BPTI with the intact cystines against proteolytic digestion. Once the disulfide bonds are broken, BPTI is very susceptible to peptic digestion and even at pH 2.0 and 0°C it yields complete and reproducible peptides in 5 minutes. Based on these peptic peptides, microbore HPLC-ESIMS and -ESIMS/MS analyses during the course of H/D exchange were performed (a) to correlate deuterium levels in each peptide amide group with the structural stability of the protein, (b) to locate the structural

regions in the molecules that were resistant to H/D exchange and (c) to compare the results to those obtained by NMR spectroscopy.[11b,24]

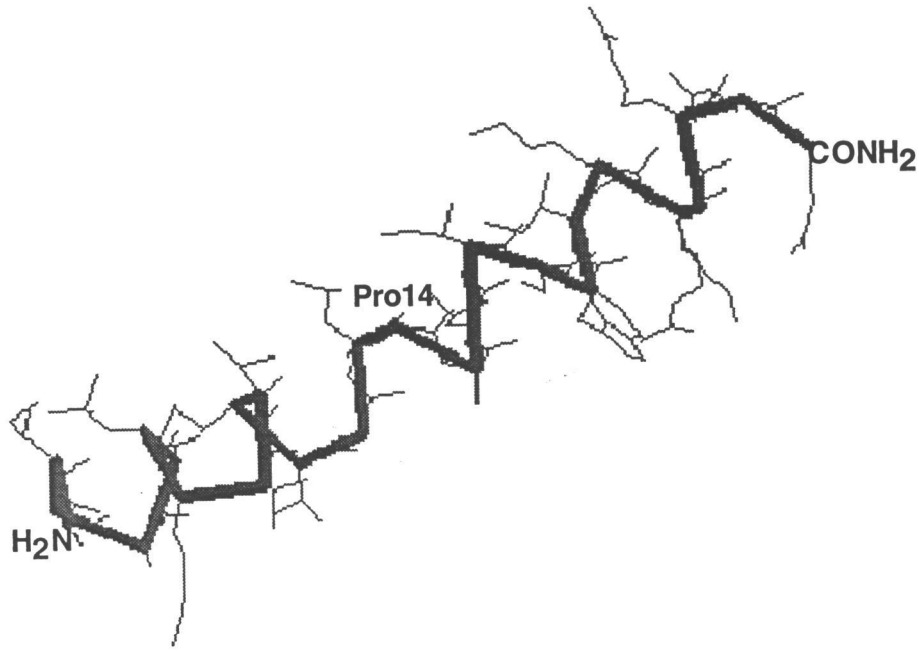

Mol. Wt .: 2845.8 ±0.16 (ESIMS)

2845.4 (Calculated)

2 α-Helical Regions :

Ile2 ~ Thr11, Leu13 ~ Gln26

50 Exchangeable Hydrogens :

24 Peptide NHs

22 Side Chain Hs

4 Terminal Hs

$$GIGAV^{5}LKVLT^{10}TGLPA^{15}LISWI^{20}KRKRQ^{25}Q\text{-}NH_2$$

Figure I.1-1: Structure of Melittin

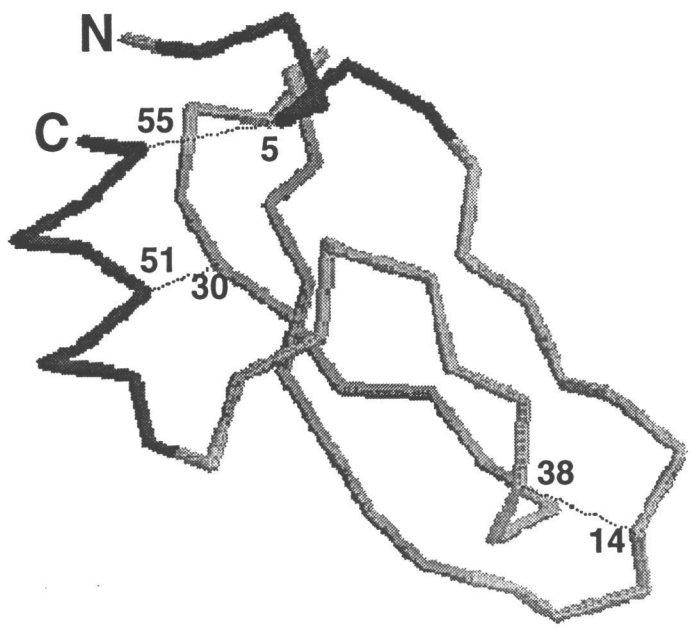

Mol. Wt. : 6510.7 ± 0.60 (ESIMS), 6509.6 (MALDI-TOFMS), 6511.5 (Calculated)

3 Disulfide Bonds, 3 α-Helices, 3 β-Strands

58 Amino Acid Residues

108 Exchangeable Hydrogens: 53 Peptide NHs, 52 Side Chain Hs, 3 Terminal Hs

Figure I.1-2: Structure of Bovine Pancreatic Trypsin Inhibitor (BPTI)

I.2 Hydrogen Exchange and Structural Dynamics of Proteins

The best probe for studying structural fluctuations of proteins is dependent on the fact that internal groups within proteins do react at a finite rate with appropriate reagents in solution, even if only very slowly. The most useful reagent is water, which can be used in isotopically labeled forms (^1H_2O, ^2H_2O and ^3H_2O) to measure exchange rates of the various hydrogen atoms of the protein. Hydrogen atoms bonded covalently to various atoms exchange at different intrinsic rates, depending on the tendency of that atom to ionize (**Figure I.2-1**).[1a] Hydrogen atoms on oxygen, nitrogen or sulfur atoms exchange rapidly, whereas those bonded to carbon atoms exchange at extremely slow rates.

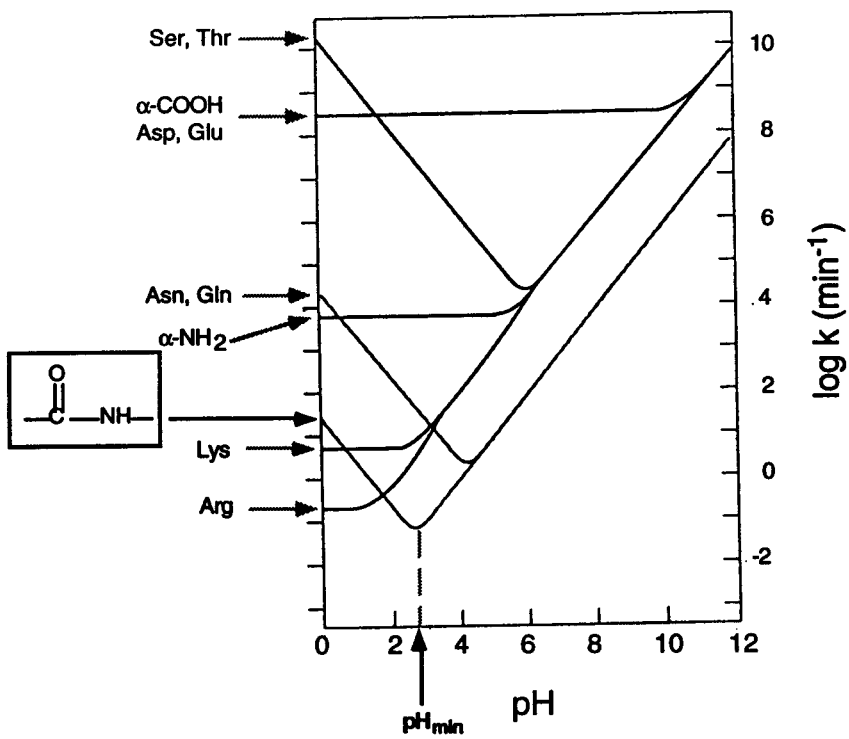

Figure I.2-1: pH Dependence of H/D Exchange Rates (k) for Model Groups (Creighton, T.E. *Proteins: Structures and Molecular Properties* **1993**, p282)

Hydrogen exchange of peptide amide hydrogens (NHs) in proteins is most often used because these hydrogens exchange on a convenient time scale and because they are often buried within the structures of the proteins, which further slows down the exchange rate. Generally, peptide amide hydrogens near the protein topological surfaces are readily accessible to water and exchange rapidly, whereas more slowly exchanging peptide amide hydrogens are buried in the interior of the molecule and are less accessible to water, and /or are involved in intramolecular hydrogen bonds such as in α-helices and β-sheets. Amide hydrogen exchange occurs by both acid- and base-catalysis in model compounds, e.g., poly-D,L-alanine[25] with a characteristic V-shape dependence of rate on pH (**Figure I.2-1**). The minimum exchange rate of an NH occurs at about pH 3 (pH_{min}) for model compounds,[25,26] where the acid- and base-catalyzed exchanges are of equal rates. The rate increases tenfold for each unit change in pH away from the minimum value.

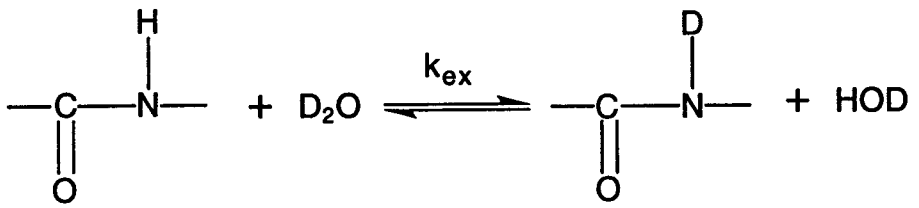

$$k_{ex} = k_H[H^+] + k_{OH}[OH^-] + k_0$$

Equation I.2-1: H/D Exchange of Peptide Amide Hydrogen

The pH dependence of amide hydrogen exchange rate (k_{ex}) can be expressed according to Woodward and Hilton[27] (**Equation I.2-1**), where k_H, k_{OH} and k_0 are the rate constants for acid-catalyzed, base-catalyzed and direct exchange with

water, respectively. Direct exchange with water (k_0) is negligible for the model compounds. The pH_{min} can be related to exchange rate constants (k_H, k_{OH}) and K_w, according to Leichtling and Klotz (1966),[28] where K_w is the ionization constant of water (**Equation I.2-2**). The pH_{min} reflects the ratio between k_H and k_{OH}. Therefore, it shifts in proteins as a consequence of unequal effects on the acid- and base-catalyzed exchange rate constants caused by structural parameters of the protein.[11a]

$$pH_{min} = 1/2 \, [\, pK_w + \log(k_H/k_{OH}) \,]$$

Equation I.2-2: pH_{min}
(Leichtling, B.M.; Klotz, I.M. *Biochemistry* **1966**, *5*, 4026)

The intrinsic rate of an NH exchange is also temperature-dependent,[11a] generally increasing about threefold with every 10°C increase in temperature. This corresponds to an activation energy of 17~20 KCal/mol.

The intrinsic rates of NH exchange depend on the chemical environments[11a] such as the presence of denaturants, salts and organic solvents. Generally, if some structures can be stabilized by these chemicals, the exchange rates of amide hydrogens are slowed down. Dependence of NH exchange on organic solvents[11a,15] has been studied more (**Figure I.2-2**). Organic solvents frequently used in reverse phase HPLC, generally slow the exchange rate, largely due to a decrease in K_w and, thus, in OH^- activity. Furthermore, the pH_{min} shifts progressively to higher values with increasing organic solvent composition. This effect can be used to reduce back-exchange of the isotopic label during HPLC analysis of proteins and peptides by keeping

the solution pH close to the value of the pH_{min} during gradient elution with organic solvents.

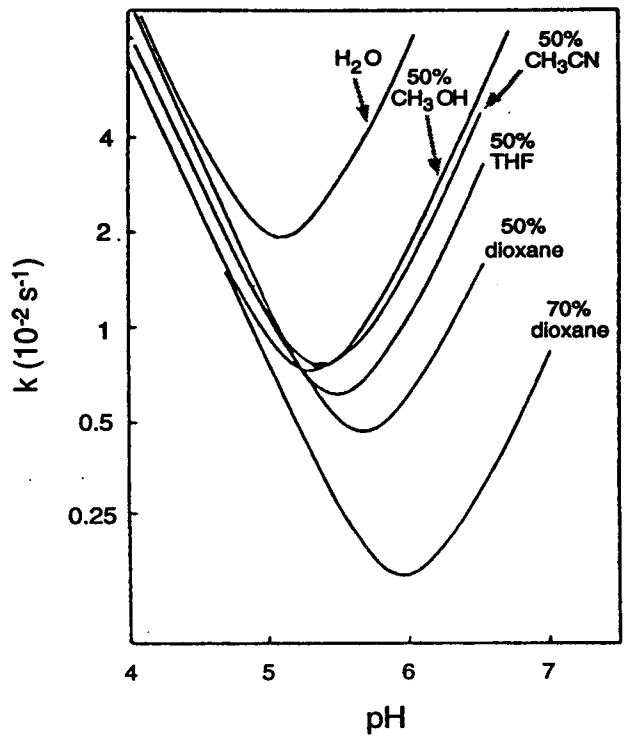

Figure I.2-2: Solvent Dependence of Amide Hydrogen Exchange Rate for Acetamide at 25°C
(Englander, J.J.; Rogero, J.R.; Englander, S.W. *Anal. Biochem.* **1985**, *147*, 234)

Generally, the exchange rates of peptide amide hydrogens in proteins are influenced by many parameters, especially the protein's structural parameters, in which each NH exchange event depends on the specific microenvironment where the individual NH is located in the molecular space of the protein. Thus, it is more complex in proteins than in model compounds. Amide hydrogen exchange theoretically can occur via the following three mechanisms.[29] The first mechanism is a **"base-catalyzed exchange"**, where a hydroxide ion removes

the amide proton to produce the imidate anion which is subsequently reprotonated (**Figure I.2-3**). The pK_a for deprotonation (pK_1) of the amide group in N-methylacetamide[27b] has been estimated to be 18.

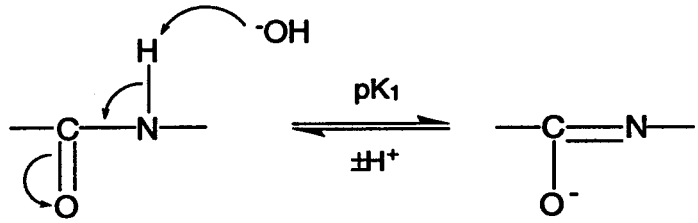

Figure I.2-3: Base-Catalyzed Exchange Mechanism

The second mechanism is an "**acid-catalyzed N-protonation**" with a pK_a value for protonation of the amide group (pK_2) around -7 (**Figure I.2-4**).[27b]

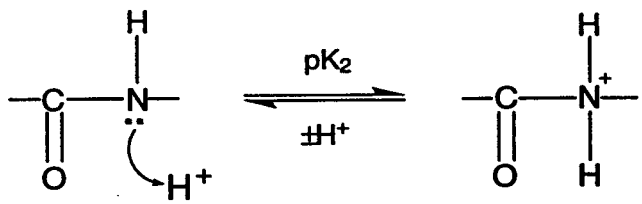

Figure I.2-4: Acid-Catalyzed N-Protonation Exchange Mechanism

The third mechanism is an "**imidic acid mechanism**", where protonation of carbonyl oxygen acidifies the amide proton so that a water molecule can remove it to produce the imidic acid, which turns into the amide through the reverse reaction (**Figure I.2-5**). The experimental pK_3 for carbonyl oxygen[30] and pK_4 for O,N-dimethyl acetimidate[31] has been estimated as ~0 and 7.5, respectively. The imidic acid mechanism (**Figure I.2-5**) has been shown to be preferred over

the N-protonation mechanism (**Figure I.2-4**) for the acid-catalyzed exchange of amide protons in proteins.[32]

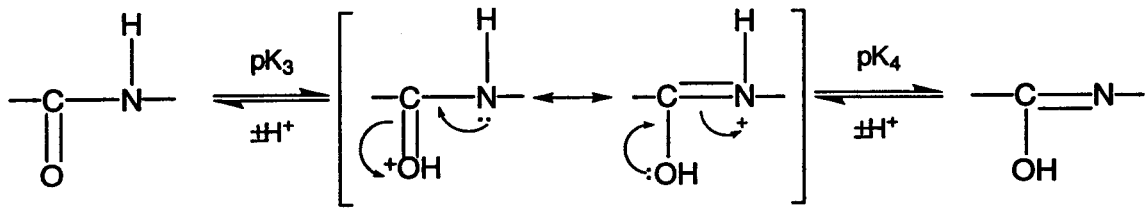

Figure I.2-5: Imidic Acid Exchange Mechanism

The transition state of the imidic acid mechanism has a delocalized positive charge though the charge is more localized on nitrogen because it is more basic than oxygen.[27b] On the other hand, the transition state for the N-protonation mechanism has a more localized positive charge on the nitrogen, which is destabilized by electron-withdrawing acyl substituents on the peptides.[29] The preferred imidic acid mechanism is further supported by Tüchsen and Woodward[33] in determining the acid-catalyzed exchange rate constants (k_H) and the base-catalyzed rate constants (k_{OH}) for the 25 most rapidly exchanging peptide amide hydrogens of BPTI at the solvent-protein interface. They found an excellent correlation of k_H, but not k_{OH} with the static accessibility and hydrogen bonding of the carbonyl oxygens of the same peptide, which indicated that the acid-catalyzed mechanism in proteins occurs via protonation at carbonyl oxygen (O-protonation). And also, agreement between the ionic strength dependence calculated for the O-protonation (imidic acid mechanism) and that observed for k_H and k_{OH}, further supported the dominance of the imidic acid mechanism. The previous three mechanisms can describe the NH exchange on model compounds, where all the NH groups are freely accessible to solvents and

catalysts. However, the exchange processes of amide hydrogens in a protein cannot be explained completely by these mechanisms, especially the amide hydrogens buried in the interior of the protein structure. According to **"the local unfolding model"** of Linderstrøm-Lang,[6] or so called **"the breathing model"**,[34] the exchange of the buried amide hydrogens of proteins occurs via a variety of transient open conformations of the protein, with the exchanging groups exposed locally to the solvent (**Figure I.2-6**). In state **A** the peptide amide hydrogens are buried within some structure and are separated from solvent and catalyst. In state **B** the peptide amide hydrogens are exposed to the solvent and the catalyst due to local unfolding of the protein structures, and in state **C** hydrogen exchange occurs. In this model, the folded state is strongly favored ($k_1 << k_{-1}$) and the rate of exchange is determined by k_1 and k_{ex} (**Equation I.2-3**).

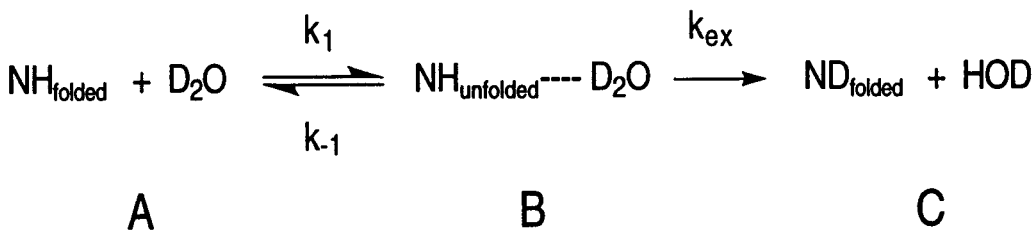

Figure I.2-6: Local Unfolding Model for H/D Exchange of Peptide NHs

$$k_{obs} = (k_1 \times k_{ex}) / (k_{-1} + k_{ex})$$

Equation I.2-3: Exchange Rate of Amide Hydrogen in Local Unfolding Model

In the **EX_1 mechanism** ($k_{-1} << k_{ex}$), the observed rate of exchange (k_{obs}) is directly related to the unfolding rate of the protein structures (k_1, **Equation I.2-4**).

$$k_{obs} = k_1 \qquad (k_{-1} \ll k_{ex})$$

Equation I.2-4: Observed Exchange Rate of NH in EX_1 Mechanism

In the **EX_2 mechanism** ($k_{-1} \gg k_{ex}$), the observed rate of exchange (k_{obs}) is proportional to the equilibrium constant ($K_{eq} = k_1/k_{-1}$) for the local unfolding process as well as on its intrinsic rate constant (k_{ex}) (**Equation I.2-5**). In this mechanism, the rate of exchange should be sensitive to factors which affect the intrinsic exchange rate (k_{ex}) in model compounds, especially on the pH of the solution.

$$k_{obs} = K_{eq} \times k_{ex} \qquad (k_{-1} \gg k_{ex})$$

Equation I.2-5: Observed Exchange Rate of NH in EX_2 Mechanism

An alternative model for the exchange of solvent-protected amide hydrogens of proteins is **"the solvent penetration model"**[34] in which hydrogen exchange occurs by diffusion of solvent molecules to various sites in the protein interior. Therefore, the exchange rate of each amide hydrogen depends in a complex manner on (a) the flexibility of the protein for creating the necessary channels of the solvents, (b) the probability of the solvent molecules diffusing to each site, and (c) the stability of the hydrogen bonds involving peptide amide hydrogens. Other models used to explain hydrogen exchange for the non-first order pH dependence, and broad and shallow minima observed in the hydrogen exchange rate of proteins, are **"the multistate model"**[35] and **"the model of the catalysis by water molecules"**[36] (k_0, **Equation I.2-1**). Unfortunately, there is

no single model which can explain the amide hydrogen exchange processes for all known proteins and even for different sites in the same protein. It is more likely that hydrogen exchange occurs by a wide range of different processes, depending on the nature of proteins and their conformations.

I.3 Electrospray Ionization Mass Spectrometry (ESIMS and ESIMS/MS)

Electrospray is a very soft ionization technique in mass spectrometry, which imparts minimal energy upon ionization to give multiply charged gaseous molecular ions directly from protein solutions.[5,37] The number of ionizable groups, their accessibility and their proximity on the protein's surface has been shown to be related to the charge state distributions of gas-phase molecular ions in the mass spectrum.[37-40] Therefore, electrospray ionization mass spectrometry (ESIMS) has been used as an analytical tool to probe conformational changes in peptides and proteins. For example, monitoring acid denaturation of myoglobin[38] and cytochrome c[39] by lowering the solution pH, has been reported. Generally, the ESI spectrum of a protein in a denaturing solution conditions, such as at the extremes of the pH range and at higher temperatures or in the presence of organic solvents, results in a charge state distribution that is broader and more centered on a higher charge than the one from the protein in its native state. In a tightly folded conformation (native state), some of the ionizable groups are close together and buried inside the folded structure and are, thus, inaccessible to the ionizing solvent. This leads to fewer charges on the protein which is reflected in the ESI mass spectrum. On the other hand, as the protein denatures, the buried ionizable groups become accessible to the ionizing solvent and move further away from the groups with the same charge

type, which lowers the free energy of the protein,[39,40] leading to a higher charge state envelope in the mass spectrum.

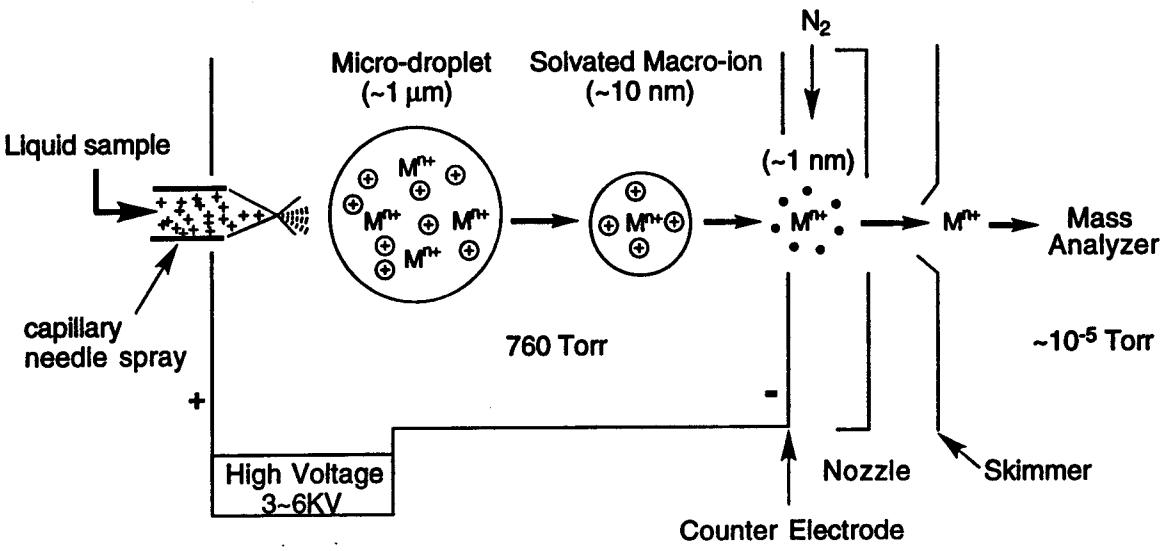

Figure I.3-1: Electrospray Ionization Mechanism

An accepted qualitative mechanism for electrospray ionization (ESI) is shown schematically in **Figure I.3-1**. The liquid sample is introduced through a capillary needle sprayer into the mass spectrometer by direct infusion, flow injection, liquid chromatography (LC) or capillary electrophoresis (CE). Due to the high electric field between the sprayer tip and the counter electrode (3-6 KV), the liquid sample obtains a net charge and small charged droplets of micrometer-size in diameter are formed from the sprayer. As the charged micro-droplets evaporate in the atmospheric pressure region, a critical point of charge to droplet size (Rayleigh instability limit) is reached at which point it is kinetically and energetically possible for desolved ions to be emitted from the surface of the droplet. The highly solvated nanometer-size droplets are formed through Coulombically driven processes. These processes are dependent on the solution

composition. This mechanism is compatible with others discussed by Smith[41], Fenn[42] and Röllgen[43] which are based on **"the ion evaporation mechanism"** proposed by Iribarne and Thomson (1976).[44] As the water molecules continue to evaporate from the nano-droplets, the desolvated molecular ions are sampled into the low pressure region through a capillary inlet[37a] or a nozzle-skimmer inlet[37b] and detected. Although a substantial loss of higher order solution-structures of proteins occurs during the desolvation process, ESI typically involves a minimum energy for the desorption and desolvation processes of the solvated molecular ions to give multiply charged molecular ions in gas phase, and can be applied to near-physiological solution conditions[37b] and thus, gives good correlations between the structural features of proteins in solution and the charge state distributions of gas phase molecular ions in mass spectrometer[37-40]. Therefore, over the last few years dramatically increasing number of the detections of non-covalent complexes involving large biomolecules have been reported by using ESIMS.[38,40,45] Especially, many of these complexes have been detected on the relatively recently developed ion-spray mass spectrometer[46] (pneumatically assisted ESIMS). Ionspray mass spectrometry uses a coaxial air-jet along the capillary needle spray to shear the droplets from the liquid stream, which can give a higher efficiency for fine droplet-formation and desolvation process of the droplets even from neutral aqueous sample solutions with a higher flow rate (up to 200 ml/min).

ESIMS has been used in combination with hydrogen/deuterium (H/D) exchange to characterize the fluctuations among different protein conformations[5,16] and to monitor the folding / unfolding processes of proteins.[14] Not only does it provide a unique ability to characterize structural differences among conformers or among folding / unfolding intermediates, but ESIMS is amenable for the analysis of relatively large proteins (~200 KDa).[47] In addition,

it is very sensitive, typically only microgram quantities of protein are required (pmole~fmole), it is accurate (0.1~0.01% error), and fast (ms-time scale) and provides continuous detection of sample molecules. Finally, it is tolerant of proteins in complex mixtures.

Although there are many practical benefits of mass spectrometric analyses in combination with H/D exchange of peptide amide hydrogens in proteins, this method can give only limited site-specific information. This limitation, however, can be addressed (a) indirectly by comparison with data obtained through NMR spectroscopy, (b) directly by using proteolytic digests of proteins and (c) by tandem mass spectrometry (MS/MS).

Mass spectrometric analysis of the H/D content of peptide amide groups in proteins can be used to measure the mass increase during deuterium exchange-in into the protein or the mass decrease during deuterium exchange-out from the protein. The resulting molecular weight profile as a function of H/D exchange time, can give global structural information, and allow one to distinguish different conformers. However, these data do not provide information about the specific sites on the protein, where H/D exchange takes place. The main interest in these studies is to correlate the H/D exchange data with structural features of the protein. To address this problem, a medium resolution method, **"protein fragmentation method"**,[8a,15] has been developed to provide more detailed information within the specific regions of the protein. In this method (**Figure I.3-2**), the protein in its native state is exposed to deuterated solvent so that the deuterium exchange-in process can occur. After a predetermined period of time, the deuterated protein is subjected to an acidic solution near its pH_{min} to quench the H/D exchange reaction. This is usually done at 0°C to slow the H/D exchange further. The protein is digested for a short period of time with pepsin at 0°C. Pepsin[48] is an acid protease which has its maximum activity in the pH

range of 2 to 3, where amide hydrogen exchange is slowest. In addition, pepsin cleaves at many sites on the protein backbone with a priority at the C-terminal side of phenylalanine, leucine and hydrophobic aromatic residues. This gives many small overlapping peptides (3-30 residues) which facilitate complete peptide mapping of the protein.. Generally, pepsin is regarded as a non-specific protease.[49] However, it shows kinetic specificity[15] at low temperature (0°C) and over shorter digestion time, which makes it possible to obtain resolvable and reproducible peptic peptides. The resulting small overlapping peptides are used to define the regions of the protein that have undergone isotopic exchange. Because this method can give only the total number of peptide amide deuterons in a segment of the protein, it is not possible to determine exchange rates for specific amide hydrogens.

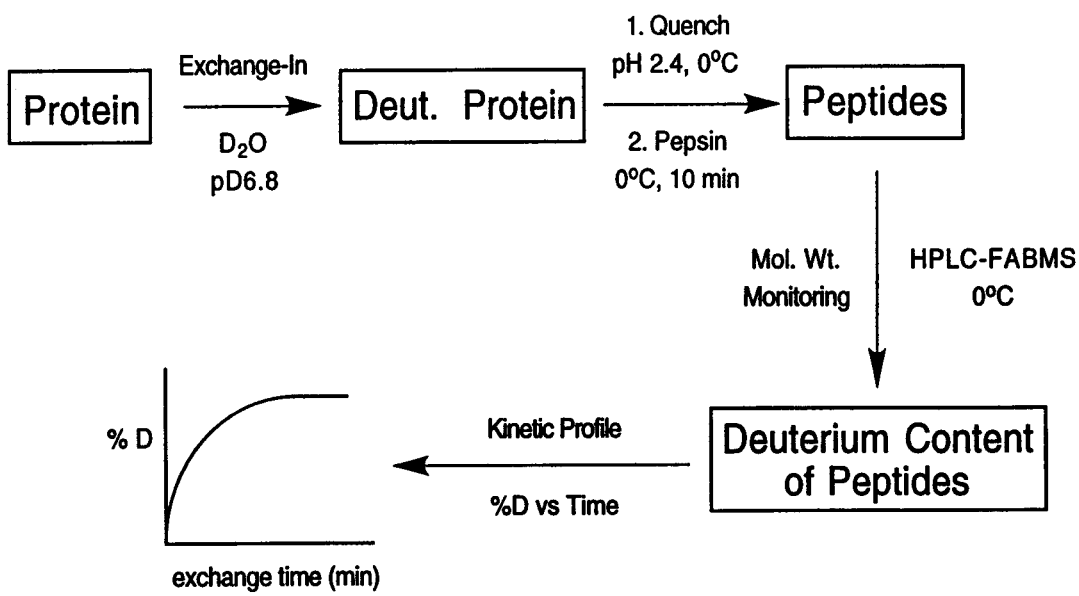

Figure I.3-2: Monitoring Deuterium Exchange-In by the Protein Fragmentation Method and HPLC-FABMS Analysis

Anderegg et. al. (1994)[18] have conducted tandem mass spectrometric experiments (ESIMS/MS) after H/D exchange on small peptides, including melittin and a growth hormone releasing factor. The data obtained in these experiments were shown to be useful for locating the α-helical regions in the peptides and the dynamic unfolding of the α-helices as a function of time.

In tandem mass spectrometry (MS/MS)[50] (**Figure I.3-3**), one can selectively transmit an ion as a parent ion which may be a molecular ion or any other ion that can give fragment ions, by using the first mass analyzer (MS-1). The parent ion is collisionally activated and dissociated into fragment ions in a high pressure region that contains an inert gas (He, Ar) between MS-1 and MS-2, and the fragment ions are then detected by the second mass filter (MS-2) to give a daughter ion spectrum of the selected parent ion.

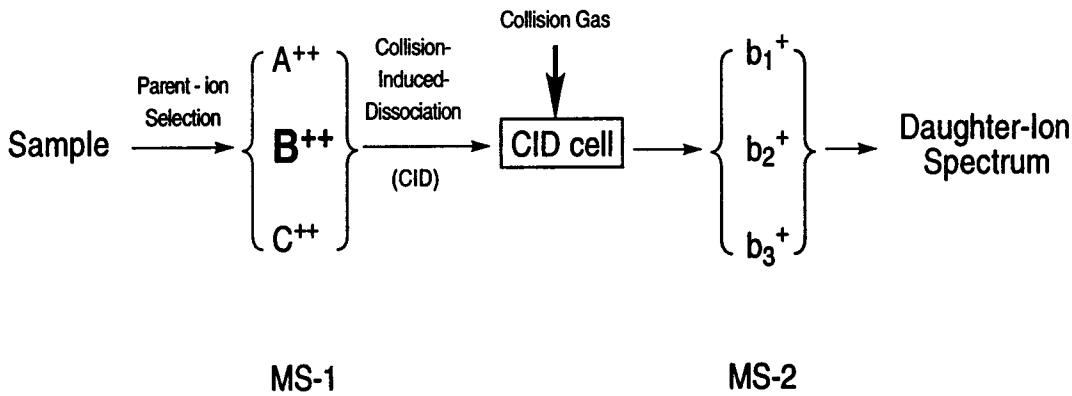

Figure I.3-3: Schematic Diagram for Tandem Mass Spectrometry

For peptides and proteins the polypeptide backbone is fragmented in a predictable way giving rise to several ion series from which most of the sequence can be deduced.[50a] According to the Roepstroff and Fohlman nomenclature [50c], the fragment ions produced from any peptide backbone cleavage are

represented (**Figure I.3-4**). Therefore, tandem mass spectrometric analysis in combination with H/D exchange of peptide amide hydrogens is a very promising technique for locating regions where exchanges in the mass reflect changes in the structural regions of peptides and proteins. This is possible if the proteins are digestible with an acid protease, such as pepsin.

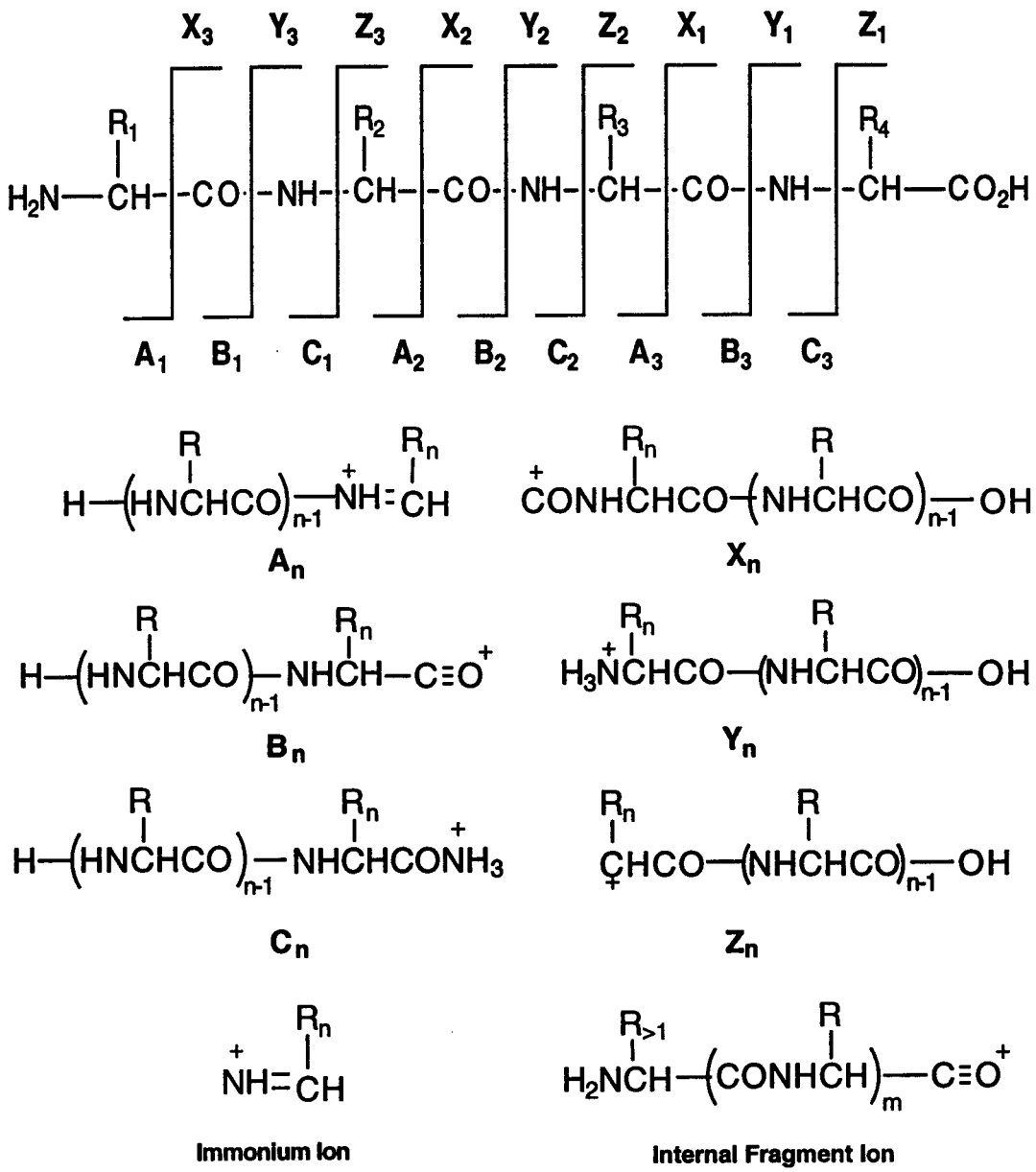

Figure I.3-4: Fragment Ions Obtained from Cleavage of a Peptide Backbone

Proteins, however have tight compact tertiary structures when they are in their native states. More often than not, proteins have one or more polypeptide chains linked through disulfide bonds. Some of these disulfide bonds may be located near the protein surface but others can be buried inside the protein structure making them inaccessible to solvent and chemical reagents. The disulfide bonds are very important to the stability of the protein's tertiary structure. So manipulation of the disulfide bonds is critical, especially in the structural analyses of complex proteins where H/D exchange and protein fragmentation-mass spectrometric methods are the experimental focal point. For example, bovine pancreatic trypsin inhibitor (BPTI) is a relatively small protein (6510 Da, 58 residues), but it has a tight compact and stable three-dimensional structure whose stability depends highly on the three disulfide bonds. Two of these disulfide bonds are completely buried in the core structure. This protein is completely resistant to pepsin digestion under slow H/D exchange conditions (pH 2.0, 0°C, up to 30 min). Chemical cleavages of the disulfide bonds are essential for successfully locating the H/D exchange sites in this protein.

In the following sections, H/D exchange experiments were carried out on the small peptide, melittin, using HPLC-ESIMS and -ESIMS/MS in the analytical schemes. The methodology has also been applied to the relatively small and complex protein, bovine pancreatic trypsin inhibitor (BPTI). In this system, the main effort was focused on reduction and oxidation reactions of the disulfide bonds to make the protein digestible by pepsin.

II. Results and Discussion

II.1 H/D Exchange of Melittin

II.1-1 Monitoring Deuterium Exchange-In of Melittin by Continuous Flow Infusion (CF)-ESIMS and CF-ESIMS/MS

Hydrogen/deuterium (H/D) exchange reactions on melittin in combination with continuous flow infusion-electrospray ionization mass spectrometric analysis (CF-ESIMS),[18] have been carried out to evaluate the protocol for probing global conformations in solution and locating the conformational changes within the amino acid residues of melittin. The overall procedure for monitoring deuterium exchange-in into melittin is depicted in **strategy I** (**Scheme II.1-1**). In this method, sample solutions were continuously forced through a microsyringe into the electrospray ionization mass spectrometer at a flow rate of 3.3 μl/min (**Figure II.1-1**).

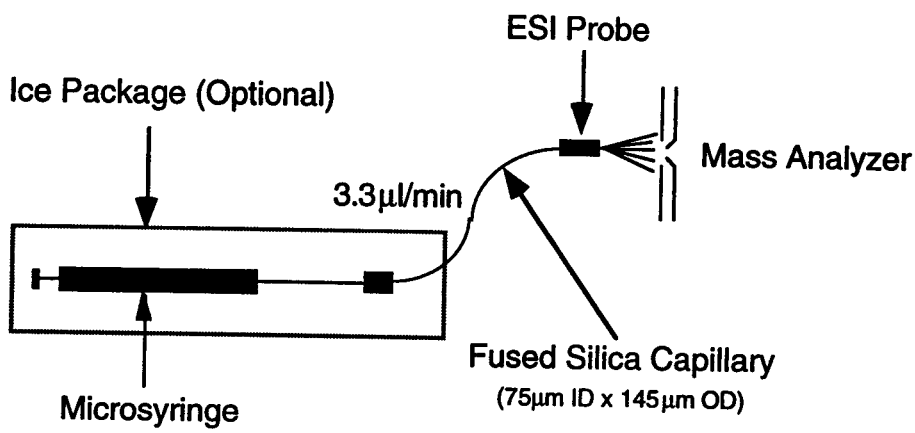

Figure II.1-1: Continuous Flow Infusion Mode of Sample Introduction

Strategy I

Deuterium Exchange-In of Melittin Monitored by Continuous Flow(CF)-ESIMS and CF-ESIMS/MS

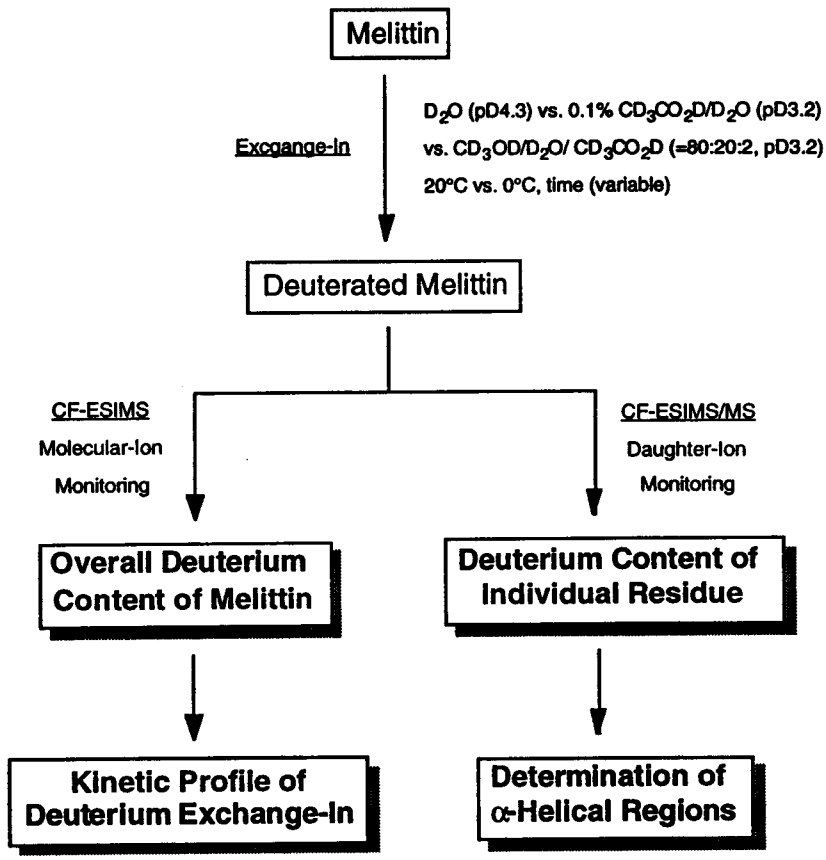

Scheme II.1-1: Strategy I

Mass increase measurements in the molecular ions of melittin during the course of deuterium exchange-in have been performed at different solution pHs (pH 4.3, pH 3.2), at different temperatures (20°C, 0°C) and in different solvents (D_2O, 0.1% CD3CO2D/D_2O, $CD_3OD/D_2O/CD_3CO_2D$ (=80:20:2)). The overall deuterium content in melittin was calculated and the data were used to obtain kinetic profiles of exchange by plotting H_t as a function of H/D exchange time (t),

where H_t represents the number of hydrogens that have not exchanged at a given time t. Nonlinear curve fitting was performed on this plot by using a program of Microcal Origin with a version 4.0 (**Equation II.1-1**). A group of hydrogens (H_n) that undergoes exchange with deuteriums with the same first-order rate constant (k_n) was determined from the obtained fitting curve where H_{total} is a total number of exchangeable hydrogens available in melittin.

$$H_t=H_0+H_1\exp(-k_1t)+H_2\exp(-k_2t)\cdots+H_n\exp(-k_nt) \quad (\Sigma H_n=H_{total})$$

Equation II.1-1: Exponential Decay of Exchangeable Hydrogens in Melittin

Tandem mass spectrometric analysis (CF-ESIMS/MS) of melittin was performed to determine the number of hydrogens that remained in each amino acid residue during the course of H/D exchange and to locate the α-helical regions within melittin. The schematic diagram of a Perkin-Elmer Sciex API III ionspray mass spectrometer equipped with a triple quadrupole mass analyzer, is shown in **Figure II.1-2**.

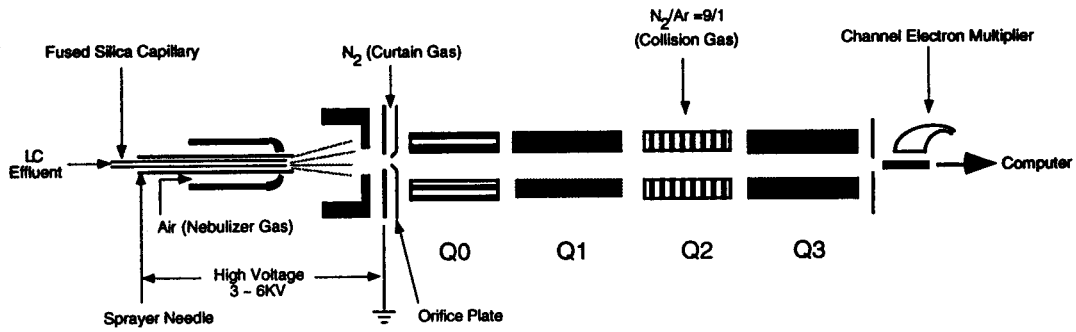

Figure II.1-2: Ionspray Triple Quadrupole Mass Spectrometer

Ionspray mass spectra were collected in the positive ion mode. The ion spray needle and the orifice potential were set to 5.3 KV and 80 V, respectively. The mass range was adjusted to observe +3-, +4- and +5-charged molecular ions with scanning parameters of 0.2 Da step size, 0.7 ms dwell time and 3.5 sec/scan (**Figure II.1-3**).

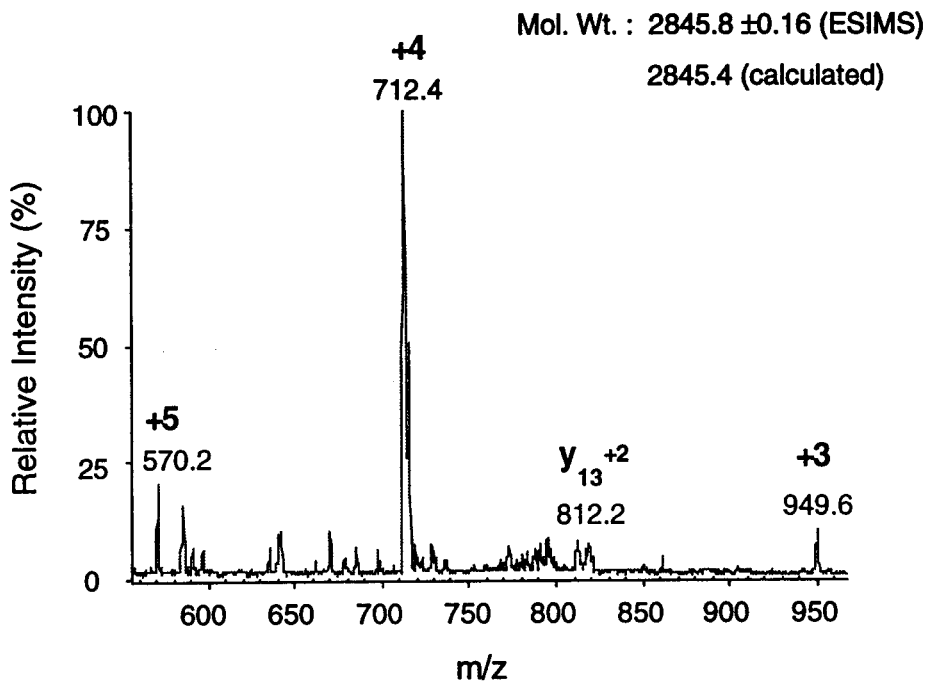

Figure II.1-3: Ionspray Mass Spectrum of Melittin (5 μM) in MeOH/H_2O/AcOH (=80:20:2) at 80 V Orifice Potential

Melittin (a 26-residue peptide) has a total of 50 exchangeable hydrogens in its sequence with 24 peptide amide hydrogens (NH), 22 side chain hydrogens and 4 terminal hydrogens (-NH_2: N-terminus, -$CONH_2$: C-terminus). When melittin is exposed to deuterated solvent, its molecular weight increases rapidly as deuterium replaces the exchangeable hydrogens in the molecule. The exchangeable hydrogens in both termini and the side chains are freely

accessible to solvent and catalyst and thus they exchange instantly. However, the hydrogens involved in intramolecular hydrogen bonds of the α-helices in melittin are expected to exchange slowly, so that one can distinguish these stabilized hydrogens from the rest of the fast-exchanging hydrogens according to their exchange rates.

The temperature-dependence of H/D exchange of melittin was studied in $CD_3OD/D_2O/CD_3CO_2D$ (=80:20:2, pD 3.2) at 20°C and 0°C. A time-dependent mass profile was obtained by plotting the percentage of deuterium incorporation versus H/D exchange time (**Figure II.1-4A** and **Table III.1-1**, **Table III.1-2**). The molecular weight of melittin would be expected to change from 2846 Da to 2896 Da upon complete deuterium exchange of all the exchangeable hydrogens. Kinetic data were obtained from plotting H_t versus H/D exchange time (**Figure II.1-4B**, **Figure II.1-4C** and **Table III.1-1**, **Table III.1-2**). In the deuterium exchange-in experiments of melittin, the first datum point was obtained 1 minute after dissolving melittin in deuterated solvent. During this period of time, the first 30 exchangeable hydrogens exchanged at 20°C, so that they could not be distinguished on the mass spectrometric time scale. These fast exchanging hydrogens included those in both termini and in the side chains as well as the four from the backbone amide groups. Fifteen peptide amide hydrogens exchanged with half-life of 7 min (**Figure II.1-4B**). Five peptide amide hydrogens were still remained after 46 minutes of deuterium exchange-in period. On the other hand, the deuterium exchange-in into melittin at 0°C showed that the first 24 exchangeable hydrogens exchanged to deuteriums in less than a minute. About 7 hydrogens and 9 peptide amide hydrogens exchanged with half-lives of 6 min and 3 hr, respectively (**Figure II.1-4C**). Another group of about 10 peptide amide hydrogens exchanged very slowly, which are more likely those of the backbone amides in the α-helices of melittin.

(A)

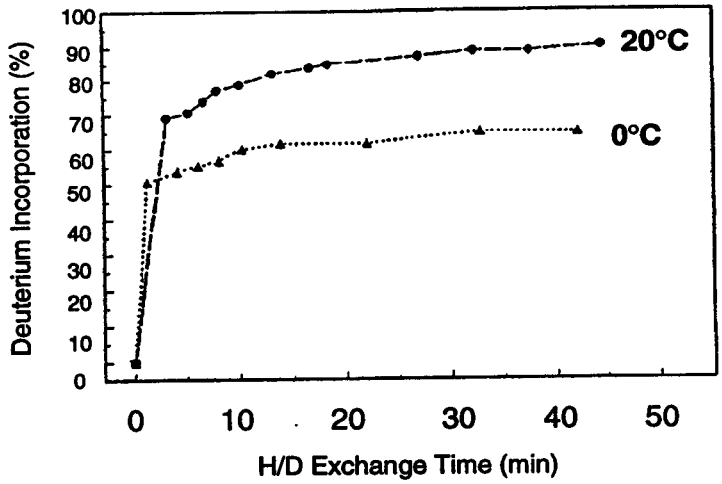

(B)

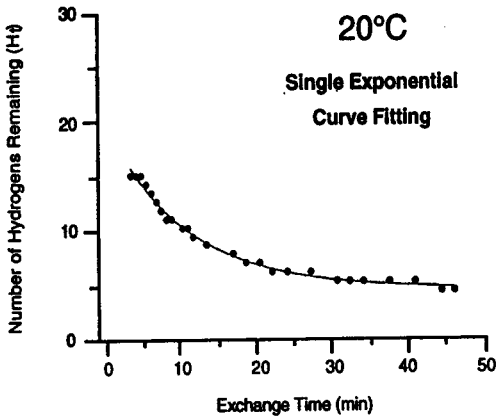

$H_t=5+15\exp(-0.10t)$ $(\chi^2=0.12)$

$H_{total} = 50$
Group 1 : $H_1=15$, $k_1=-0.10$ min^{-1}, $t_{1/2}=6.9$ min
Group 2 : $H_0=5.0$ (too slow to be observed)

(C)

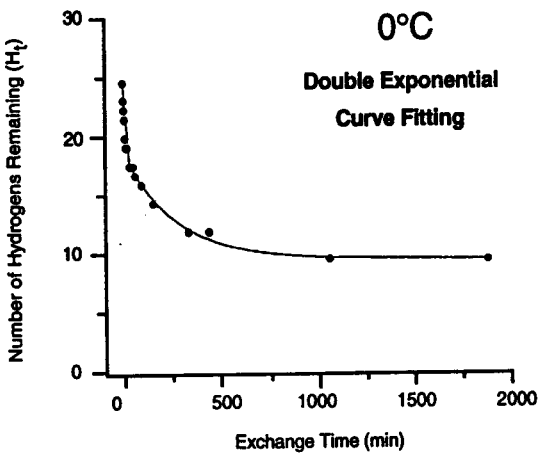

$H_t=9.6+7.2\exp(-0.12t)+9.2\exp(-0.0038t)$
$(\chi^2=0.18)$

$H_{total} = 50$
Group 1 : $H_1=7.2$, $k_1=-0.12$ min^{-1}, $t_{1/2}=5.8$ min
Group 2: $H_2=9.2$, $k_2=-0.0038$ min^{-1}, $t_{1/2}=3.0$ hr
Group 3 : $H_0=9.6$ (too slow to be observed)

Figure II.1-4: Temperature Dependence of H/D Exchange of Melittin

The dependency of H/D exchange on solution pH (pD 3.2 vs. pD 4.3) and on solvent composition (D_2O vs. 0.1% CD_3CO_2D/D_2O vs. $CD_3OD/D_2O/CD_3CO_2D$ (=80:20:2) in melittin was also studied at 20°C. Time-dependent profiles of deuterium incorporation into melittin were obtained from three different solvent systems (**Figure II.1-5** and **Table III.1-1**, **Table III.1-3**, **Table III.1-4**).

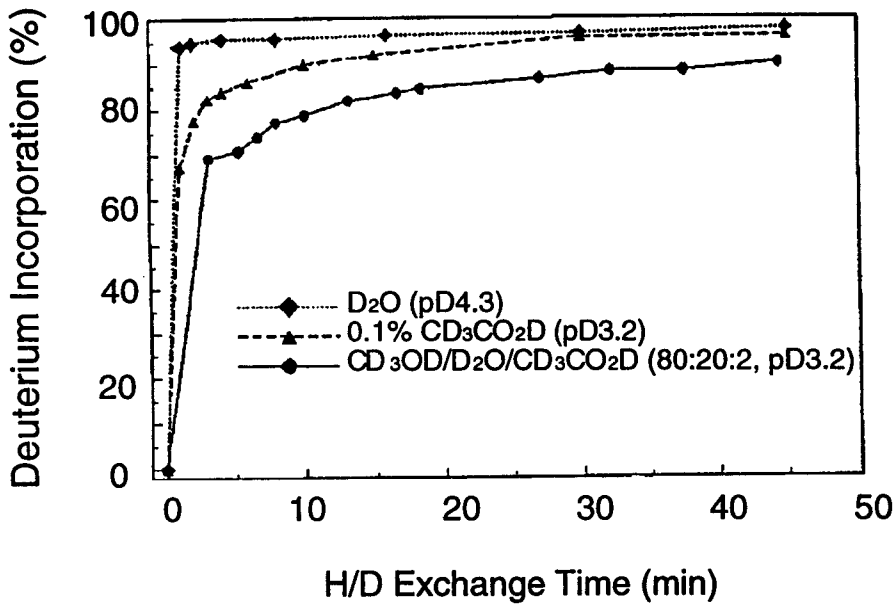

Figure II.1-5: Deuterium Incorporation into Melittin in Different Solvents

Deuterium exchange-in into melittin in D_2O (pD 4.3) showed the fastest exchange profile. About 94% of exchangeable hydrogens were replaced by deuterium in less than a minute. It is well known that melittin adopts a random coil structure in water and this was confirmed by CD analysis (**Figure II.1-6**). Melittin in 0.1% CD_3CO_2D/D_2O (pD 3.2) showed a medium-exchange profile. The slowest exchange profile on melittin was obtained in $CD_3OD/D_2O/CD_3CO_2D$ (=80:20:2, pD 3.2) (**Figure II.1-5**). The secondary structure of

melittin in MeOH/H_2O/AcOH (=80:20:2) consisted of about 84% α-helix as measured by CD spectroscopy (**Figure II.1-6**). Therefore, the solution pH and methanol composition did have influences on the H/D exchange of melittin.

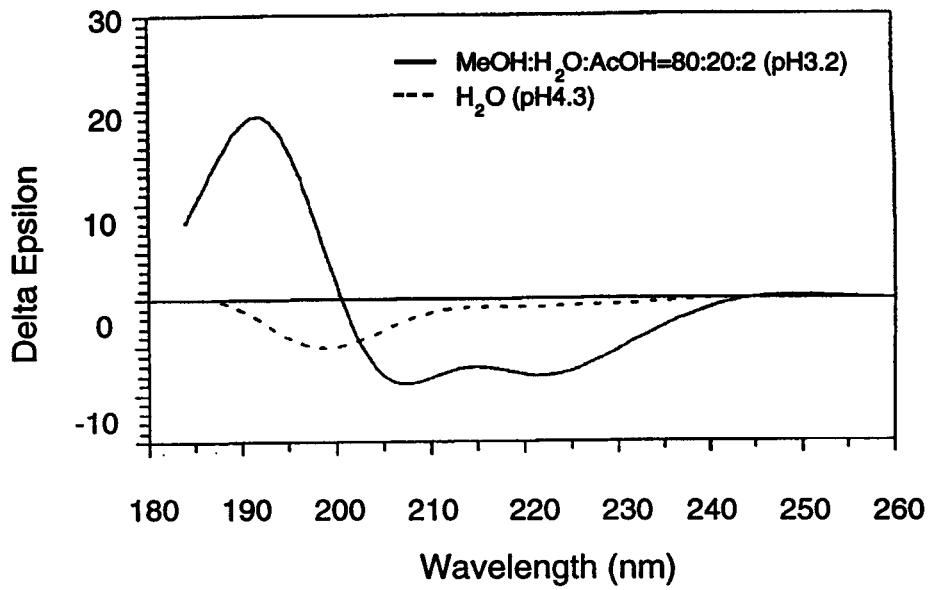

Figure II.1-6: CD Spectra of Melittin in Different Solvents

The kinetic results were calculated from plots of H_t versus H/D exchange time (t) (**Figure II.1-7, Figure II.1-4B** and **Table III.1-1, Table III.1-3, Table III.1-4**). In H/D exchange of melittin in D_2O (pD 4.3), 47 exchangeable hydrogens (94%) exchanged rapidly in less than a minute (**Figure II.1-7A**). In H/D exchange in 0.1% CD_3CO_2D/D_2O (pD 3.2), about 15 hydrogens exchanged rapidly in less than a minute. Another 24 and 9 hydrogens exchanged with half-lives of 34 sec and 7 min, respectively (**Figure II.1-7B**). H/D exchange of melittin in $CD_3OD/D_2O/CD_3CO_2D$ (=80:20:2, pD 3.2) showed the slowest-exchange profile (**Figure II.1-4B**). According to these results, mass spectrometric analyses did show similar dependencies of H/D exchange

in melittin on temperature, pH and solvent composition as those observed by NMR spectroscopic experiments.[19]

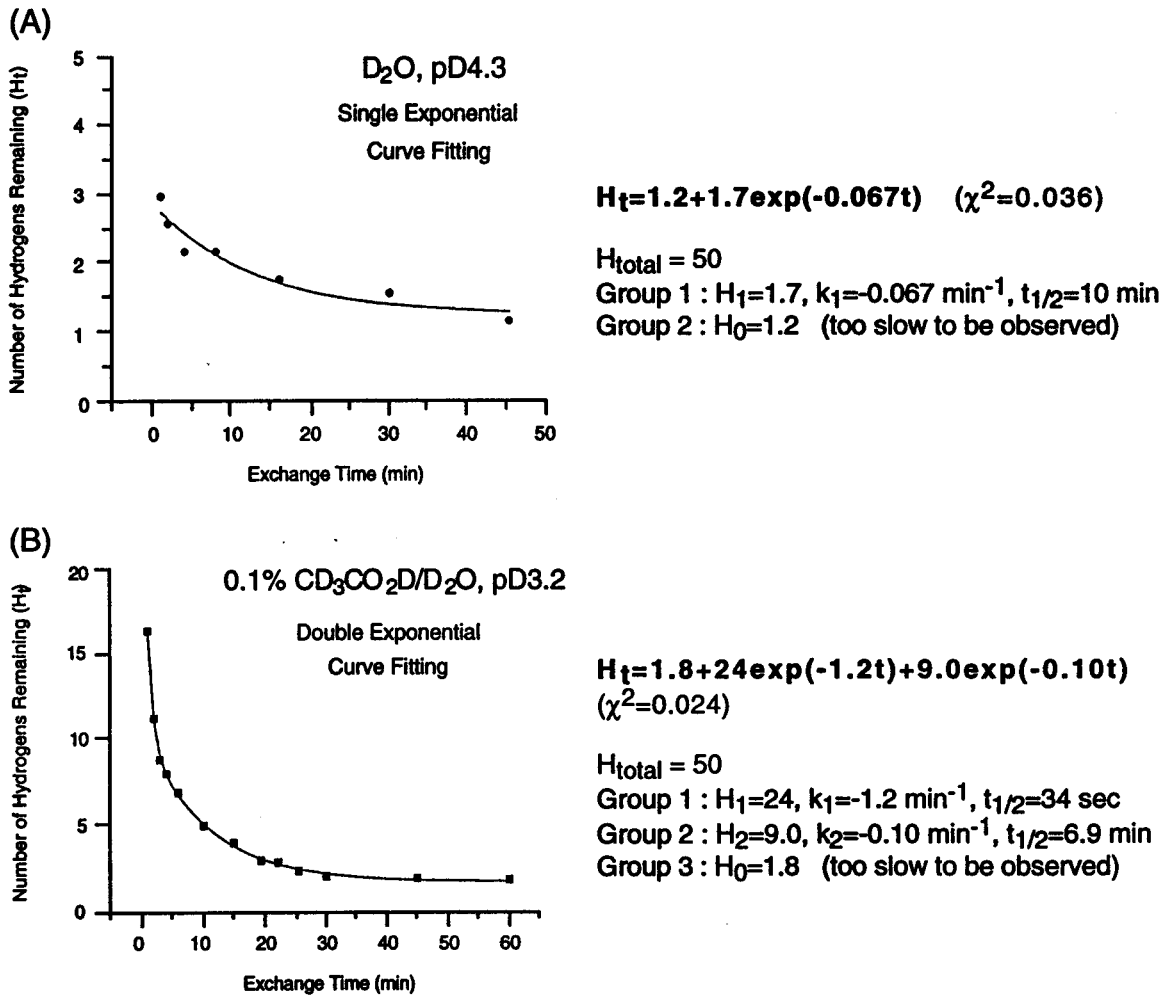

Figure II. 1-7: pH and Solvent Dependence of H/D Exchange of Melittin

Although the shift in molecular ion masses during H/D exchange can give information on the global structure of melittin in solution, it can't provide any information on specific regions of melittin where the deuterium atoms were incorporated. To obtain this type of regional information, tandem mass

spectrometric experiments (CF-ESIMS/MS) were conducted after H/D exchange into melittin.

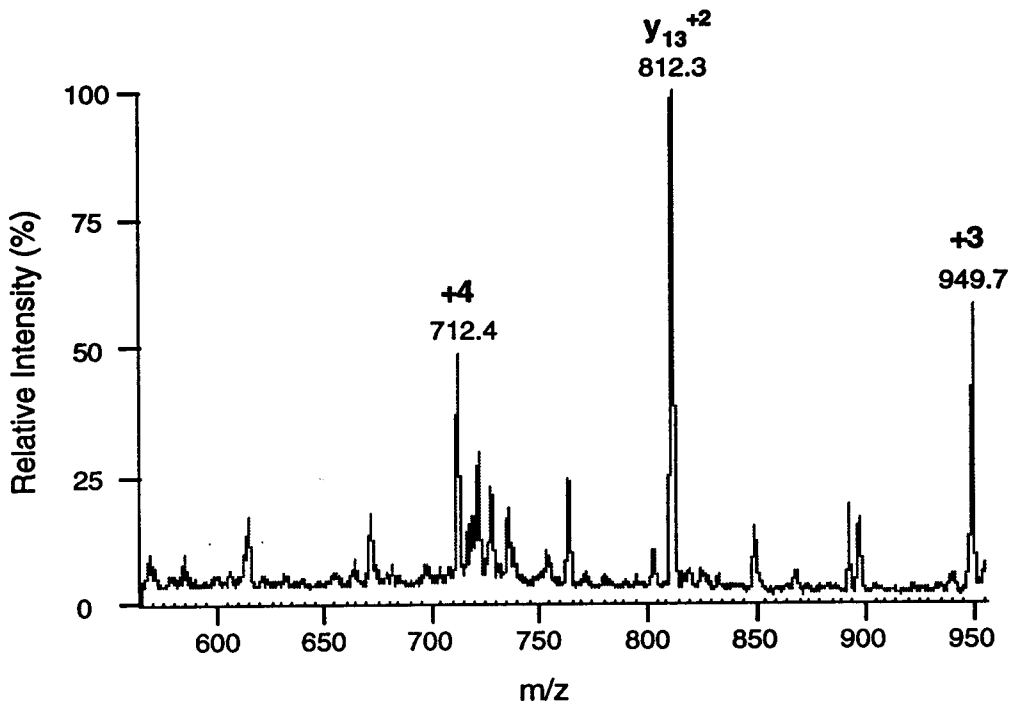

Figure II.1-8: Ionspray Mass Spectrum of Melittin (5 μM) in MeOH/H_2O/AcOH (=80:20:2, pH 3.2) at 120 V Orifice Potential

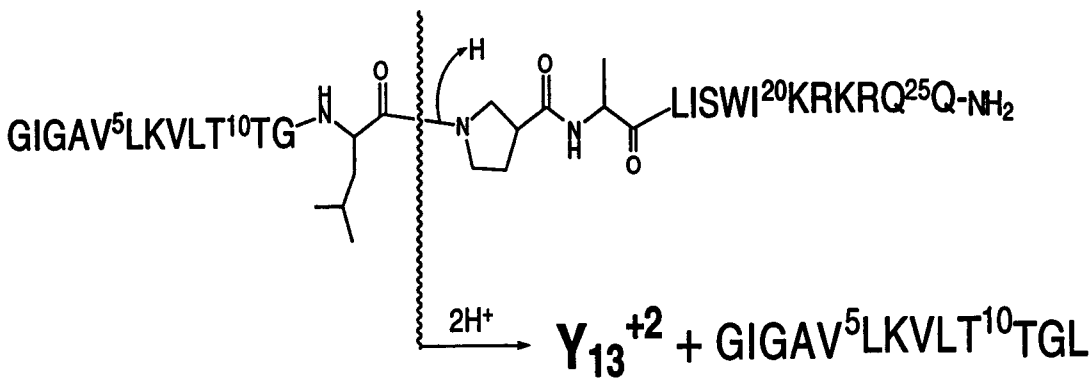

Figure II.1-9: Generation of Y_{13}^{+2} Fragment Ion

Tandem mass spectrum (**Figure II.1-10**) was obtained for the +4-charge state molecular ion which was the most intense at 80 V orifice potential (**Figure II.1-3**). A similar tandem mass spectrometric study (**Figure II.1-11**) was carried out on the +2-charge state of the Y_{13} fragment ion which was formed with high abundance in the free jet expansion region of the mass spectrometer before the first quadrupole when the orifice potential was increased from 80 V to 120 V (**Figure II.1-8, Figure II.1-9**). The Y_{13}^{+2} fragment ion was used to obtain additional sequence-specific information on the C-terminal α-helix of melittin.

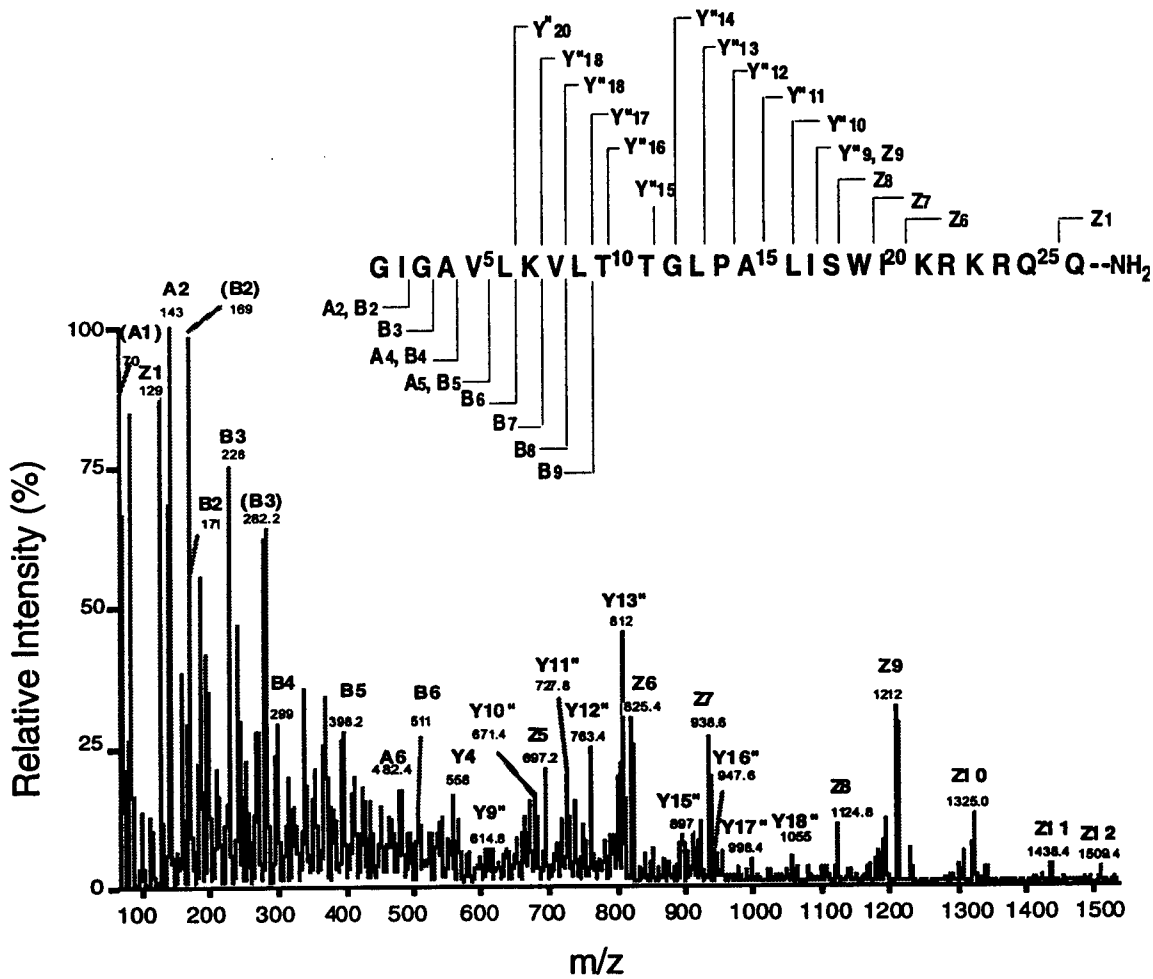

Figure II.1-10: Daughter Ion Spectra of +4-Charge State Molecular Ion (m/z 712, 80 V Orifice)

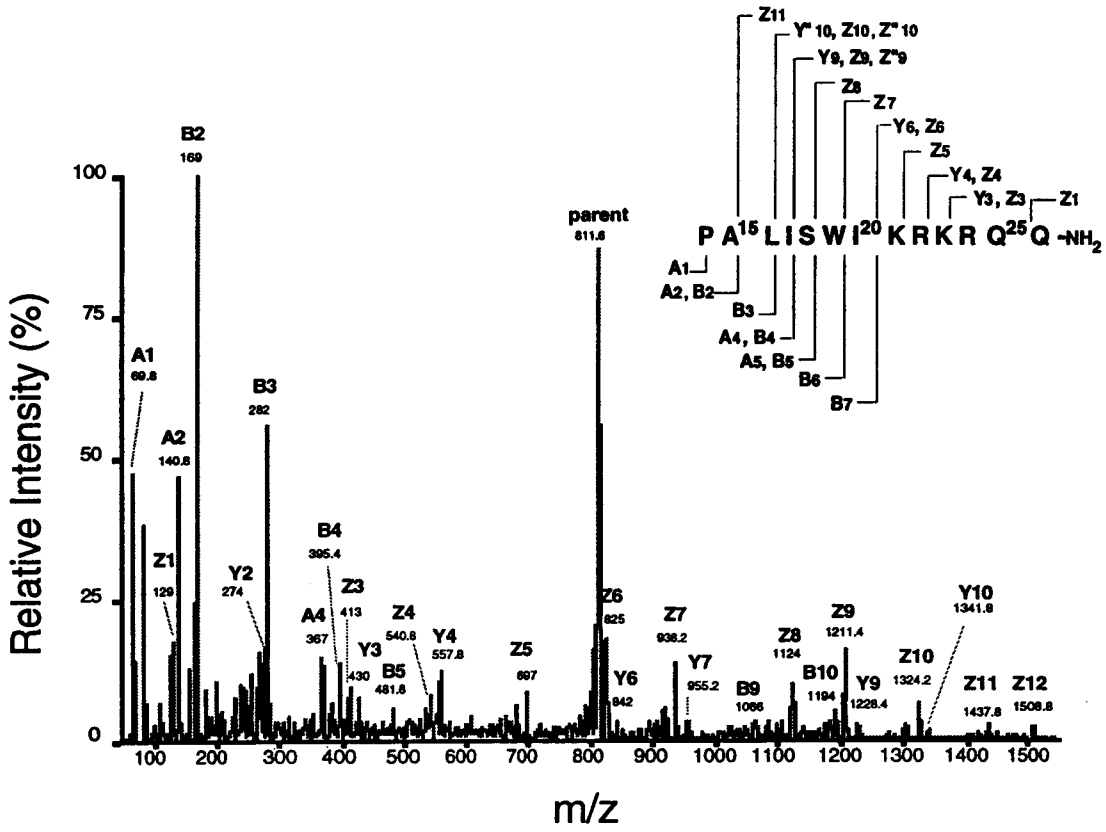

Figure II.1-11: Daughter Ion Spectra of Y_{13}^{+2} Fragment Ion (m/z 812, 120 V Orifice)

During ESIMS/MS analysis, the mass range was scanned from m/z 50 to m/z 1550 with 0.2 Da step size and 0.7 ms dwell time. A-, B-, Y- and Z-series fragment ions derived from the +4-charge state molecular ion (**Figure II.1-10**) and the +2-charge state Y_{13} fragment ion (**Figure II.1-11**) predominated . The mass shifts in the fragment ions during H/D exchange were determined and the information was used to calculate the number of deuterium atoms in the ion and the number of hydrogens remaining after the H/D exchange period. This was done by comparing the masses of the observed protonated and the calculated fully deuterated ions. The results were averaged and tabulated (**Table II.1-1**, **Table II.1-2**).

Table II.1-1: Observed Sequence Ions from Collision-Induced Dissociation (CID) on +4-Charge State Molecular Ion of Melittin and Deuterium Incorporation as a Function of Time

Ions	Protonated Mass (a) (Observed) 0% D	Deuterated Mass (b) (Calculated) 100% D	Number of Hydrogens Remaining after Time (min)					
			Total H	Total NH	4	7	11	19
(+1)								
A_2	143.1	146.1	3	1	0.5	0.4	0.4	0.2
A_4	271.3	276.3	5	3	1.0	1.0	1.0	0.8
A_5	370.2	376.2	6	4	2.0	1.7	1.5	1.3
B_2	171.0	174.0	3	1	0.9	0.8	0.6	0.4
B_3	228.1	232.1	4	2	1.4	1.4	0.8	0.6
B_4	229.2	304.2	5	3	1.9	1.4	0.9	0.7
B_5	398.2	404.2	6	4	1.6	1.4	1.4	1.0
B_6	511.1	518.1	7	5	1.9	1.8	1.7	1.3
B_7	639.1	649.2	10	6	1.9	1.8	1.8	1.7
B_8	738.0	749.1	11	7	2.1	2.0	2.0	1.8
B_9	851.3	863.4	12	8	2.4	2.3	2.3	1.8
Z_1	129.2	133.2	4	0	2.1	1.9	1.7	1.1
Z_6	825.5	848.7	23	5	7.4	6.7	6.5	5.5
Z_7	938.4	962.6	24	6	8.4	7.4	7.4	7.4
Z_8	1124.5	1150.7	26	7	8.5	7.7	7.6	7.4
Z_9	1211.2	1239.4	28	8	8.5	8.0	7.8	6.1
(+2)								
Y_9	614.6	630.2	31	9	6.8	6.0	5.4	4.8
Y_{10}	671.4	687.5	32	10	7.0	6.4	5.4	5.1
Y_{11}	727.7	743.8	33	11	7.2	6.9	5.4	5.2
Y_{12}	763.3	779.9	34	12	7.8	6.7	6.4	6.2
Y_{13}	811.8	828.9	34	12	8.4	7.2	6.2	6.2
Y_{14}	868.3	885.9	35	13	8.8	7.5	6.5	6.2
Y_{15}	897.0	915.1	36	14	9.0	7.7	6.6	6.2
Y_{16}	947.4	966.6	38	15	9.0	8.2	7.8	6.8
Y_{17}	997.9	1018.1	40	16	10.0	9.0	8.3	7.0
Y_{18}	1054.6	1075.1	41	17	10.4	9.2	8.3	7.4
Y_{19}	1104.2	1125.3	42	18	10.6	9.8	8.3	7.5
Y_{20}	1168.2	1190.9	45	19	11.4	9.8	9.0	8.2

(a) 100% protonated melittin, (b) 100% deuterated melittin

Table II.1-2: Observed Sequence Ions from Collision-Induced Dissociation (CID) on Y_{13}^{+2} Fragment Ion of Melittin and Deuterium Incorporation as a Function of Time

Ions	Protonated Mass (a) (Observed) 0% D	Deuterated Mass (b) (Calculated) 100% D	Number of Hydrogens Remaining after Time(min)					
			Total H	Total NH	4	7	11	19
(+1)								
A_1	70.0	71.0	1	0	0.2	0.2	0.2	0.2
A_2	141.2	143.2	2	1	0.4	0.6	0.4	0.4
A_4	367.2	371.2	4	3	1.2	1.2	1.2	1.2
A_5	454.2	460.2	6	4	2.2	2.2	1.6	1.6
B_2	169.2	171.2	2	1	0.6	0.6	0.4	0.4
B_3	282.2	285.2	3	2	1.0	0.8	0.8	0.8
B_4	395.6	399.6	4	3	2.0	2.0	2.0	1.0
B_5	482.0	488.0	6	4	2.0	1.8	1.8	1.2
B_6	668.2	676.2	8	5	3.0	2.9	2.4	2.0
B_7	782.2	791.2	9	6	4.0	4.0	3.0	2.7
Y_3	430.2	444.3	13	3	3.3	3.3	3.0	3.0
Y_4	558	575.1	16	4	3.1	3.1	3.1	3.1
Y_6	714.4	867.2	24	6	5.0	4.6	4.1	3.4
Y_9	1228.2	1258.4	29	9	6.4	6.4	5.6	5.6
Y_{10}	1341.8	1373.0	30	10	6.5	6.5	6.5	6.5
Z_1	129.0	134.0	4	0	2.2	2.2	2.2	2.0
Z_3	413.2	426.3	12	2	4.9	4.9	4.3	4.3
Z_4	541.2	557.3	15	3	5.3	5.1	5.1	4.5
Z_5	697.2	718.3	20	4	6.5	6.3	5.9	5.9
Z_6	825.4	849.6	23	5	7.4	7.4	7.2	6.6
Z_7	938.2	963.4	24	6	7.4	7.4	7.2	6.8
Z_8	1124.4	1151.6	26	7	7.4	7.4	7.4	7.2
Z_9	1211.4	1240.4	28	8	8.0	8.0	7.6	7.4
Z_{10}	1324.4	1354.6	29	9	8.0	8.0	8.0	7.6
Z_{11}	1437.4	1468.6	30	10	8.2	8.4	8.4	8.4
(+2)								
Z_9	606.2	1242.6	28	8	8.2	8.2	8.2	7.4
Z_{10}	663.0	1357.2	29	9	9.2	8.8	8.4	7.5

(a) 100% protonated melittin, (b) 100% deuterated melittin

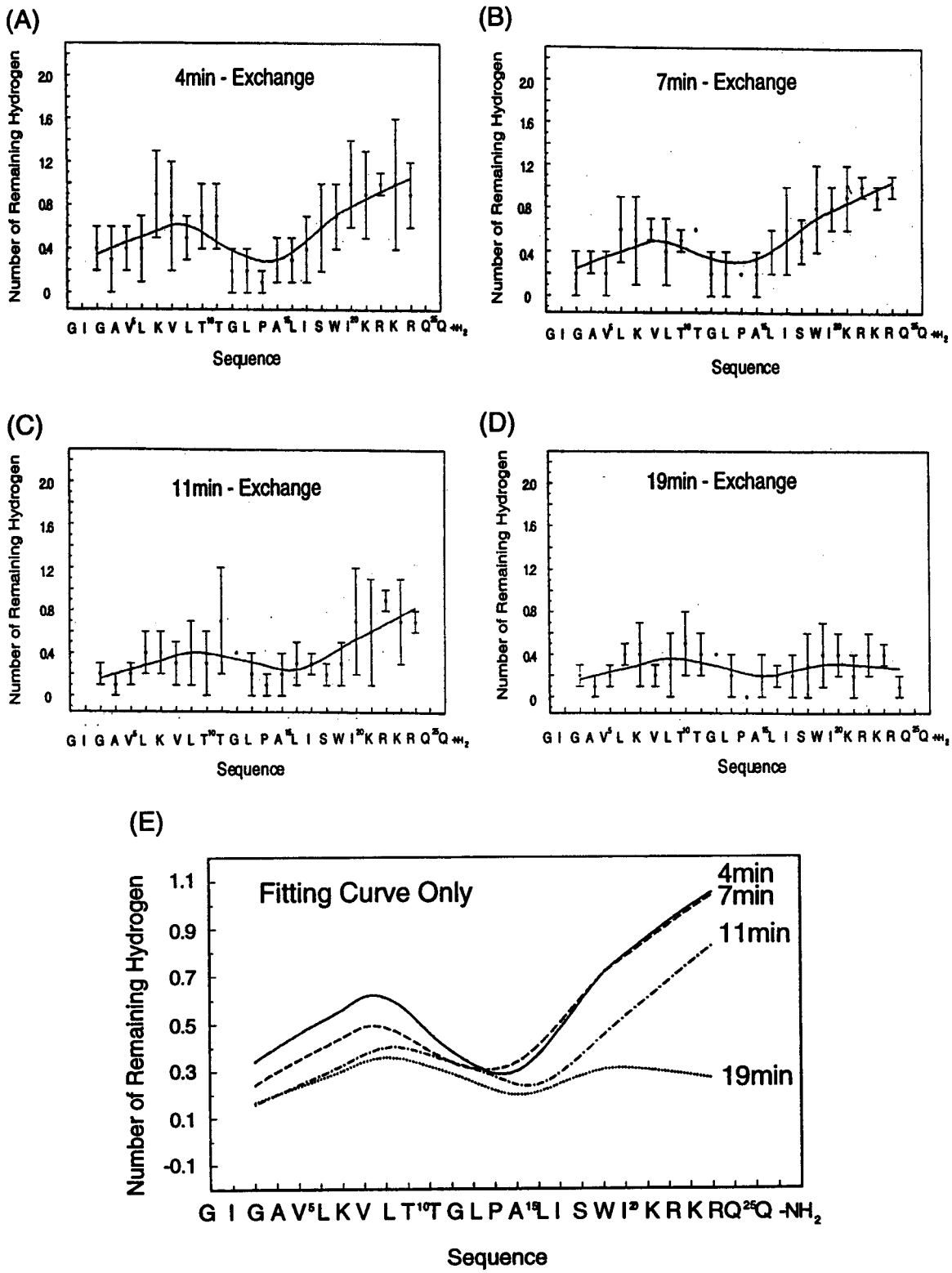

Figure II.1-12: Deuterium Exchange-In of the Individual Amino Acid Residue of Melittin in $CD_3OD/D_2O/CD_3CO_2D$ (=80:20:2, pD 3.2) at 20°C Monitored by CF-ESIMS/MS

To determine whether or not a particular peptide amide hydrogen was involved in intramolecular hydrogen bonding, the number of hydrogens remaining in each residue was calculated. The peptide amides with a high number (close to 1) of remaining hydrogens, are more likely to have been involved in intramolecular hydrogen bonding within the α-helices of melittin. Accordingly, the α-helical regions retained the highest number of remaining hydrogens after H/D exchange. The number of hydrogens remaining in an A_n-ion was subtracted from that in the A_{n+1}-ion after a certain time of H/D exchange (t), which gave the number of hydrogens remaining at the residue n at time t. The same kind of subtractions were conducted on the B_n-, Y_n- and Z_n-fragment ions, respectively to calculate the number of hydrogens remaining in each residue. The results were averaged and plotted for each amino acid residue at different H/D exchange times (**Table III.1-5, Figure II.1-12**). The number of hydrogens remaining at the individual residues can be related to the relative strength of the original hydrogen bonds in the α-helices of melittin. These results were plotted as a function of H/D exchange time. In these diagrams, two distinct slow-exchanging regions were observed and these were separated approximately around Pro14 with the C-terminal region apparently being more stabilized by intramolecular hydrogen bonds. These results were compatible with the known data obtained by X-ray crystallography and NMR spectroscopy[18,19] which showed two helices: Ile2-Thr11 and Leu13-Gln26 (**Figure I.1-1**).

II.1-2 Monitoring Deuterium Exchange-In of Melittin by HPLC-ESIMS and HPLC-ESIMS/MS

Deuterium exchange of peptide amide hydrogens (NHs) in melittin was followed by microbore HPLC-ESIMS and HPLC-ESIMS/MS analysis under slow-exchange conditions (0°C, pH 2-3). These conditions are necessary to minimize back-exchange of the deuteriums to hydrogens. In this method, sample solutions were injected onto the microbore HPLC system which was directly coupled to the electrospray ionization mass spectrometer (ESIMS) (**Figure II.1-13**). Solvent reservoirs containing 0.1% trifluoroacetic acid (TFA) in water and 0.08% TFA in acetonitrile, respectively, were placed in an ice-bath. All of the compartments from injection valve to column outlet line just before the UV detector also were immersed in an ice-bath. The retention time of melittin through an Aquapore C-8 reverse phase column, was 8-10 min, and under these conditions the measurement of the deuterium content was reproducible.

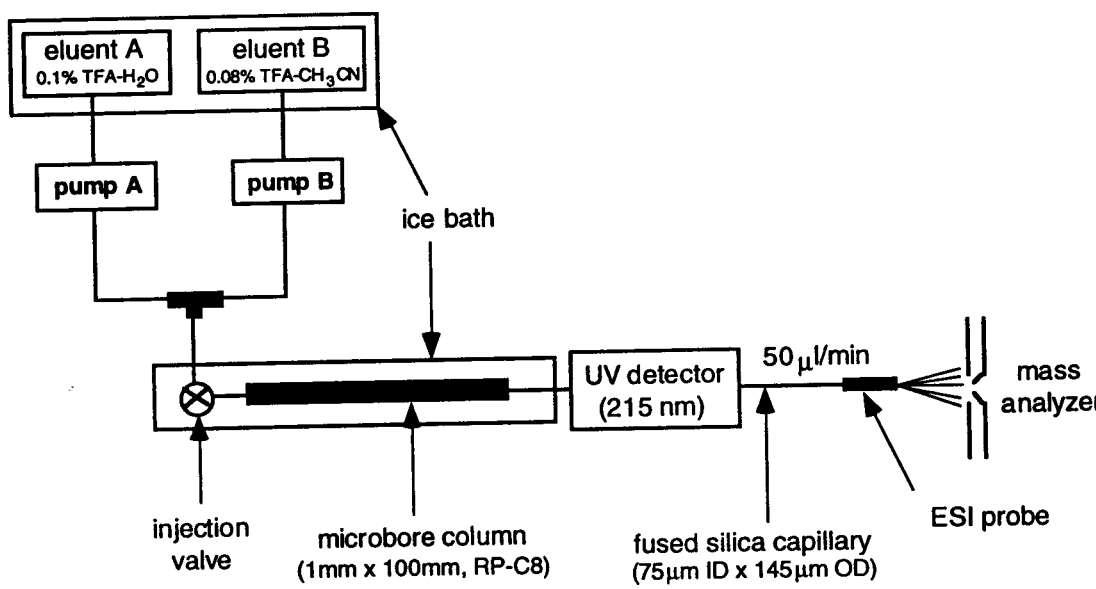

Figure II.1-13: Sample Injection onto HPLC-ESIMS System

The purpose of this study was to compare the results with those obtained from previous H/D exchange experiments with melittin using continuous flow infusion ESIMS (CF-ESIMS) for the analysis. Furthermore, sample introduction through an HPLC system is more practical, especially for complex proteins dissolved in a salt-containing solvent system. Although ESIMS is compatible with solvent systems containing volatile salts such as NH_4OAc (<100 mM) and volatile organic solvents (AcOH, HCO_2H and MeOH), the sensitivity for the detection of the analyte diminishes as the amount of salts in the solution increases. Phosphate buffer can not be infused directly into the ESI mass spectrometer because of the very strong signals from background ions. Alkaline ions such Na^+ and K^+ also decrease the detection sensitivity for the analyte by distributing the analyte ion through adducts such as $(M+H)^+$, $(M+Na)^+$, $(M-H+2Na)^+$, $(M-nH+nNa+Na)^+$, etc., where M is the mass of the analyte. Therefore, sample injection into an HPLC system can be used to desalt the sample and help to concentrate it, with dramatical increases in the absolute detection sensitivity. Another benefit of using the HPLC-ESIMS system is that the fast-exchanging hydrogens can be distinguished from the slow-exchanging peptide amide hydrogens (NHs).[4] The fast-exchanging hydrogens from the side chains and from both terminal sites are completely deuterated in the deuterium exchange-in process but they are completely back-exchanged to hydrogens during HPLC analysis of the sample, even at 0°C and pH 2-3. However the peptide amide hydrogens will retain their deuterium labels during the HPLC run under the right conditions (pH 2-3, 0°C). In fact the half-life of H/D exchange of peptide amide hydrogens is in the range of 40-50 min under these slow-exchange conditions (0°C, pH 2-3).[51] The overall procedure for monitoring H/D exchange of the peptide amide hydrogens of melittin using HPLC-ESIMS and HPLC-ESIMS/MS, is depicted in **strategy II (Scheme II.1-2)**.

Strategy II

Deuterium Exchange-In of Melittin Monitored by HPLC-ESIMS and HPLC-ESIMS/MS

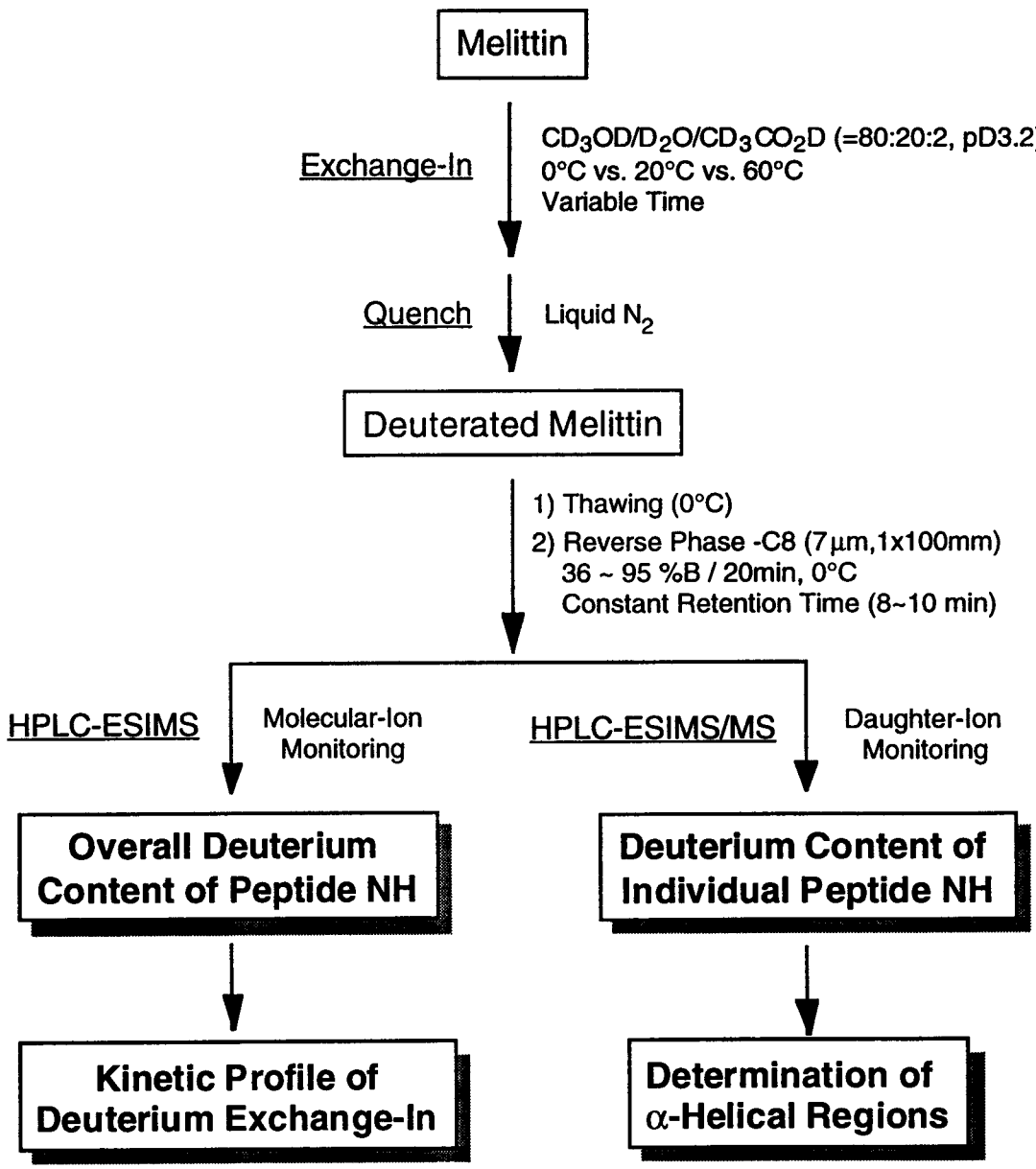

Scheme II.1-2: Strategy II

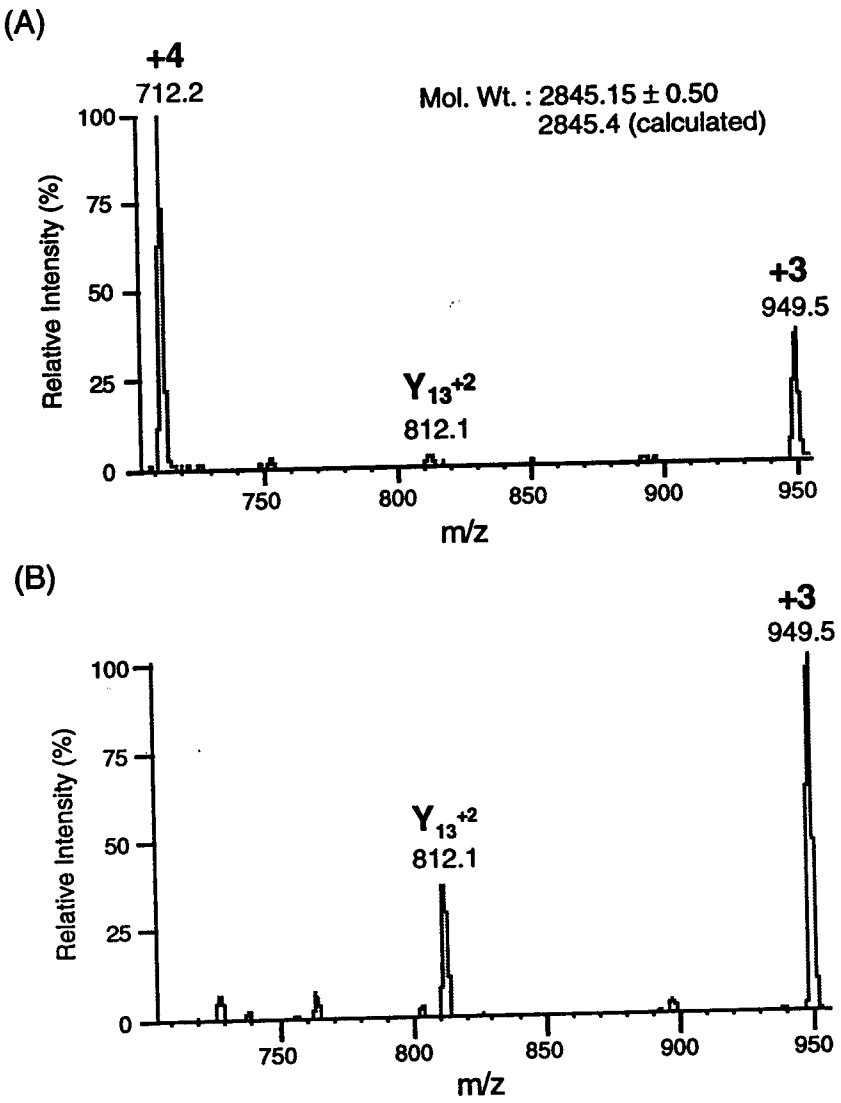

Figure II.1-14: Microbore HPLC-Ionspray Mass Spectra of Melittin (40 μM, 200 pmole Injection) (A) at 80 V Orifice Potential and (B) at 120 V Orifice Potential

Melittin (40 μM, 200 pmole) in MeOH/H_2O/AcOH (=80:20:2, pH 3.2) was injected into the microbore HPLC-ESIMS system under the slow-exchange conditions. The melittin peak which had a retention time of 8-10 min was analyzed by scanning the mass region between 705 and 955 using 0.1 step size and 1 ms dwell time (**Figure II.1-14**). Molecular ions with +4- and +3-

charge states were detected at 80 V orifice potential (**Figure II.1-14A**). At 120 V orifice potential, only the +3-charge state molecular ion of melittin and the Y_{13}^{+2} fragment ion were observed (**Figure II.1-14B**). The relative intensity of the Y_{13}^{+2} fragment ion was much lower than the corresponding one observed by CF-ESIMS (**Figure II.1-8**).

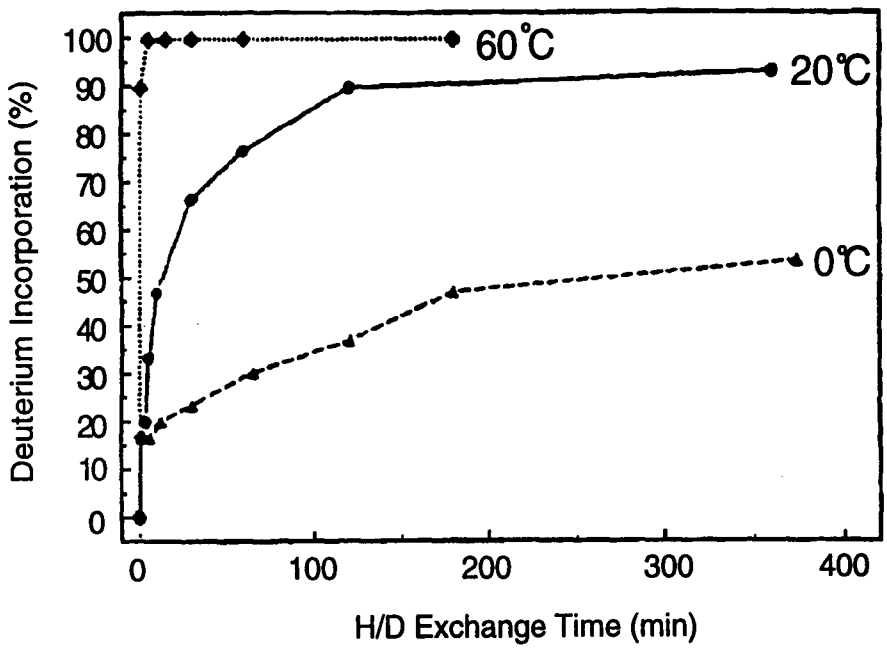

Figure II.1-15: Monitoring Deuterium Incorporation into Melittin in $CD_3OD/D_2O/CD_3CO_2D$ (=80:20:2) at Different Temperatures by HPLC-ESIMS

The temperature dependence of H/D exchange of peptide amide hydrogens was studied by following the deuterium incorporation when melittin was dissolved in $CD_3OD/D_2O/CD_3CO_2D$ (=80:20:2, pD 3.2) and the temperature was set to 60°C, 20°C and 0°C. Calculation of the percentage of deuterium incorporation was based upon a total of 24 peptide amide hydrogens which give a molecular weight of 2870 Da when the peptide amide groups are fully

deuterated. A time-dependent mass profile of melittin was obtained by plotting the percentage of deuterium incorporation in the +4- and +3-charge state molecular ions during the exchange time period (**Figure II.1-15** and **Table III.1-6~Table III.1-8**). The peptide amide hydrogens of melittin were completely deuterated within 5 min at 60°C, which indicated complete unfolding of the helical structures in melittin. On the other hand, it required 6 hours for 93% of the peptide amides to be deuterated at 25°C, whereas in 0°C experiment, only 53% of the peptide amides were deuterated for 6.2 hours. From these mass profiles, kinetic data were obtained from plotting NH_t vs. deuterium exchange-in time (t), where NH_t represents the number of peptide amide hydrogens that have not yet exchanged by time t at a given temperature and NH_{total} is a total number of exchangeable peptide amide hydrogens available (**Figure II.1-16** and **Table III.1-6~Table III.1-8**). Deuterium exchange-in into melittin at 60°C occurred very rapidly, so that a proper non-linear fitting curve could not be found. On the other hand, deuterium exchange-in profiles at 20°C and 0°C could be represented by single exponential decay curves, respectively. According to these fitting curves, three groups of peptide amide hydrogens were observed at 20°C (**Figure II.1-16A**) and 0°C (**Figure II.1-16B**), respectively. The fastest- and the slowest-exchanging groups of peptide amide hydrogens could not provide detailed kinetic data in these analyses. The medium-exchanging group of amide hydrogens (group 1) were exchanged with half-lives of 18 min at 20°C and 4.0 hr at 0°C, respectively. These results were not comparable with those obtained from the H/D exchange experiments using CF-ESIMS analysis at 20°C and 0°C (**Figure II.1-4B, II.1-4C**). Especially, deuterium exchange-in profile at 0°C monitored by CF-ESIMS, showed a double exponential fitting curve, in which two exchange rate constants were determined (k_1=-0.12 min^{-1} and k_2=-0.038 min^{-1}).

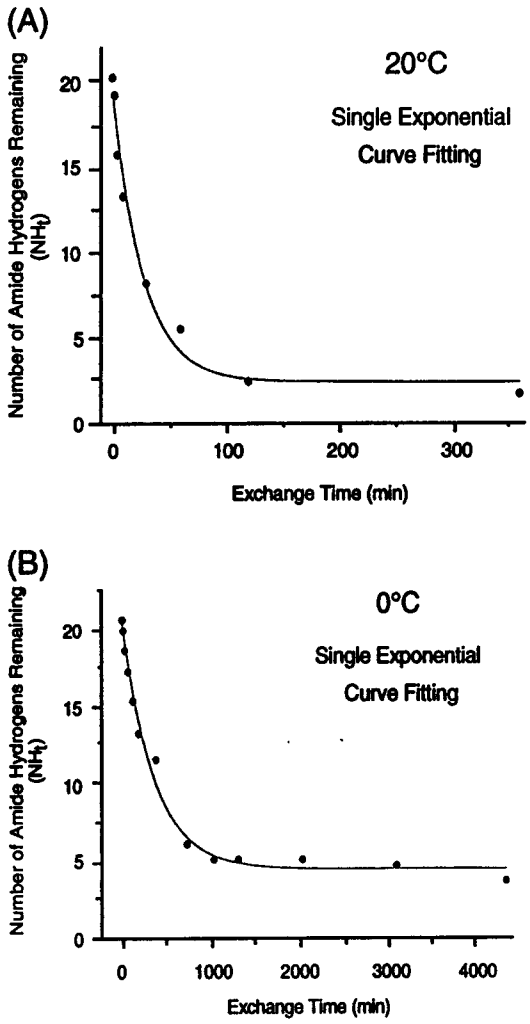

NH_t=2.5+18exp(-0.038t) (χ^2=1.3)

NH_{total}=24
Group 1 : NH_1=18, k_1=-0.038 min^{-1}, $t_{1/2}$=18 min
Group 2 : NH_0=2.5 (too slow to be observed)

NH_t=4.3+16exp(-0.0028t) (χ^2=0.46)

NH_{total}=24
Group 1 : NH_1=16, k_1=-0.0028 min^{-1}, $t_{1/2}$=4.0 hr
Group 2 : NH_0=4.3 (too slow to be observed)

Figure II.1-16: Temperature Dependence of H/D Exchange of Melittin

To observe the specific amide hydrogens in the sequence of melittin that have exchanged, tandem mass spectrometric analysis (HPLC-ESIMS/MS) was performed. The daughter ion spectra of the +4-charge state molecular ion and the +2-charge state Y_{13} fragment ion (**Figure II.1-17**) resulted in similar sequence ions with those obtained by CF-ESIMS/MS (**Figure II.1-10, Figure II.1-11**). The Y_{13}^{+2} fragment ion (**Figure II.1-14B**) was much weaker in intensity at 120 V orifice potential than the one observed by CF-ESIMS (**Figure**

II.1-8). The collisionally induced dissociation (CID) of the +4-charge state molecular ion (**Figure II.1-17A**) and the Y_{13}^{+2} fragment ion (**Figure II.1-17B**) provided A-, B-, Y- and Z-series of fragment ions predominantly.

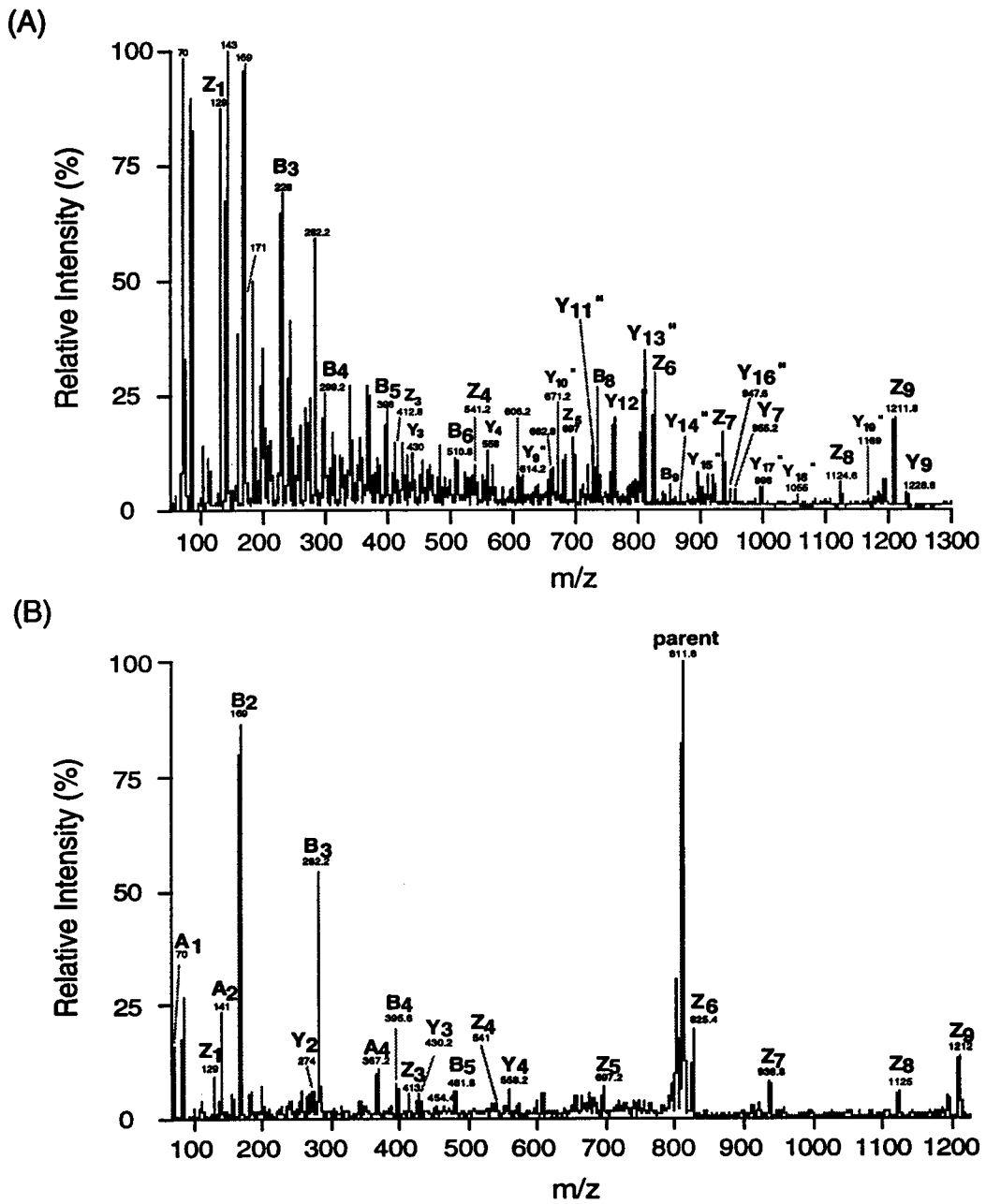

Figure II.1-17: Daughter Ion Spectra of (A) +4-Charge State Molecular Ion (m/z 712, 80 V Orifice) and (B) Y_{13}^{+2} Fragment Ion (m/z 812, 120 V Orifice) of Melittin Obtained by Microbore HPLC-ESIMS/MS at 0°C

Table II.1-3: Observed Sequence Ions from Collision-Induced Dissociation on +4-Charge State Molecular Ion of Melittin and Deuterium Incorporation as a Function of Time

Ions	Protonated Mass (Observed) 0% ND	Deuterated Mass (Calculated) 100% ND	Number of Amide Hydrogens Remaining after a Time (min)			
			Total NH	4	11	19
(+1)						
B_3	228.0	230.0	2	1.8	1.2	1.0
B_4	299.2	302.2	3	2.6	1.8	1.8
B_5	398.0	402.0	4	3.0	2.6	2.6
B_6	510.8	515.8	5	3.6	3.4	3.0
B_8	738.2	745.2	7	4.6	3.8	3.6
B_9	851.4	859.4	8	5.6	4.4	4.0
Y_3	430.0	433.0	3	1.4	0.6	0
Y_4	558.0	562.0	4	2.0	1.2	0
Y_7	955.2	962.2	7	3.4	2.8	0.7
Y_9	1228.8	1237.8	9	5.9	3.6	2.2
Z_3	412.8	414.8	2	0.8	0.4	0
Z_4	541.2	544.2	3	1.4	0.8	0.2
Z_5	697.0	701.0	4	1.6	0.6	0.2
Z_6	825.2	830.2	5	2.4	1.0	0.6
Z_7	938.4	944.4	6	3.0	1.8	1.0
Z_8	1124.6	1131.6	7	3.6	2.4	1.4
Z_9	1211.8	1219.8	8	4.4	2.8	1.4
(+2)						
Y_9	614.2	619.1	9	5.0	3.4	2.6
Y_{10}	671.2	676.2	10	6.0	4.4	2.8
Y_{11}	727.8	733.3	11	7.0	5.4	3.4
Y_{12}	763.4	769.4	12	8.0	6.4	4.8
Y_{13}	811.8	817.8	12	8.0	6.4	4.8
Y_{14}	868.4	874.9	13	8.0	6.2	4.6
Y_{15}	896.6	903.6	14	8.8	6.4	4.8
Y_{16}	947.6	955.1	15	9.4	7.8	5.8
Y_{17}	998.0	1006.0	16	10.0	8.0	5.6
Y_{18}	1055.0	1063.6	17	11.2	9.6	6.8
Y_{20}	1169.0	1178.5	19	12.6	11.4	9.0
Z_9	606.2	610.2	8	4.4	2.4	2.0
Z_{10}	662.8	667.3	9	5.4	4.2	1.4
Z_{11}	719.6	724.6	10	6.4	5.6	4.0
Z_{12}	754.6	760.1	11	7.0	5.8	3.8

Table II.1-4: Observed Sequence Ions from Collision-Induced Dissociation on Y_{13}^{+2} Fragment Ion of Melittin and Deuterium Incorporation as a Function of Time

Ions	Protonated Mass (Observed) 0% ND	Deuterated Mass (Calculated) 100% ND	Number of Amide Hydrogens Remaining after a Time (min)			
			Total NH	4	11	19
(+1)						
A_1	70.0	70.0	0	0	0	0
A_2	141.0	142.0	1	0.8	0.8	0.6
A_4	367.2	370.2	3	2.6	1.6	1.6
B_2	169.0	170.0	1	0.8	0.8	0.6
B_3	282.2	284.2	2	1.8	1.8	1.6
B_4	395.6	398.6	3	2.2	1.6	1.4
B_5	481.8	485.8	4	3.2	2.8	2.8
Y_2	274.0	276.0	2	1.4	1.4	1.2
Y_3	430.2	433.2	3	1.5	1.0	1.0
Y_4	558.2	562.2	4	2.0	1.4	1.0
Z_3	413.0	415.0	2	0.4	0	0
Z_4	541.0	544.0	3	1.0	0.2	0
Z_5	697.2	701.2	4	1.6	0.4	-
Z_6	825.4	830.4	5	2.0	1.4	0.6
Z_7	938.8	944.8	6	3.4	2.4	2.2
Z_8	1125.0	1132.0	7	3.2	2.4	-
Z_9	1212.0	1220.0	8	4.2	3.0	-

For tandem mass spectrometric monitoring of deuterium exchange-in, melittin was dissolved in $CD_3OD/D_2O/CD_3CO_2D$ (=80:20:2, pD 3.2) at 20°C for a predetermined period of time and then injected immediately into a microbore HPLC-ESIMS/MS system under the slow exchange conditions. Mass shifts of the sequence-specific ions from +4-charge state molecular ions and from Y_{13}^{+2} fragment ions were used to calculate the deuterium level incorporated in the individual backbone amide groups of each amino acid residue. The number of peptide amide hydrogens remaining in a given ion after 4 min, 11 min and 19

min under deuterium exchange-in conditions was determined and the results were tabulated in the 5th to 7th column in **Table II.1-3** and **Table II.1-4**. The observed sequence ions, their observed m/z values, the calculated m/z values of the corresponding ions with fully deuterated peptide amide groups, and the total number of peptide amide hydrogens in each ion, were also tabulated in the 1st to the 4th column of **Table II.1-3** and **Table II.1-4**. From these values, the number of peptide amide hydrogens remaining in each amino acid residue was calculated, averaged (**Table III.1-9**) and plotted (**Figure II.1-18**).

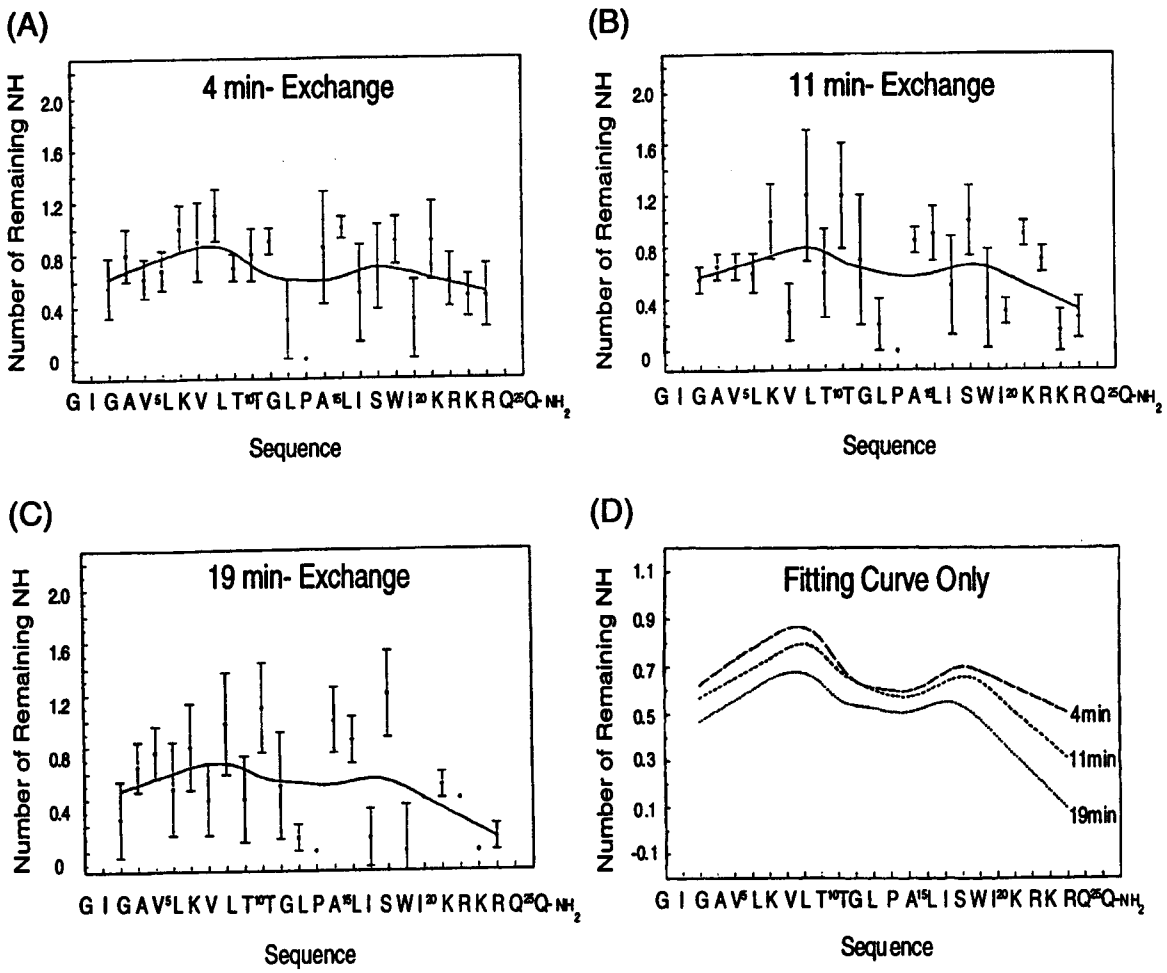

Figure II.1-18: Deuterium Exchange-In of the Individual Amino Acid Residue of Melittin in $CD_3OD/D_2O/CD_3CO_2D$ (=80:20:2, pD 3.2) at 20°C Monitored by Microbore HPLC-ESIMS/MS at 0°C

Generally, the numbers of backbone amide hydrogens remaining after a given deuterium exchange-in time (**Table III.1-9**) were higher than those obtained from the deuterium exchange-in experiments using CF-ESIMS/MS (**Table III.1-5**). The numbers of remaining peptide amide hydrogens in the a-helical region at the C-terminal side, were smaller than those in the a-helical region at the N-terminal side. This is opposite to what was obtained by NMR spectroscopy[19] and by our H/D exchange experiments using CF-ESIMS/MS for the analysis (**Figure II.1-12**). This discrepancy could be explained in the following way. The peptide amide hydrogens observed in the spectrum could arise in one of two ways. They could have exchanged to deuterium atoms during the deuterium exchange-in period and then back-exchanged to hydrogens during HPLC analysis or they had not been exchanged at all during the deuterium exchange-in period. One can not distinguish between these two processes. So the final calculated value will be the sum of these two contributions. Our results also showed large variations of values for each amino acid residue, making curve-fitting difficult (**Figure II.1-18**).

To overcome these problems, melittin was first completely deuterated and then deuterium was exchanged out from the fully deuterated melittin. The analysis was carried out by microbore HPLC-ESIMS and HPLC-ESIMS/MS under the slow exchange conditions as described in the following section.

II.1-3 Monitoring Deuterium Exchange-Out of Fully Deuterated Melittin by HPLC-ESIMS and HPLC-ESIMS/MS

Deuterium exchange-out from deuterated peptide amides (NDs) of fully deuterated melittin was studied. Microbore HPLC-ESIMS and -ESIMS/MS under slow exchange conditions (pH 2-3, 0°C) were used in the analyses. In these experiments, all the possible compartments were cooled to ice-bath temperature to minimize deuterium loss during analysis (**Figure II.1-13**). The overall processes are depicted in **strategy III (Scheme II.1-3)**.

Melittin was fully deuterated in D_2O at room temperature for 2 hrs and then freeze-dried.[18,19] The freeze-dried fully deuterated melittin was dissolved in $CH_3OD/D_2O/ CD_3CO_2D$ (=80:20:2, pD 3.2) at 20°C and immediately analyzed by microbore HPLC-ESIMS under slow H/D exchange conditions to obtain molecular weight of the fully deuterated melittin and to provide the data for time t=0. At 80V orifice potential, the +3 and the +4-charge state molecular ions of the fully deuterated melittin were observed, which gave a molecular weight of 2868 Da after deconvolution (**Figure II.1-19**). Melittin that was 100% protonated, was observed with a molecular weight of 2846 Da. Therefore, 22 deuteriums from the fully deuterated melittin were preserved and detected when analyzed by microbore HPLC-ESIMS. This mass indicates that 44% of the deuteriums remained based on a total of 50 exchangeable deuteriums available. Among these 50 exchangeable deuteriums, there are 24 peptide amide deuteriums. Based on these 24 peptide amide deuteriums, the 22 Da mass increase indicates that 96% of the peptide amide deuteriums remained.

To obtain the time-dependent mass changes due to deuterium exchange-out from fully deuterated melittin, the fully deuterated melittin was

dissolved in $CH_3OH/H_2O/CH_3CO_2H$ (=80:20:2) at 20°C for a predetermined period of time and immediately analyzed by microbore HPLC-ESIMS under slow exchange conditions.

Strategy III

Deuterium Exchange-Out of Fully Deuterated Melittin Monitored by HPLC-ESIMS and HPLC-ESIMS/MS

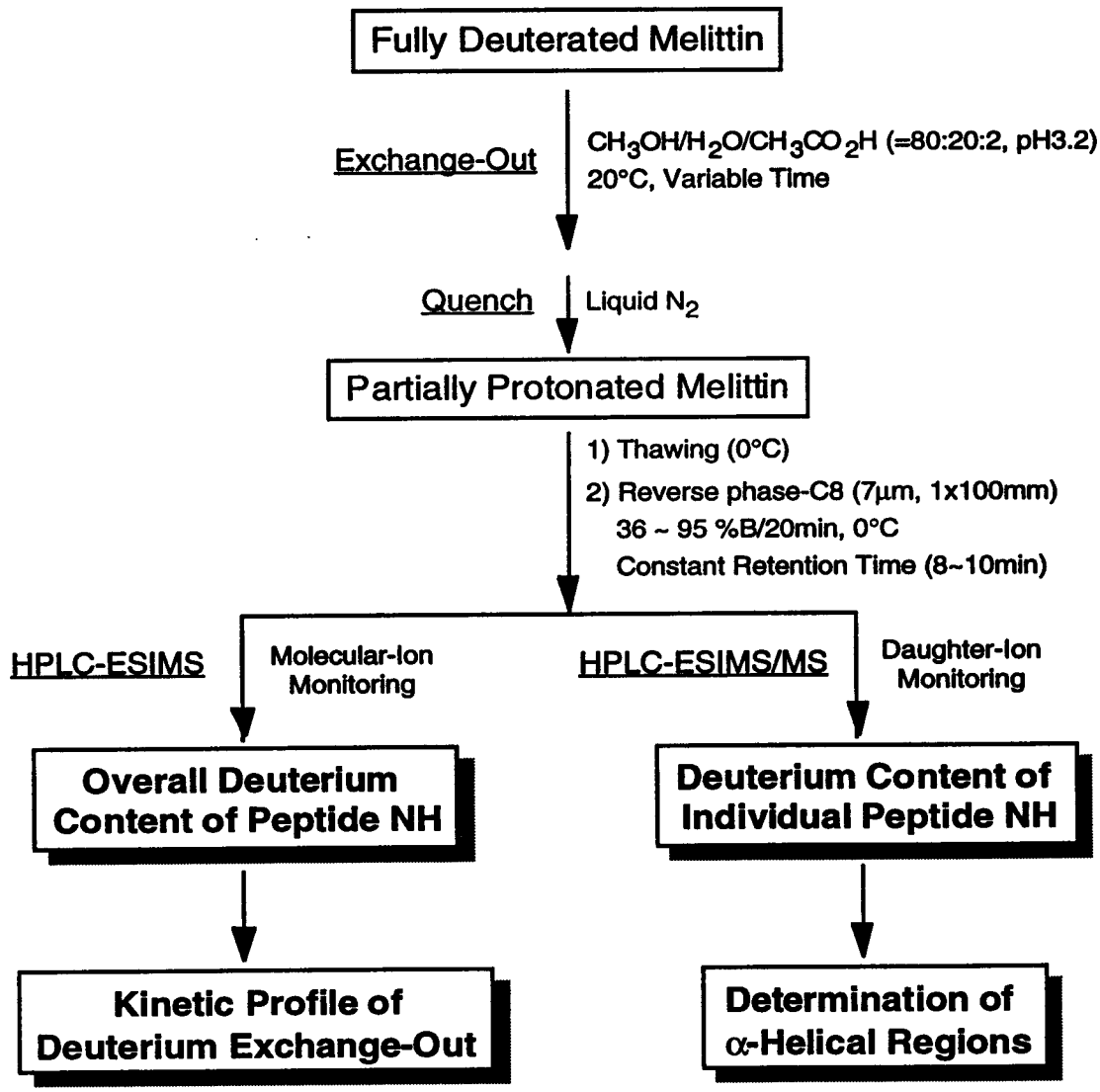

Scheme II.1-3: Strategy III

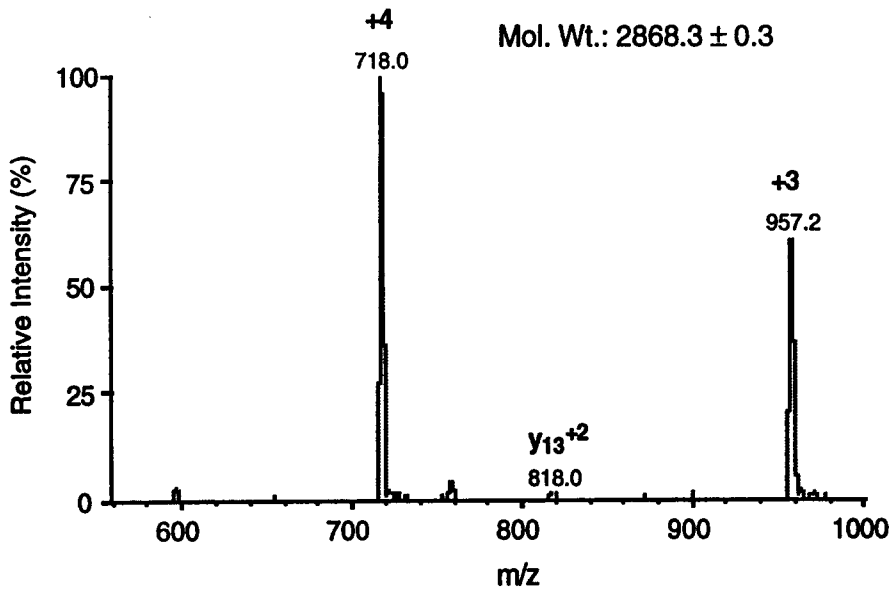

Figure II.1-19: Microbore HPLC-Ionspray Mass Spectrum of Fully Deuterated Melittin (40 μM, 200 pmole Injection) in $CD_3OD/D_2O/CD_3CO_2D$ (=80:20:2, pD 3.2) at 80 V Orifice Potential

Hydrogen incorporation into the fully deuterated melittin during deuterium exchange-out process was determined (**Figure II.1-20A** and **Table III.1-10**) and kinetic data were obtained by plotting the number of remaining peptide amide deuteriums (ND_t) as a function of deuterium exchange-out time (t) , in which ND_{total} represents a total of 24 peptide amide deuteriums available (**Figure II.1-20B, Table III.1-10**). Single exponential fitting curve was found, from which kinetic values were determined. In the fastest-exchanging group, about 6 peptide amide deuteriums exchanged rapidly in less than a minute. Fourteen of backbone amide deuteriums exchanged with a half-life of 6.9 min in group 1. Another about 4.3 amide deuteriums in group 2 exchanges too slowly to provide kinetic data in an hour time scale. The Peptide amide deuteriums in the fastest-exchanging group are represented by peptide amide deuteriums located in the most flexible regions of melittin. Peptide amide

deuteriums in group 1 and group 2 are representative of the medium- and the slowest-exchanging peptide amide deuteriums located in the two α-helices of melittin.

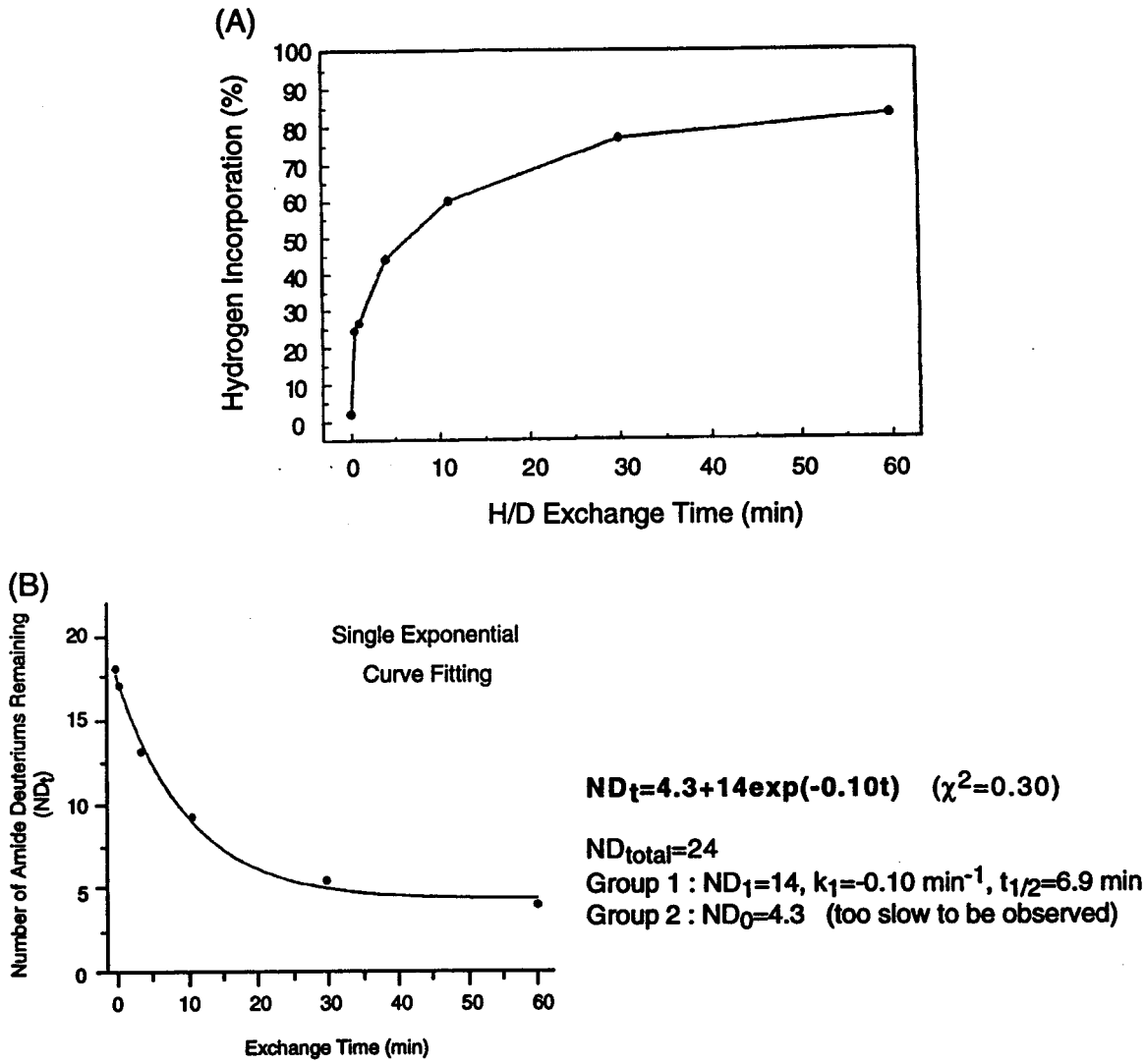

Figure II.1-20: Deuterium Exchange-Out of Fully Deuterated Melittin in MeOH/H_2O/AcOH (=80:20:2, pH 3.2) at 20°C by Microbore HPLC-ESIMS at 0°C

These kinetic data clearly show a similarity with those obtained from the deuterium exchange-in on melittin using CF-ESIMS for the analysis (**Figure**

II.1-4B). The comparability of these two methods is also reflected in the following diagrams (**Figure II.1-21**).

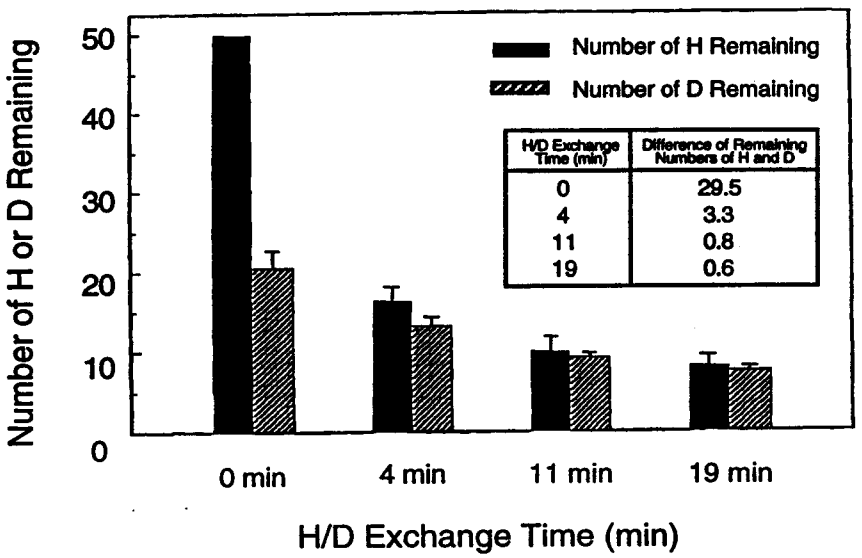

Figure II.1-21: Comparison Between Deuterium Exchange-In on Melittin Using CF-ESIMS Analysis and Deuterium Exchange-Out from Fully Deuterated Melittin Using Microbore HPLC-ESIMS Analysis

The number of remaining hydrogens from the deuterium exchange-in into melittin using CF-ESIMS analysis and the number of remaining peptide amide deuteriums from the deuterium exchange-out from fully deuterated melittin using HPLC-ESIMS analysis are presented. The difference in the number of remaining hydrogens and deuteriums at time t=0 was about 30 which consists of 26 fast-exchanging hydrogens and 4 flexible peptide amide hydrogens. As H/D exchange continued, the difference with time decreased. In 4 min, the difference was 3.3 and in 11 min, the difference was less than 1. Considering the possible deuterium-loss during HPLC-ESIMS analysis, these differences are negligibly small.

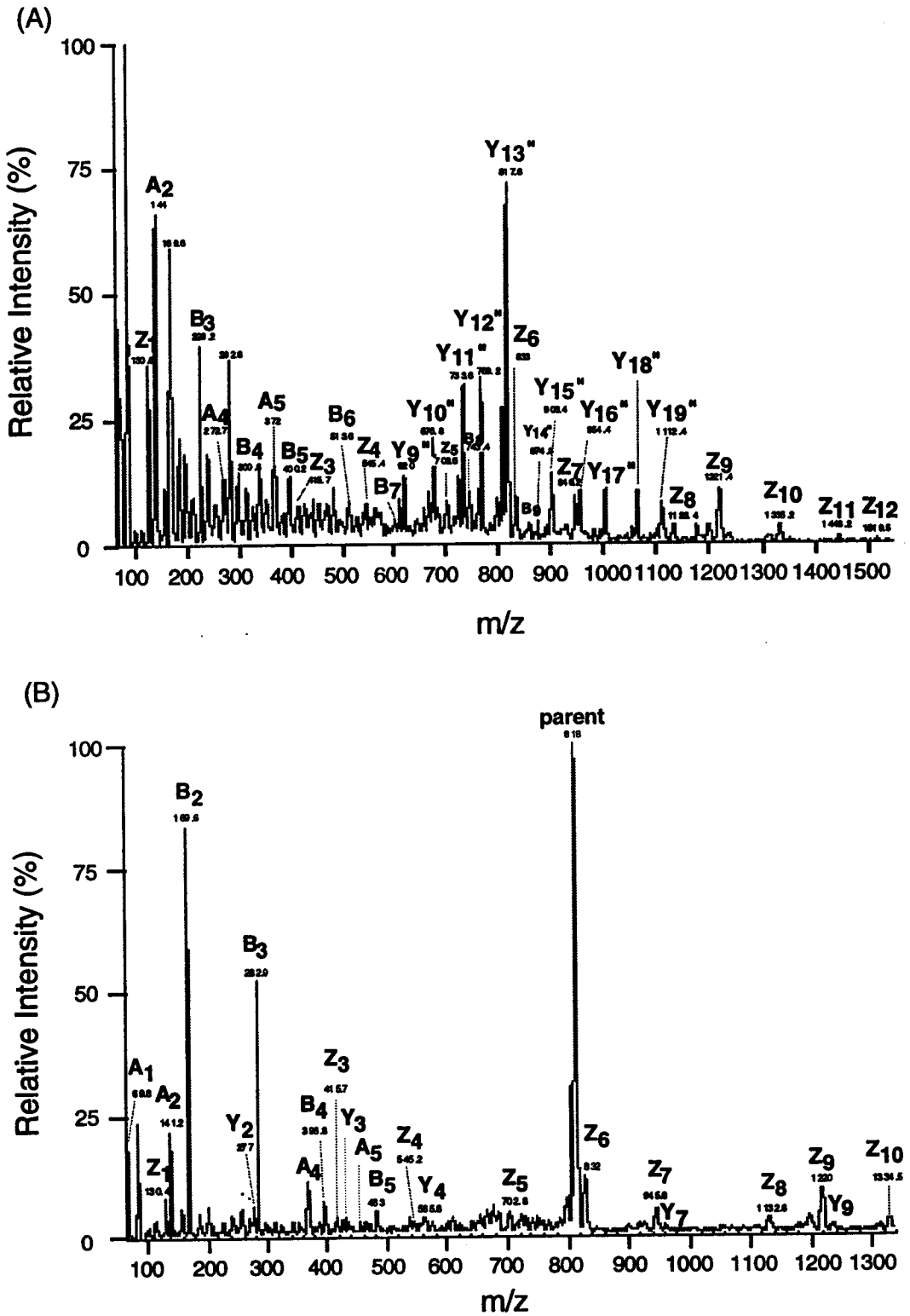

Figure II.1-22: Daughter-Ion Spectra of (A)+4-Charge State Molecular Ion (m/z 718, 80 V Orifice) and (B) Y_{13}^{+2} Fragment Ion (m/z 818, 120 V Orifice) of Fully Deuterated Melittin Using Microbore HPLC-ESIMS/MS Analysis at 0°C

To determine the time-dependent deuterium exchange-out from each amino acid residue of melittin, tandem mass spectrometric experiments were performed on the 4-charge state molecular ions and on the Y_{13}^{+2} fragment ions of deuterated melittin after 0 min-, 4 min-, 11 min- and 19 min-exchange. A-, B-, Y- and Z- series of fragment ions were produced from these two parent ions (**Figure II.1-22A, Figure II.1-22B**) for all four runs.

The mass shifts of the sequence-specific fragment ions were averaged and tabulated (**Table II.1-5, Table II.1-6**). In these tables, the observed m/z values of ions for normal protonated melittin, the calculated m/z values for the corresponding ions with fully deuterated peptide amides and other exchangeable hydrogens completely protonated, and the total number of peptide amides in the corresponding fragment ions are shown in the 2nd-, 3rd- and 4th-columns, respectively. The number of remaining peptide amide deuteriums in each fragment ion after 0 min-, 4 min-, 11 min- and 19 min-exchange, was calculated and are shown in columns 5 through 8. The A- and B-ions from the +4-charge state molecular ions of fully deuterated melittin (t=0 min) showed acceptable values for the remaining peptide amide deuteriums. However the composition of the Y- (Y_9^{+2}-Y_{11}^{+2}) and Z-ions (Z_1-Z_{11}) reflected larger values than the total number of peptide amide deuteriums available in the corresponding ions even under the slow exchange conditions used for their analyses (**Table II.1-5**). The A- and B-ions from the Y_{13}^{+2} ions of the fully deuterated melittin (t=0 min) also showed acceptable values for the remaining peptide amide deuteriums, but the Y- (Y_2-Y_4) and Z-ions (Z_1-Z_{10}) also reflected larger values than the total number of peptide amide deuteriums available in the ions. The data after 4 min, 11 min and 19 min under deuterium exchange-out conditions, however, showed much smaller numbers of amide deuterium labels left. Therefore, these data can be used to locate the deuterium

exchange-out in each amino acid residue and to follow the unfolding of the original α-helices in melittin.

Table II.1-5: Observed Sequence Ions from Collision-Induced Dissociation on +4-Charge State Molecular Ion of Fully Deuterated Melittin and Hydrogen Incorporation as a Function of Time

Ions	Protonated Mass (Observed) 0% ND	Deuterated Mass (Calculated) 100% ND	Number of Amide Deuteriums Remaining after a Time (min)				
			Total ND	0	4	11	19
(+1)							
A_2	143.2	144.2	1	0.8	0.3	0.1	0
A_4	271.0	274.0	3	1.7	0.8	0.6	0
A_5	369.9	373.9	4	2.1	1.1	0.6	-
B_3	228.0	230.0	2	1.2	0.4	0.2	0
B_4	299.0	302.2	3	1.8	0.6	0.2	0
B_5	398.0	402.0	4	2.2	0.8	0.4	0
B_6	511.2	516.0	5	2.4	1.0	0.6	0
B_7	639.8	645.8	6	3.4	0.6	0.6	0
B_8	739.0	746.0	7	4.4	1.8	1.4	0.2
B_9	852.2	860.2	8	4.8	1.8	1.3	0.2
Z_1	129.0	129.0	0	1.6	0.6	0.4	0
Z_3	413.0	415.0	2	2.7	1.0	0.7	0.2
Z_4	541.2	544.2	3	4.2	1.8	1.5	0.6
Z_5	697.4	701.4	4	6.2	2.3	2.0	1.0
Z_6	825.8	830.8	5	7.2	3.2	3.0	1.3
Z_7	939.2	945.2	6	7.0	3.8	3.2	1.6
Z_8	1124.8	1131.8	7	8.6	4.0	3.8	1.8
Z_9	1212.2	1220.2	8	9.2	4.3	3.8	1.6
Z_{10}	1324.8	1333.8	9	10.4	4.7	4.0	1.6
Z_{11}	1437.9	1447.9	10	10.3	4.7	3.9	-
Z_{12}	1508.9	1519.9	11	10.6	4.6	4.1	-
(+2)							
Y_9	614.9	619.4	9	10.2	5.0	2.4	1.6
Y_{10}	671.4	676.4	10	10.8	5.2	2.6	1.8
Y_{11}	728.0	733.5	11	11.2	5.2	2.6	1.8
Y_{12}	763.5	769.5	12	11.4	5.4	2.4	2.0
Y_{13}	812.0	818.0	12	11.6	5.8	3.2	2.8
Y_{14}	868.5	875.0	13	12.6	4.8	3.0	2.6
Y_{15}	897.1	904.1	14	12.6	5.2	3.0	2.6
Y_{16}	947.6	955.1	15	13.6	6.0	3.6	2.8
Y_{17}	998.1	1006.1	16	15.4	6.4	3.8	2.6
Y_{18}	1054.6	1063.1	17	16.4	7.0	4.0	3.2
Y_{19}	1104.2	1113.2	18	16.4	7.4	3.6	3.2

Table II.1-6: Observed Sequence Ions from Collision-Induced Dissociation on Y_{13}^{+2} Fragment Ion of Fully Deuterated Melittin and Hydrogen Incorporation as a Function of Time

Ions	Protonated Mass (Observed) 0% ND	Deuterated Mass (Calculated) 100% ND	Number of Amide Deuteriums Remaining after a Time (min)				
			Total ND	0	4	11	19
(+1)							
A_1	69.8	69.8	0	0	0	0	0
A_2	140.9	141.9	1	0.3	0	0	0
A_4	367.3	370.2	3	1.7	0.3	0.3	0
A_5	454.3	458.2	4	1.1	0.4	0.1	0
B_2	168.8	169.8	1	0.8	0	0	0
B_3	282.0	284.0	2	0.9	0.1	0	0
B_4	395.3	398.3	3	1.5	0.3	0.1	0
B_5	481.9	485.9	4	1.1	0.3	0.1	0
Y_2	274.2	276.2	2	2.8	0	0	0
Y_3	430.2	433.2	3	3.4	1.1	0.7	0.2
Y_4	558.4	562.4	4	5.4	1.2	0.8	0.2
Y_7	955.6	962.6	7	6.2	1.9	1.7	0.8
Y_9	1228.8	1237.8	9	8.8	2.6	1.7	1.0
Z_1	128.9	128.9	0	1.5	0.1	0	0
Z_3	413.0	415.0	2	2.7	0.6	0.3	0.1
Z_4	541.3	544.3	3	3.9	1.4	0.7	0.4
Z_5	697.4	701.4	4	5.4	1.4	0.9	0.6
Z_6	825.5	830.5	5	6.5	1.5	0.9	0.6
Z_7	938.6	944.6	6	7.2	1.8	1.5	1.0
Z_8	1124.7	1131.7	7	8.1	2.0	1.5	1.2
Z_9	1211.7	1219.7	8	8.3	2.3	1.6	1.2
Z_{10}	1324.8	1333.8	9	9.7	2.5	1.7	1.2

The number of peptide amide deuteriums remaining within each amino acid residue was calculated (**Table III.1-11**) and plotted in **Figure II.1-23.** Large deviations in the number of remaining peptide deuteriums were shown at the C-terminal side residues of the fully deuterated melittin (**Figure II.1-23A**). But the deviations gradually decreased in the residues for 4 min-, 11 min- and 19 min-exchange time points (**Figure II.1-23B~Figure III.1-23D**). The overall trend of structural integrity in the α-helices is shown in **Figure II.1-23E.**

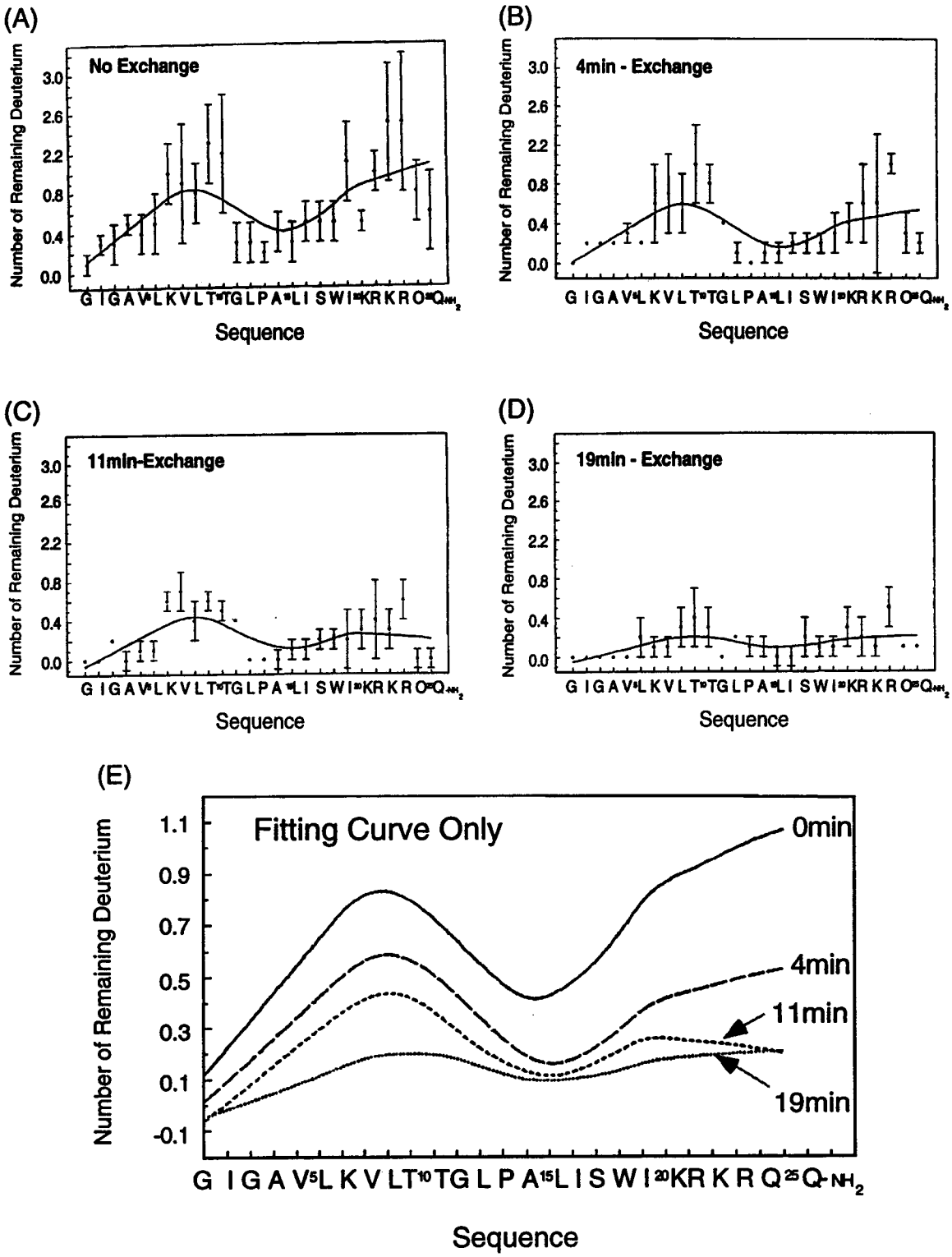

Figure II.1-23: Deuterium Exchange-Out at the Individual Amino Acid Residue of Fully Deuterated Melittin in MeOH/H_2O/AcOH (=80:20:2, pH 3.2) at 20°C Monitored by Microbore HPLC-ESIMS/MS at 0°C

From the results shown, it is clear that the α-helical region at the C-terminal end is less stable than that at the N-terminal side, which is the opposite result obtained by NMR studies and also by CF-ESIMS analysis (**Figure II.1-11E**). This discrepancy might be partially addressed by interactions between the reverse phase stationary column materials (C-8) and melittin during HPLC analysis, whereby the relatively more hydrophobic α-helix at the N-terminal side interacts more stronger with the column materials than the more hydrophilic α-helix at the C-terminal end. Because of this interaction, some deuteriums might be preserved better at the N-terminal side. Despite this discrepancy, the structural regions of the two α-helices in melittin could be roughly determined by the deuterium exchange-out from fully deuterated melittin using HPLC-ESIMS/MS analysis.

II. 2 H/D Exchange of Bovine Pancreatic Trypsin Inhibitor (BPTI)

II.2-1 Disulfide Folding Pathway of BPTI

The folding/unfolding pathway of bovine pancreatic trypsin inhibitor (BPTI)[21] has been extensively studied because its folding/unfolding is linked to disulfide bond formation/breakage and detailed information on the nature of folding/unfolding intermediates can be obtained by trapping the intermediates to produce a stable form.[52] Not only can the sulfhydryls that form specific disulfide bonds in the protein be trapped, but also the conformation of the protein can be effectively trapped because of the linkage relationship[53] between the disulfide bonds and the protein conformation that favors them. Whatever conformation favors formation of a particular disulfide bond must be favored to the same extent by the presence of the disulfide bond in the trapped intermediate.

Disulfide bond formation between two thiols occurs in two one-electron oxidation reaction requiring an oxidant such as molecular oxygen (**Figure II.2-1A**). Protein disulfide bond formation[54] results from a bimolecular thiol-disulfide exchange reaction (k_{ex}) that transfers oxidizing equivalents from a low molecular weight disulfide reagent to the protein. This transfer reaction produces a mixed disulfide intermediate which further reacts with the other sulfhydryl group nearby through an intramolecular thiol-mixed disulfide exchange process (k_{intra}) to form a protein disulfide bond (**Figure II.2-1B**). The intramolecular step (k_{intra}) is related to protein folding that involves protein conformational transitions which bring two sulfhydryl groups into proximity to form a disulfide bond. Thiol-disulfide exchange occurs via direct nucleophilic attack of thiolate anion of the thiol group on one of the sulfurs of the disulfide group.[55] The intrinsic pK_a values of

cysteine thiol groups are in the region of 8 to 9, so the rate of thiol-disulfide exchange (k_{ex}) increases with increasing pH until the attacking thiol is in the thiolate anion form.

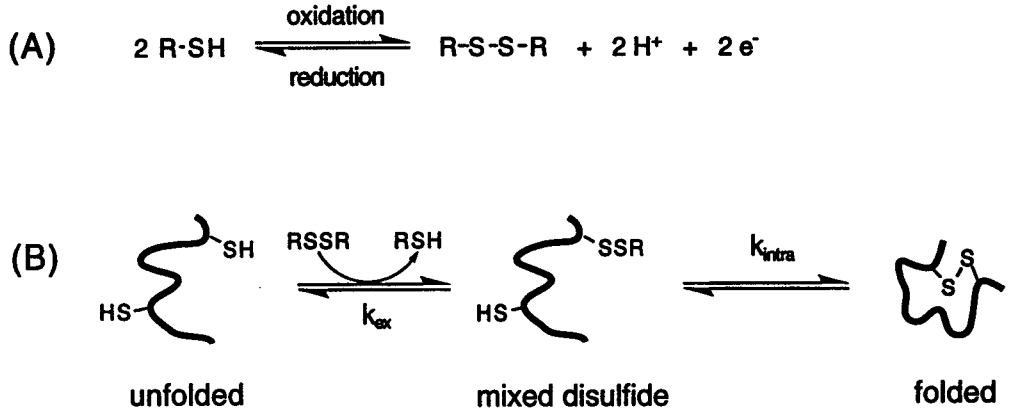

Figure II.2-1: Disulfide Formation and Cleavage

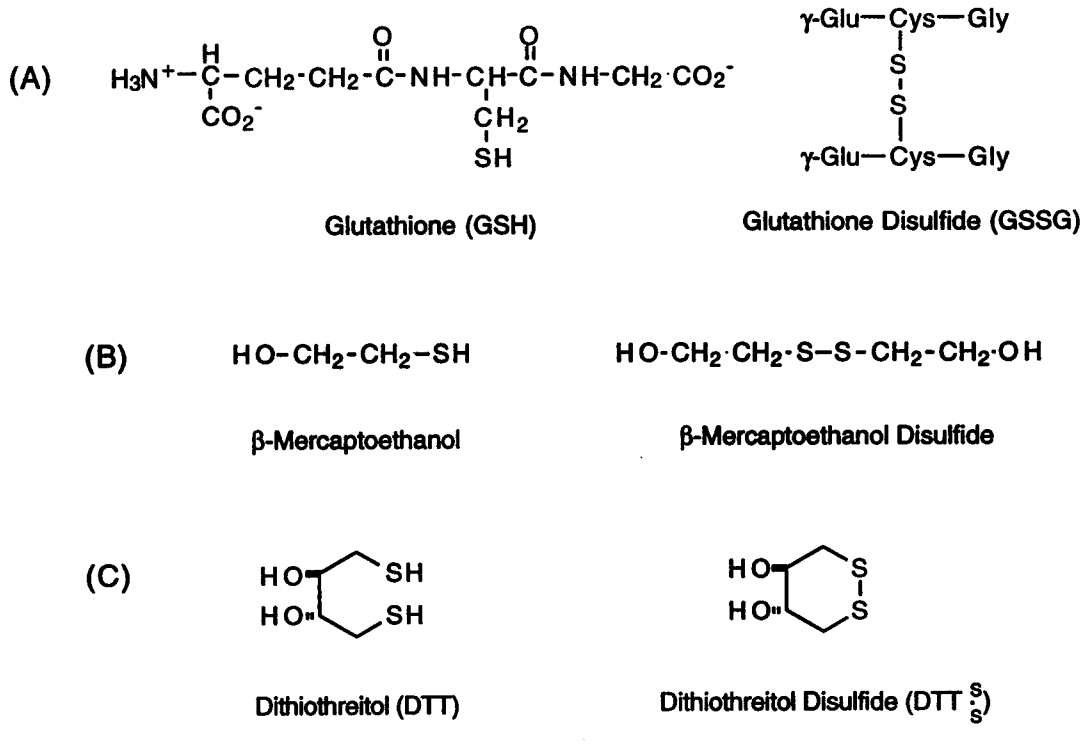

Figure II.2-2: (A,B) Intermolecular and (C) Intramolecular Disulfide Reagents

Two types of disulfide reagents are used for protein disulfide formation and cleavage (**Figure II.2-2**). One type consists of intermolecular reagents such as glutathione disulfide (GSSG; **Figure II.2-2A**) and mercaptoethanol disulfide (**Figure II.2-2B**) which results from disulfide bond formation between the two corresponding molecules. The other type is an intramolecular reagent where the disulfide bond is formed by two thiol groups in the same molecule as in dithiothreitol disulfide ($^{DTT^S_S}$; **II.2-2C**) which is very stable.

Creighton and coworkers[21a, 21b] have been actively studying the oxidative folding pathway of BPTI by trapping all free sulfhydryl groups in the folding intermediates by alkylation with iodoacetic acid or iodoacetamide. The alkylation reaction is fast, irreversible and very specific. It works under basic conditions (pH 8-9) because the reactive species are the thiolate anions of the sulfhydryl groups. Alkylation of free sulfhydryl groups is much faster than many of the intermolecular thiol-disulfide exchange reactions that take place during oxidative folding. Under these basic conditions however, intramolecular disulfide bond rearrangements (disulfide shuffling) which interconvert intermediates of the same oxidation state, are comparable in rate to, or even faster than, the rate of the alkylation reaction, especially when the access of the alkylating reagents is limited by conformational restrictions in the protein. The conformationally restricted and inaccessible thiols cannot be trapped effectively by alkylation and, therefore, their populations can be easily underestimated.

The other method for preventing thiol-disulfide exchange, is to add acid to the medium to lower the pH below 2.[21c] Acid quenching occurs very rapidly at a diffusion controlled rate and is not limited by steric inaccessibility. It provides an advantage over alkylation in that the intermediates trapped at low pH can subsequently be examined at high pH to define the kinetic roles of specific disulfide bonds more directly. However, it is a reversible process that does not

completely arrest thiol-disulfide exchange. Therefore, samples must be analyzed promptly after rapid acid quenching.

The oxidative folding mechanism of BPTI[21] is depicted below where the intermediates are designated by the numbers of the cysteine residues that are paired as disulfide bonds. The fully reduced BPTI and the native BPTI are represented as **N** and **R**, respectively (**Figure II.2-3**). The boxed intermediates at both one- and two-disulfide oxidation states are in equilibrium under most folding conditions.

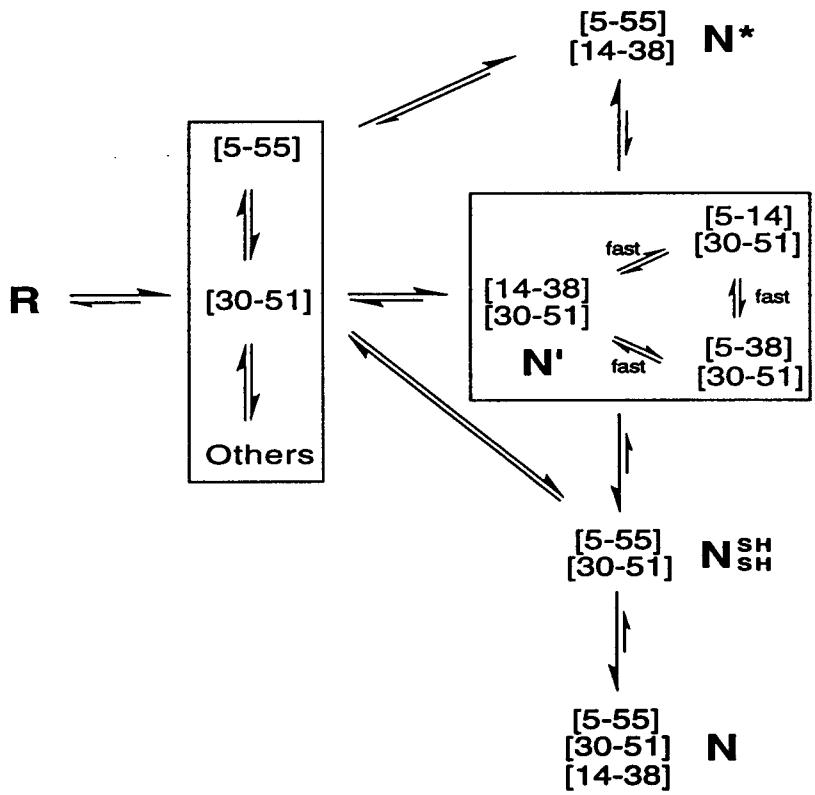

Figure II.2-3: Oxidative Folding Mechanism of BPTI

The number of intermediates observed during the folding pathway is relatively large suggesting that oxidative folding is not a simple, sequential formation of

native disulfides in BPTI. Weissman and Kim[21c] observed that after acid quenching at least eight disulfide-bonded species existed in the course of the oxidative folding pathway, including two non-native disulfide-bonded species ([5-14:30-51], [5-38:30-51]). These were originally reported by Creighton[21a, 21b] who used the alkylation method to trap these species. The native disulfide-bonded species predominated at each oxidation stage. The eight intermediates were stabilized by specific, native or non-native interactions during the course of folding. One of the doubly disulfide-bonded intermediates ([5-55]:[30-51], N^{SH}_{SH}) was the only intermediate which could proceed through a productive pathway toward native BPTI. It's structure is known to be almost identical to that of native BPTI.[21] But the stability of this intermediate was found to be much lower because of the absence of the third disulfide bond between C14-C38. The doubly disulfide-bonded intermediate with disulfide bonds between C5-C55 and C14-C38 (**N***) goes through a non-productive pathway and accumulates in the folding mixture. This intermediate has two cysteine residues at C30 and C51 which are not within range for a disulfide bond because of the conformational restrictions. This intermediate, therefore, cannot directly produce the third disulfide bond (C30-C51). But it does fold into the native BPTI through conformational rearrangements giving non-native intermediates, which are energetically unfavorable and slow processing. Native BPTI completely loses its folded conformation when the three disulfide bonds are reduced. It refolds by reforming these disulfide bonds in the presence of a disulfide reagent and it's reduced thiol form ($GSSG/GS^-$) in an appropriate ratio. In the one-disulfide oxidation state, all possible intermediates except the singly disulfide-bonded one with one disulfide bond at C14-C38 ([14-38]), are formed in rapid equilibrium. The major singly disulfide-bonded intermediates are those species with one disulfide bond at C30-C51 ([30-51]) and C5-C55 ([5-55]) in about 5:1 ratio for [30-

51]:[5-55]. These intermediates are stabilized by native-like interactions. In the doubly disulfide-bonded intermediates, the major species is [30-51]:[14-38] (**N'**) which is formed rapidly from the oxidation of the intermediate [30-51]. Intramolecular thiol-disulfide rearrangements convert the [30-51]:[14-38] (**N'**) via non-native intermediates ([5-14:30-51] and [5-38:30-51]) into the more stable doubly disulfide-bonded intermediates, [30-51]:[5-14] (N^{SH}_{SH}) and [5-55]:[14-38] (**N***).

II.2-2 H/D Exchange of BPTI in Combination with Protein Fragmentation-HPLC Separation-ESIMS and -ESIMS/MS

Previous H/D exchange experiments with melittin using microbore HPLC-ESIMS and HPLC-ESIMS/MS under slow exchange conditions for the analysis of hydrogen/deuterium content, have shown that these methods are useful for monitoring structural fluctuations in solution and determining their locations within the sequence of a small peptide. From a practical point of view, however, proteins have more complex three dimensional structures that change during the course of folding/unfolding pathways. This complexity is essential in living systems.

In our studies, H/D exchange in combination with protein fragmentation and HPLC separation-ESIMS and -ESIMS/MS for analysis have been used to observe and locate structural changes in the course of oxidative folding of bovine pancreatic trypsin inhibitor (BPTI) (**Strategy IV; Scheme II.2-1**).

Global structural changes of BPTI during the oxidative folding pathway can be obtained by monitoring molecular weight changes in the course of deuterium exchange-out from the deuterated proteins using microbore HPLC-ESIMS analysis under slow exchange conditions (pH 2-3, 0°C). Similar results can be

obtained using the continuous flow infusion-ESIMS for the analysis of the deuterium content in proteins under deuterium exchange-in conditions. The folding intermediates can be trapped in a stable form by alkylating free sulfhydryl groups with iodomethylacetamide. To locate the structural changes in the folding intermediates from the folding pathway, fully deuterated BPTI is dissolved in normal protic solvent to initiate the deuterium exchange-out process. After cleavage of the disulfide bonds by reduction (pH 2-4, 0°C, 5-10 min) or oxidation (pH 2-3, -20°C, 2 hr), the protein can be quickly digested with immobilized pepsin (pH 2.0, 0°C, 5 min). The peptic peptides, whose sequences are known, are analyzed by microbore HPLC-ESIMS/MS under slow exchange conditions to locate the deuteriums remaining at each amino acid residue. This method is highly dependent upon pepsin-digestion of BPTI under slow H/D exchange conditions because the undigested BPTI molecule is too large to obtain enough sequence-specific fragmentation ions by tandem mass spectrometry analysis.

This protein fragmentation-tandem mass spectrometric method was tested on native BPTI to follow H/D exchange, and to locate the sites of exchange by determining the deuterium content at each amino acid residue. From this information, the secondary structural elements in various regions of the protein could be determined. Before performing the H/D exchange experiments, all conditions were set up under normal non-deuterated solution conditions. To make BPTI digestible with pepsin, the three disulfide bonds (C5-C55, C14-C38, C30-C51) within native BPTI should be cleaved by reduction or oxidation in advance. Once the three disulfide bonds are broken, BPTI adopts a completely open structure which makes all buried residues in the native structure freely accessible to the protease and gives very reproducible peptic peptides from native BPTI.

Strategy IV

Monitoring Structural Changes During Disulfide Folding Pathway of Fully Reduced BPTI by H/D Exchange and Protein Fragmentation-HPLC-ESIMS and -HPLC-ESIMS/MS

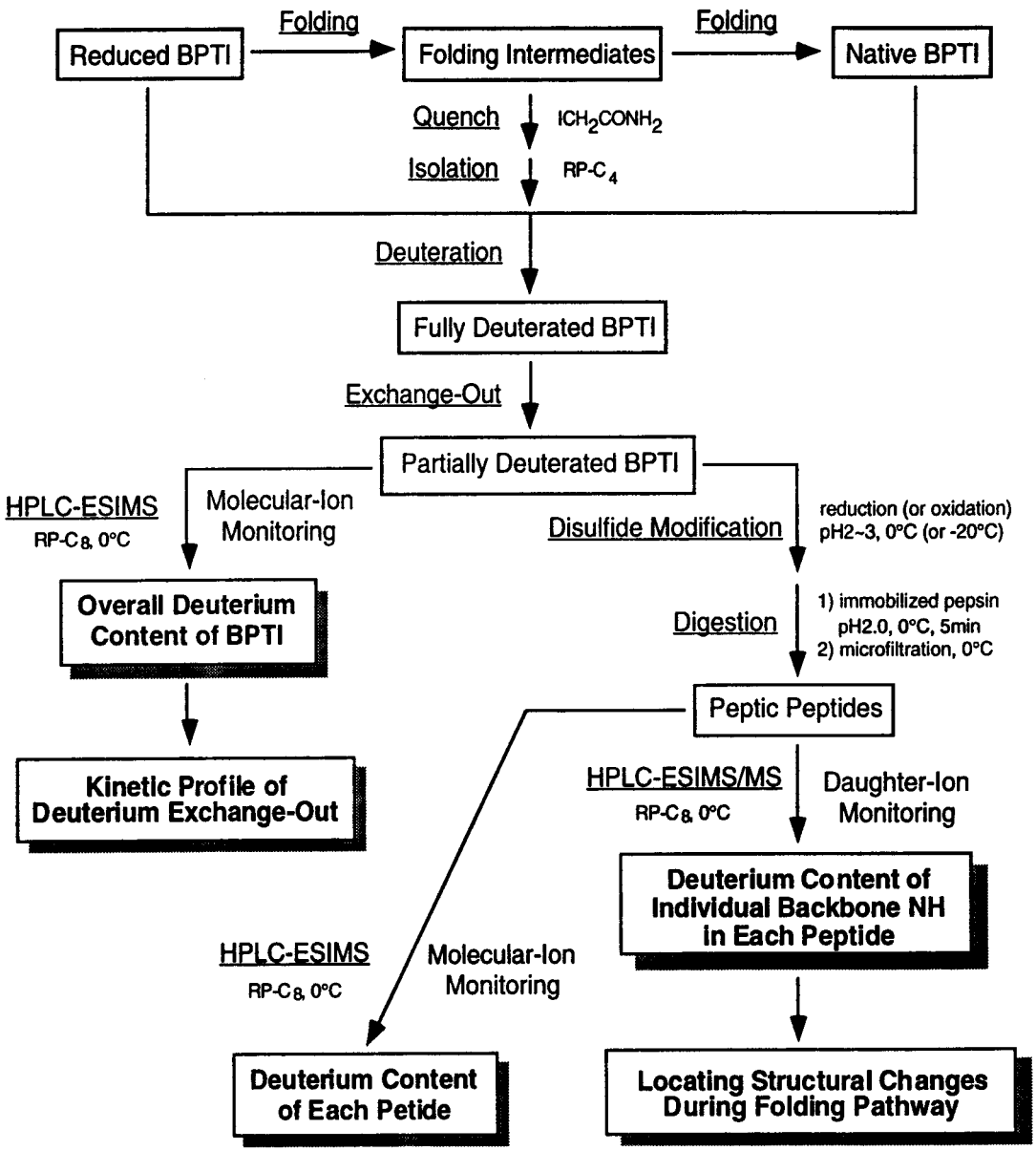

Scheme II.2-1: Strategy IV

II.2-3 Reduction of BPTI

II.2-3-1 Reduction of Native BPTI

Disulfide bond reduction of native BPTI was studied under slow H/D exchange conditions (pH 2-3, 0°C, a short period of time) where disulfide bond shuffling is largely suppressed and loss of deuterium labels is minimized. The disulfide bond at C14-C38[20] is located at the molecular surface so that it is easily accessible to reductant and alkylating reagent. The other two disulfide bonds, however, are buried in the core structural region of BPTI[20] so that they are completely inaccessible to the reacting agents. Tris-(2-carboxyethyl)-phosphine hydrochloride salt (TCEP·HCl)[22] was tested as a reducing agent under non-exchange conditions. TCEP·HCl is a water-soluble reductant that selectively reduces disulfides into thiols even under acidic conditions (pH ≥ 2.0) and commercially available. The rate of reduction of native BPTI with TCEP·HCl, however, was found to be highly pH-dependent. The native protein was completely resistant to an excess of TCEP·HCl under the conditions of pH < 3.0 at 0°C with or without denaturants such as urea (up to 8 M) and acetonitrile (up to 40 %). At pH ≥ 3.0 and 0°C, only partial reduction occurred which caused the reduction of one disulfide bond (C14-C38) (**Figure II.2-4B**). Completely reduced BPTI was obtained only under the most stringent reduction conditions for example; TCEP·HCl (100 fold molar excess, pH 3.0, 70°C, 10 min)[22a] or DL-dithiothreitol (DTT, 120 fold molar excess, pH 8.5, 39°C, 30 min)[56] (**Figure II.2-4C, Figure II.2-4D**). TCEP-reduction of native BPTI was also tried at ambient temperature (up to pH 4.5) but only partially reduced BPTI was obtained. The same partially reduced BPTI with disulfide cleavage at C14-C38[57] was also

obtained by selective reduction of the native structure using DTT (25 fold molar excess) in 0.1 M Tris-HCl buffer (pH 8.2, 20°C, 2 min).

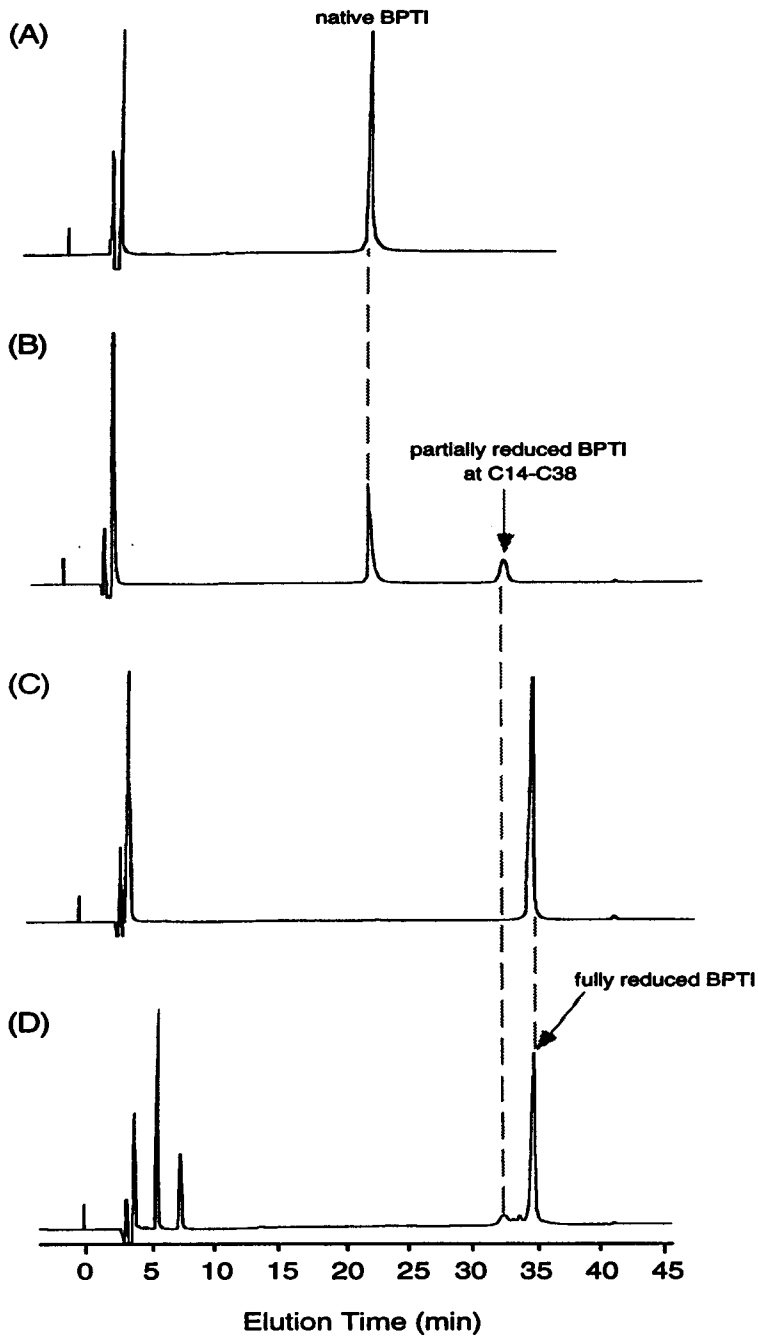

Figure II.2-4: HPLC-Chromatograms of (A) Native BPTI, (B) Partially Reduced BPTI in C14-C38 Disulfide with TCEP·HCl, (C) Completely Reduced BPTI with TCEP·HCl and (D) Completely Reduced BPTI with DTT

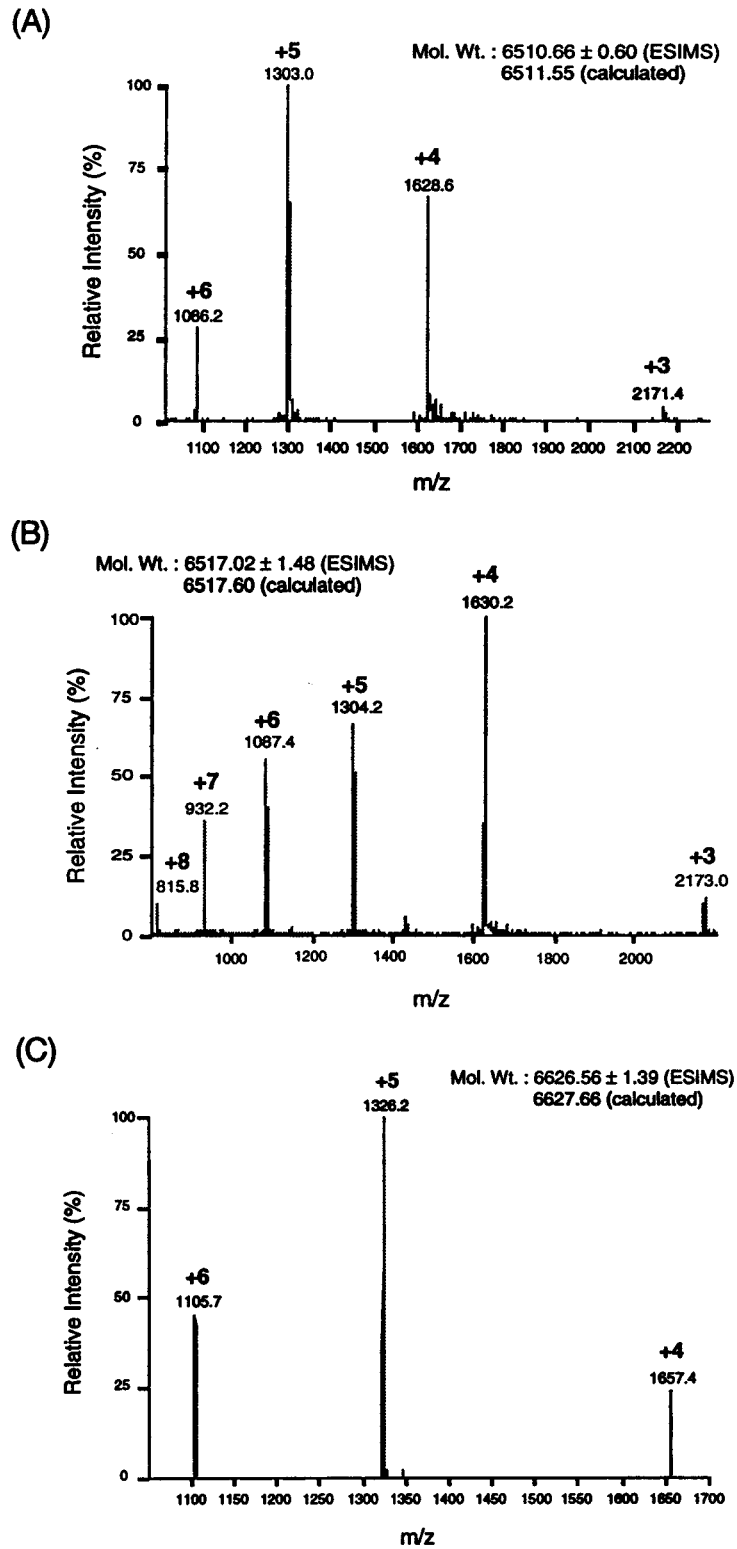

Figure II.2-5: Microbore HPLC-Ionspray Mass Spectra of (A) Native BPTI, (B) Fully Reduced BPTI and (C) Partially Reduced and Carboxyamidomethylated BPTI at C14 and C38

Microbore HPLC-ESIMS of native BPTI, of fully reduced BPTI, and of partially reduced and carboxyamidomethylated BPTI at C14 and C38, (CAM(14,38)-BPTI) yielded molecular weights of 6511 Da, 6517 Da and 6627 Da, respectively (**Figure II.2-5**). It is well known that the maximum charge state among molecular ions and the charge state distribution of molecular ions which are observed in mass spectra of proteins, can be related to the structural compactness of the protein.[16, 58] For proteins with completely open structures (denatured proteins), the maximum charge state of molecular ions observable in mass spectra correlates well with the total number of basic amino acid residues available (Arg, Lys, His) plus 1 (N-terminus) under the positive-ion detection mode and with a total number of acidic amino acid residues (Asp, Glu) plus 1 (C-terminus) under the negative-ion detection mode. However, these correlations do not work for proteins which have complex higher-order structures because these molecules normally have ionizable amino acid residues buried in structural regions where these residues are not freely accessible to the ionizing medium. The charge state distributions of molecular ions in mass spectra of proteins, however, have been shown to be dependent on the overall structure of the protein. Generally, compact-structured proteins have narrower distributions of multiple charge states and a lower weighted average values (A_W) of charge states than the corresponding open-structured proteins. The mass spectra of native BPTI (+6 ~+3, A_W=+4.84) and CAM(14,38)-BPTI (+6 ~+4, A_W=+5.07) showed relatively narrower distributions of molecular ions and lower weighted average values (A_W) than reduced BPTI (+8 ~+3, A_W=+5.11). This indicates that native BPTI has the most compact structure, CAM(14,38)-BPTI has a little less compact structure and reduced BPTI has the least compact structure. These result were very comparable to the H/D exchange behavior (**Figure II.2-30**) and CD spectra (**Figure II.2-31**) observed for these molecules.

Other reduction methods that were tested, included Zn/HCl or Zn/AcOH[59] with or without denaturants (pH 2.0, 0°C or 20°C, up to 30 min) and $NaBH_3CN$/AcOH[60] with or without EtOH (pH 2.0, 20°C, up to 30 min), but these reagents failed to reduce the disulfide bonds and only native BPTI was isolated. All these results clearly showed that the native disulfides, especially at C5-C55 and C30-C51 could not be cleaved under these reducing conditions (pH 2-3, 0°C, short time period).

II.2-3-2 Pepsin Digestion of Fully Reduced BPTI

Proteolytic digestion of native BPTI with an immobilized pepsin gel at a weight ratio of enzyme to substrate E/S=5 under slow H/D exchange conditions (pH 2.0, 0°C, up to 30 min) with or without 2M urea failed to give any peptic peptides. However, fully reduced BPTI was completely digested yielding several overlapping small peptides under these same conditions (E/S=5, pH 2.0, 0°C, 5 min). Peptic peptides from fully reduced BPTI were isolated and identified by peptide-mapping and the peptide-sequencing procedures (**Scheme II.2-2**).

The immobilized pepsin gel turned out to be very handy for fast digestions and for obtaining the peptic peptides with minimum contamination from pepsin autoproteolysis. The digestion was quenched simply by microfiltration of the reaction mixture over a microcentrifuge tube having a filter unit inside. From the peptic digest, a total of 15 peptides (**Table III.2-1**) were identified using matrix assisted laser desorption/ionization-time of flight mass spectrometry (MALDI-TOFMS), fast atom bombardment mass spectrometry (FABMS), ESIMS, ESIMS/MS and on-line microbore HPLC-ESIMS as well as off-line analytical HPLC (**Scheme II.2-2**).

Strategy V

Peptide Mapping and Sequencing of Fully Reduced BPTI

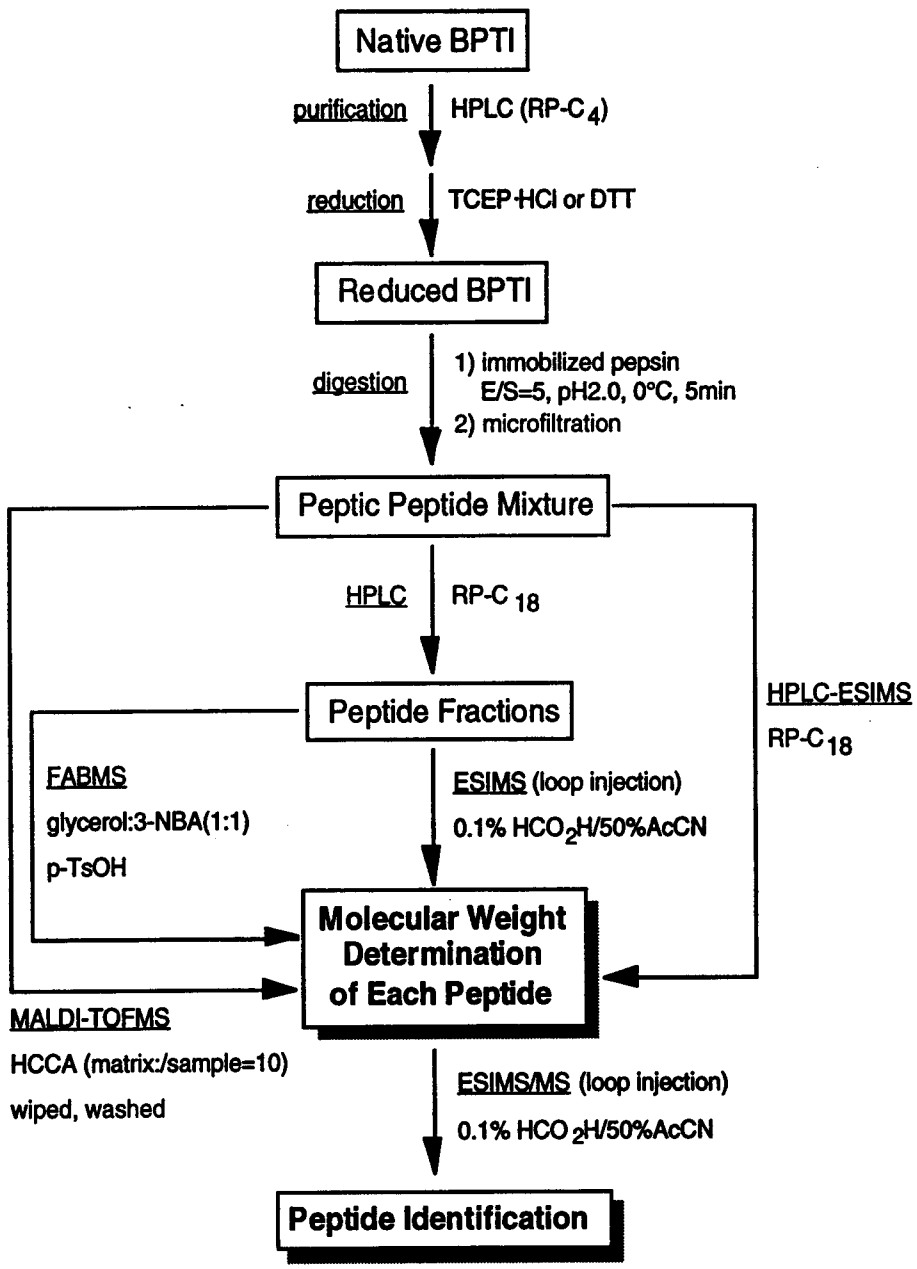

Scheme II.2-2: Strategy V

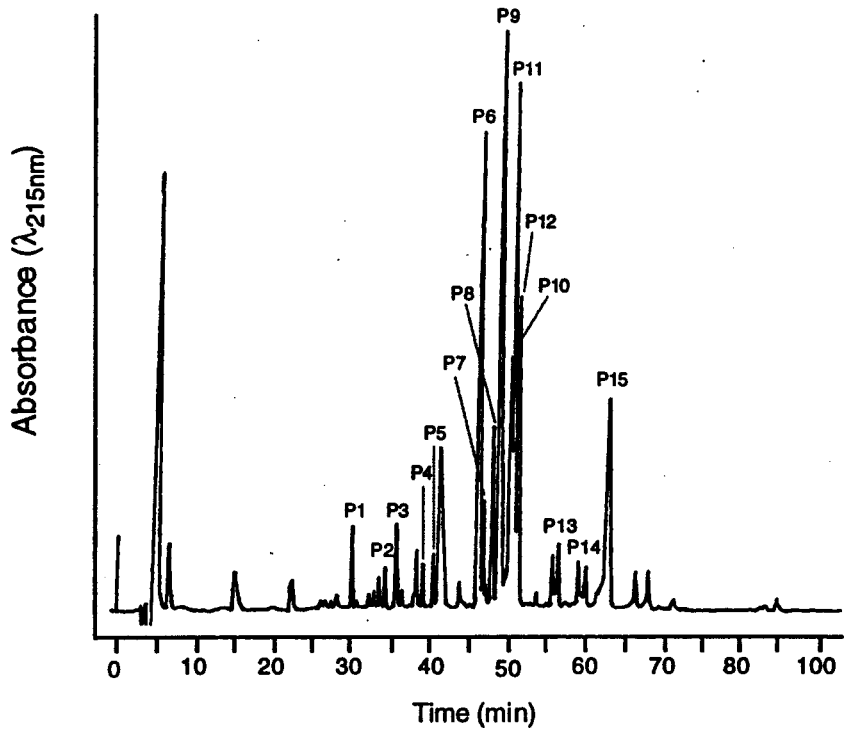

Figure II.2-6: HPLC Chromatogram (RP-C18) of Peptic Digest from Fully Reduced BPTI

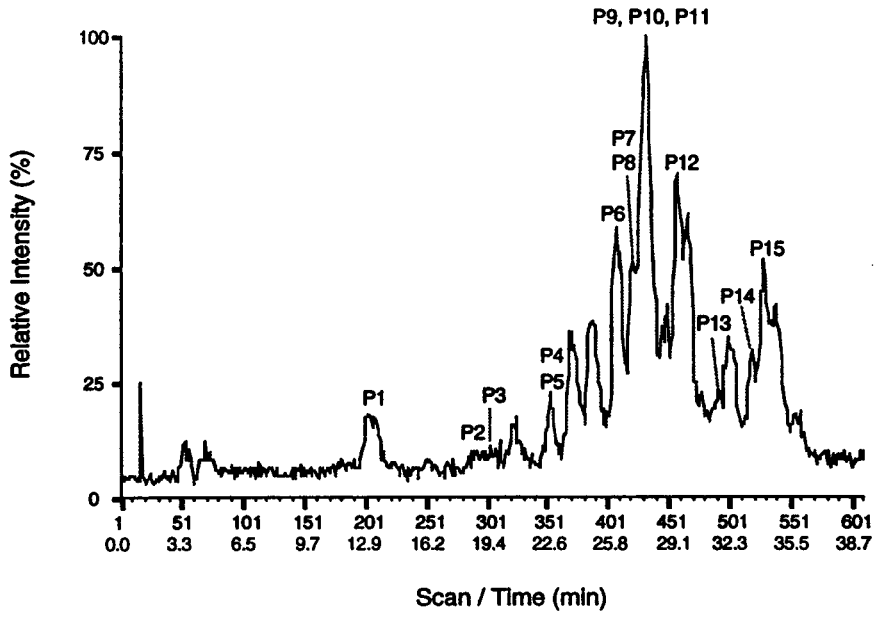

Figure II.2-7: Total Ion Chromatogram of Peptic Digest from Fully Reduced BPTI by Microbore HPLC-ESIMS Analysis at 0°C (RP-C8)

The peptic digest from fully reduced BPTI was separated by reverse phase C-18 column chromatography (**Figure II.2-6**). The total ion chromatogram of this digest was obtained using microbore HPLC-ESIMS analysis under slow H/D exchange conditions (pH 1-2, 0°C). Fifteen peptides were determined to be present (**Figure II.2-7**, **Table III.2-1**). The digest was loaded into an injection loop in which a tiny reverse phase desalting cartridge was inserted, and separated by elution through a reverse phase C_8 column (1 mm ID x 150 mm length) at 0°C. The desalting loop was used to prewash the sample mixture with 2 % AcCN/H_2O to remove most of the buffer salts and denaturants while the peptides were still adsorbed onto the tiny reverse phase column material in the cartridge. By using this desalting loop, the detection sensitivities for the peptides was increased.

MALDI-TOF mass spectra of the digest showed nine peptide peaks (P1, P6, P7, P8, P9, P10, P11, P12 and P15, **Figure II.2-8**). The peptide map of this digest is shown in **Figure II.2-10**. Ionspray mass spectra and daughter-ion spectra of the 7 major peptide are shown in **Figure II.2-10 ~ Figure II.2-16**. The observed mass values for the daughter ions of these peptides are shown in **Table III.2-2 ~ Table III.2-8**.

Pepsin digestion of fully reduced BPTI gave very reproducible peptides under slow H/D exchange conditions (E/S=5, pH 2.0, 0°C, 5 min). In seven major peptides (**P6**, **P8**, **P9**, **P10**, **P11**, **P12** and **P15**) identified, peptide bonds were cleaved at the sites before and after phenylalanine residues as well as at the C-terminal side of alanine and glutamic acid residues. It has been known that the alanine residue is not a cleavage site for pepsin[61]. In our experiments, however, the C-terminal side of alanine was easily cleaved by the immobilized pepsin which gave 5 peptides including **P6**, **P7**, **P11**, **P14** and **P15**.

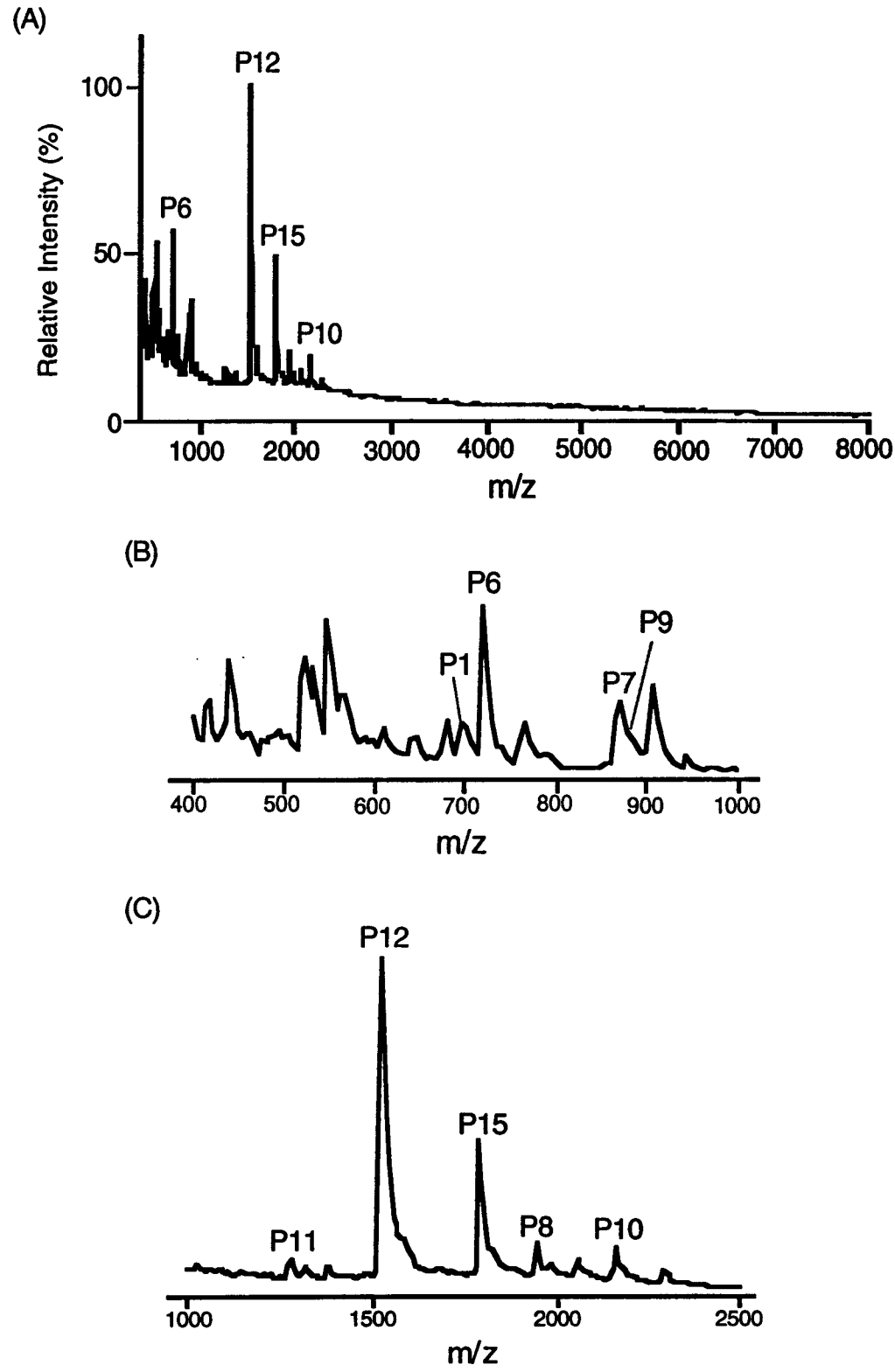

Figure II. 2-8: MALDI-TOF Mass Spectrum of (A) Peptic Digest from Fully Reduced BPTI and (B, C) Extended Spectra

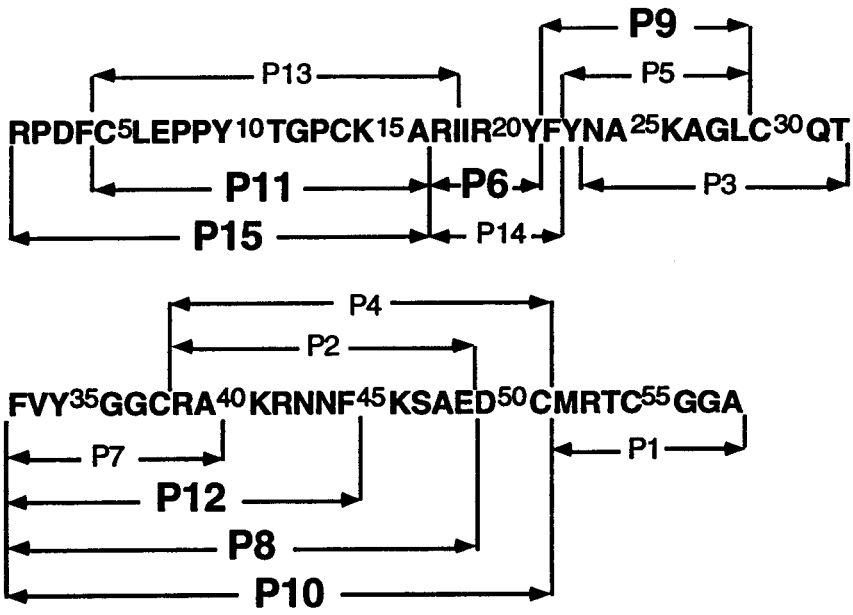

Figure II.2-9: Peptide Map of Peptic Digest from Fully Reduced BPTI with Seven Major Peptides of P6, P8, P9, P10, P11, P12 and P15

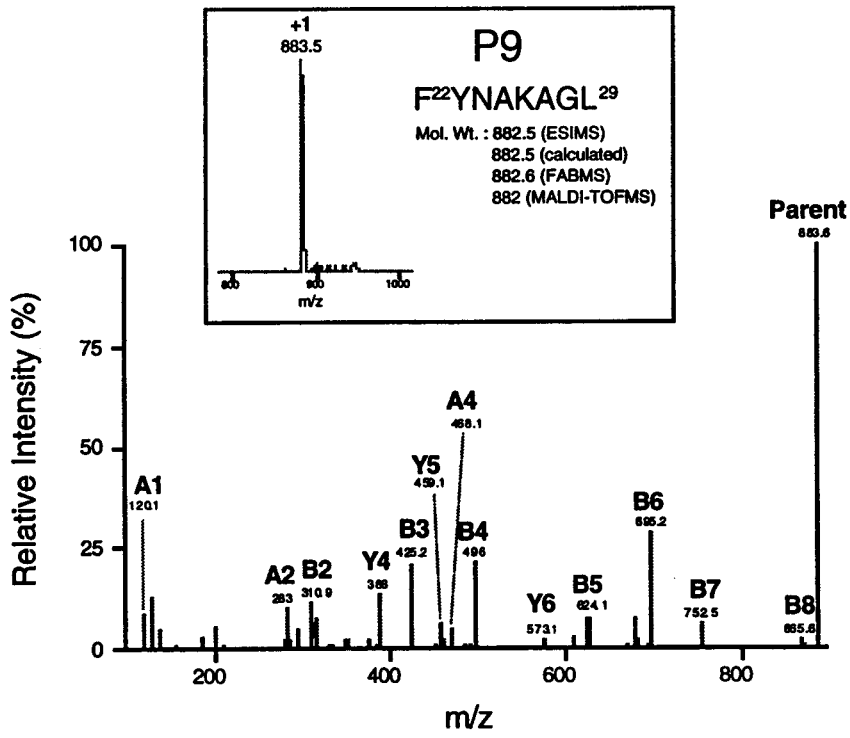

Figure II.2-10: Ionspray Mass Spectrum (Insert) and Daughter-Ion Spectrum (Parent Ion; m/z 884) of Peptide 9

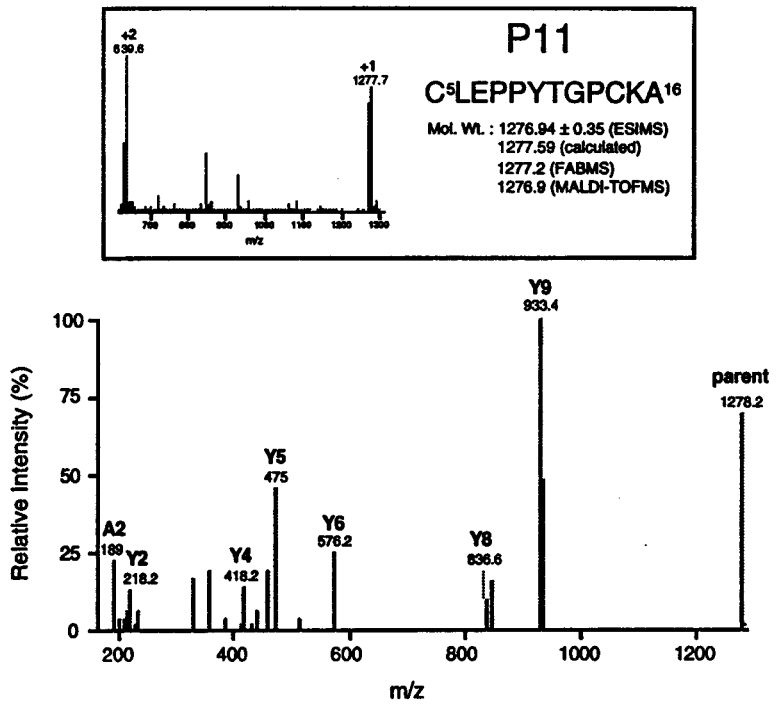

Figure II.2-11: Ionspray Mass Spectrum (Insert) and Daughter-Ion Spectrum (Parent Ion; m/z 1279) of Peptide 11

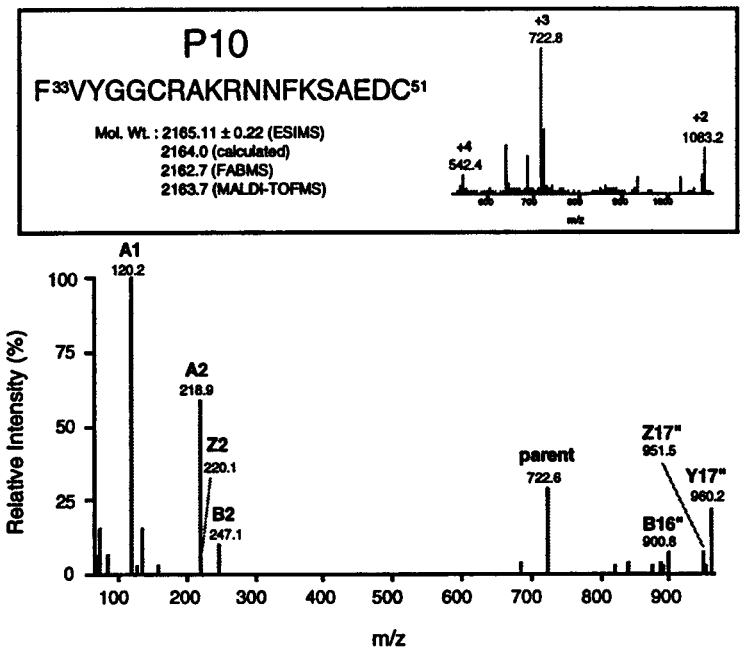

Figure II.2-12: Ionspray Mass Spectrum (Insert) and Daughter-Ion Spectrum (Parent Ion; m/z 723) of Peptide 10

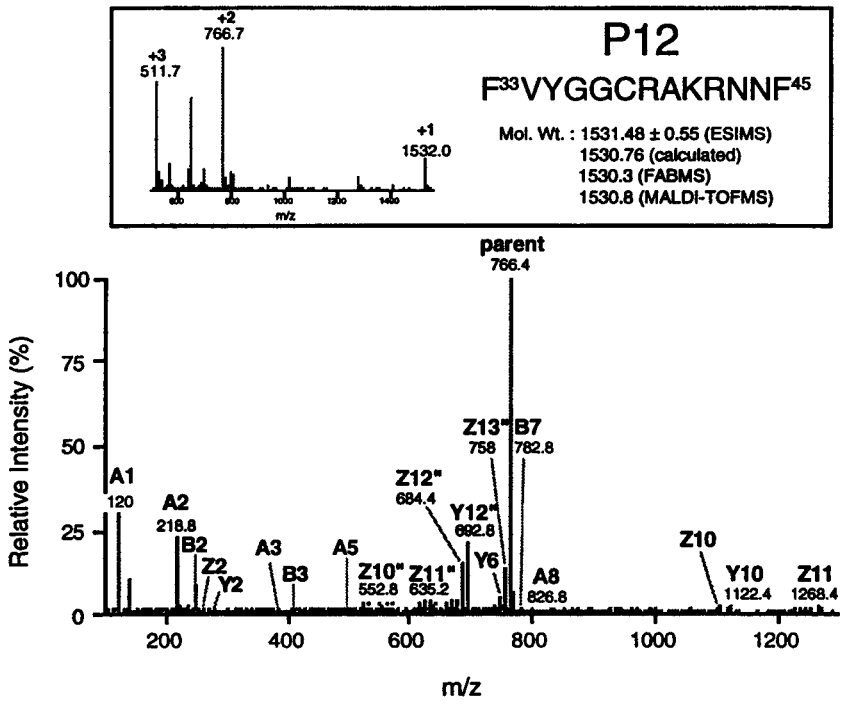

Figure II.2-13: Ionspray Mass Spectrum (Insert) and Daughter-Ion Spectrum (Parent Ion; m/z 767) of Peptide 12

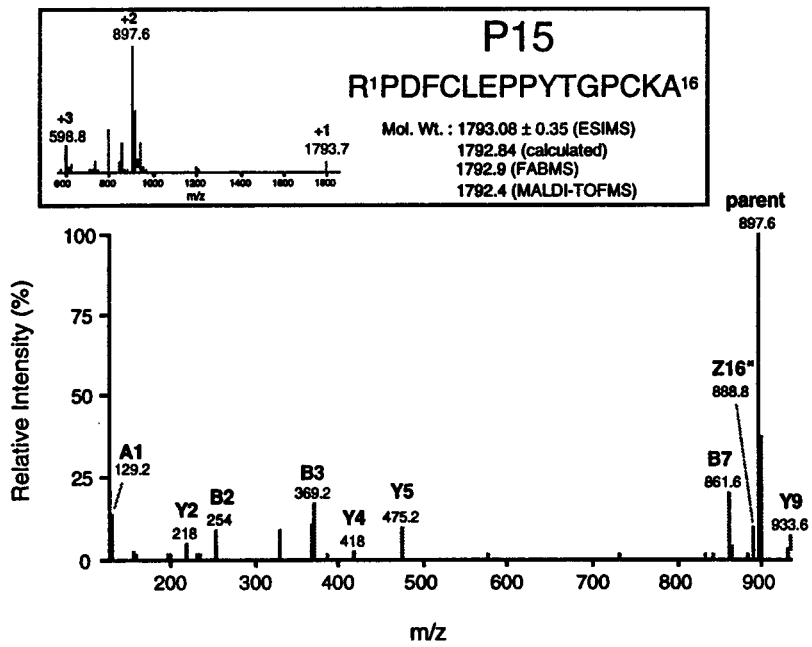

Figure II.2-14: Ionspray Mass Spectrum (Insert) and Daughter-Ion Spectrum (Parent Ion; m/z 898) of Peptide 15

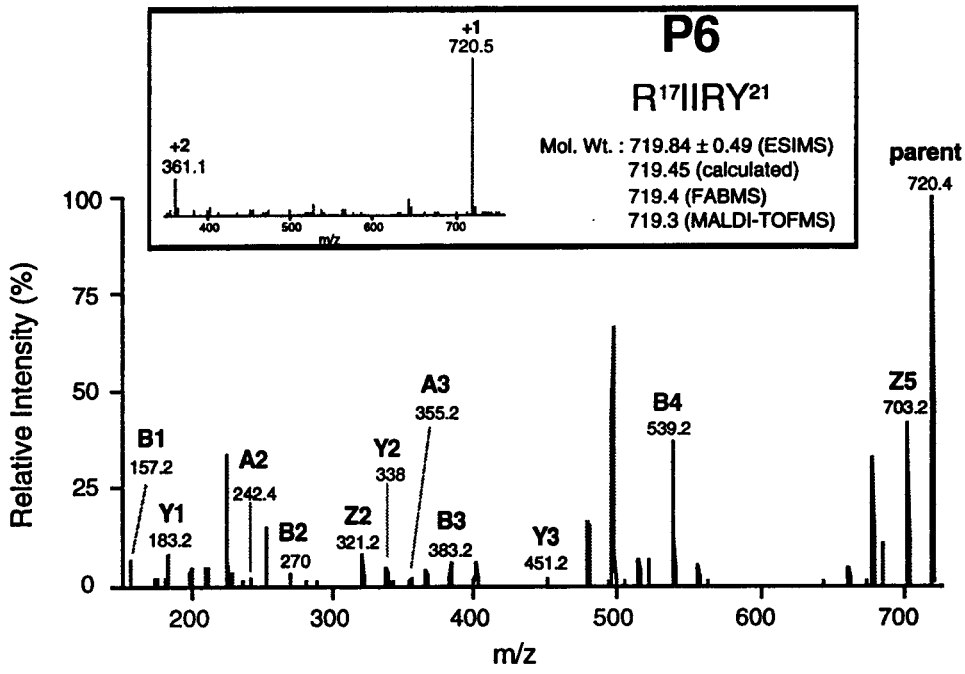

Figure II.2-15: Ionspray Mass Spectrum (Insert) and Daughter-Ion Spectrum (Parent Ion; m/z 720) of Peptide 6

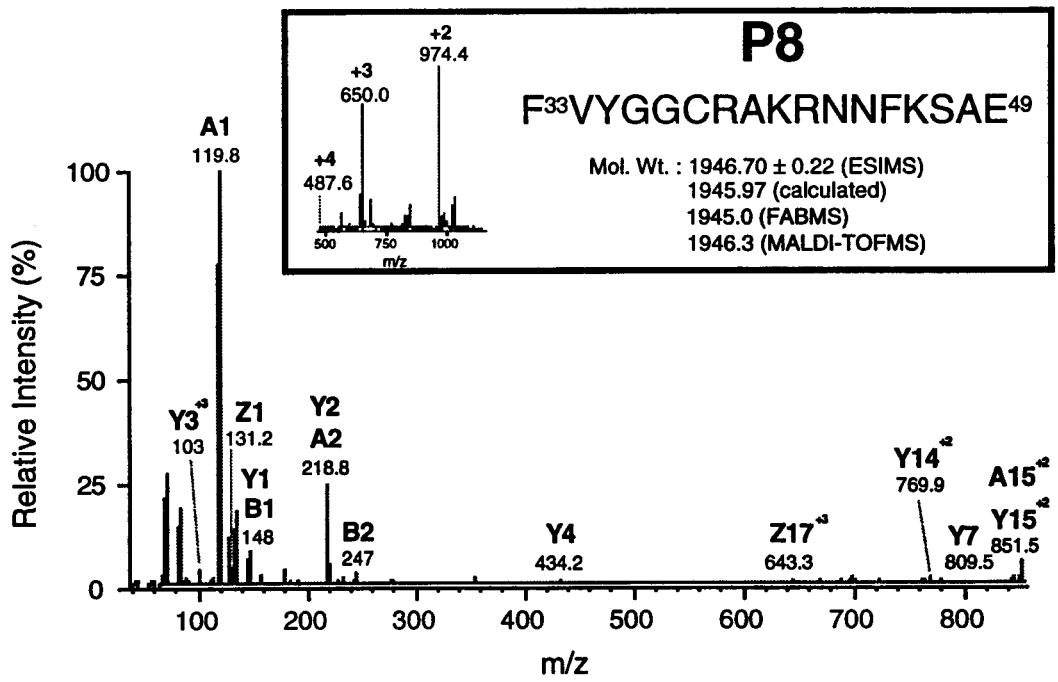

Figure II.2-16: Ionspray Mass Spectrum (Insert) and Daughter-Ion Spectrum (Parent Ion; m/z 650) of Peptide 8

II.2-4 Performic Acid Oxidation of BPTI

II.2-4-1 Performic Acid Oxidation of Peptides and Proteins

Cleavage of disulfide bonds by oxidation with performic acid has been used in protein chemistry as a standard technique since the advent of Sanger's sequencing method.[62] The oxidizing reagent[23] is obtained by mixing formic acid and 30 % hydrogen peroxide, usually in a volume ratio of 95 to 5 at room temperature for 2.5 hours (**Figure II.2-17A**). Performic acid oxidation transforms thiols and disulfide groups into sulfonic acid functionalities, which results in a stable oxidation state (**Figure II.2-17B, -17C**). The methyl sulfide group of methionine residues is oxidized to methyl sulfones (**Figure II.2-17D**).

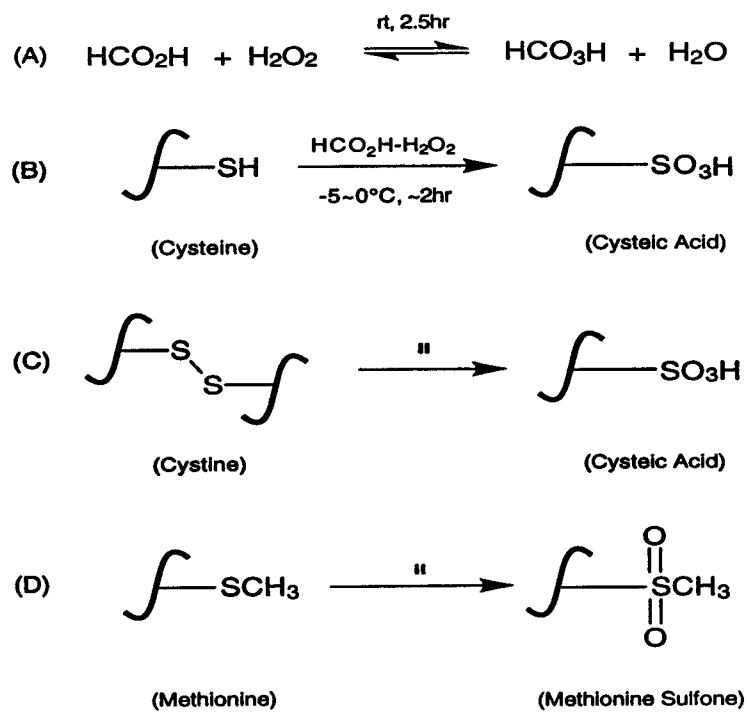

Figure II.2-17: (A) Formation of Performic Acid Reagent and Oxidation of (B) Thiol, (C) Disulfide and (D) Methyl Sulfide Group

These oxidation products of sulfur-containing amino acid residues are stable and allow accurate information from amino acid analysis. The oxidation of disulfides can occur by one of the following pathways[63] (**Figure II.2-18**). In pathways (A) or (B), the disulfide bond is split and the final product mixture consists of 2 moles of sulfonic acid per mole of disulfide precursor. Pathway (C) proceeds by scission of the C-S bond and formation of equimolar quantities of sulfonic acid and sulfuric acid.

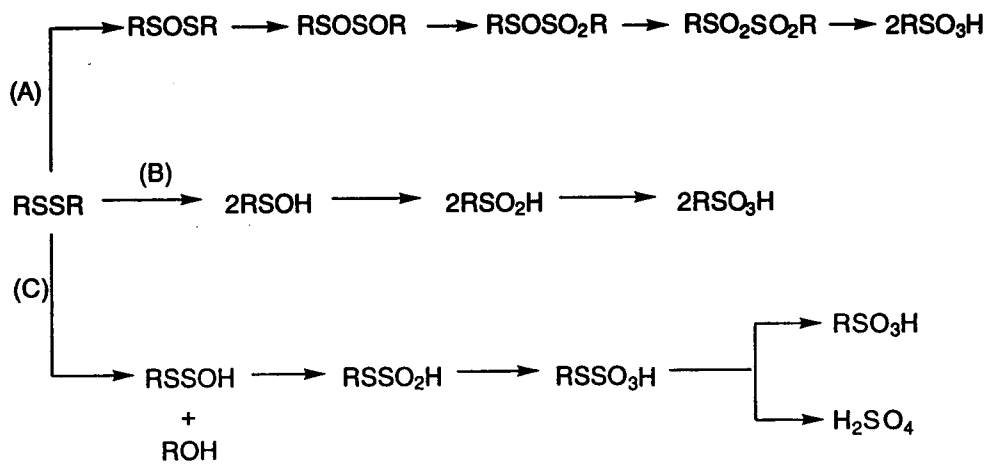

Figure II.2-18: Oxidative Cleavage Pathways of Disulfide Bond

This oxidation method,[23] however, has a significant drawback in that the indole ring of the tryptophan residue is opened and several derivatives, including N-formylkynurenine, are formed. All attempts to minimize indole ring opening and to obtain oxidation products in constant proportion, have been fruitless. Because this oxidizing agent is extremely potent, other functional groups can also be oxidized. It will oxidize the aromatic group of phenylalanine residue and the hydroxy groups of serine and threonine residues. However, the oxidation of cysteine to cysteic acid and of methionine to methionine sulfoxide

are the most rapid reactions. Transformation of cystine to cysteic acid and methionine sulfoxide to methionine sulfone are somewhat slower, which occur in comparable rate at which the indole ring is attacked. The oxidation of tyrosine occurs much less readily. The oxidations of serine and threonine require very drastic conditions. Conversion yield of cystine to cysteic acid is in the range of 85-90% whereas methionine converts to the corresponding sulfone quantitatively. Another complex situation occurs when halide ions are present in the oxidation mixture. Due to the strong oxidizing ability of the oxidant, the halide ions are converted to the corresponding halogens which attack the aromatic ring of the tyrosine residues and give a mixture of mono- and di-haloaromatic compounds by electrophilic aromatic substitution reactions. Even a trace amount of halide ion present in commercially available buffer salts can give these side products.

The reaction with performic acid is usually quenched under mild conditions using reducing reagents such as ascorbic acid, sulfide or sodium sulfite. Alternatively, the oxidation mixture may be diluted with water and subjected to lyophilization.

II.2-4-2 Performic Acid Oxidation of Native BPTI

Performic acid oxidation of native BPTI was studied to produce a product that could be digested under minimum H/D exchange conditions. The performic acid reagent was made from mixing formic acid and 30% H_2O_2 solution with a volume ratio of 90 to 10 at room temperature for 2.5 hours and at -20°C. At first, the oxidation of native BPTI was studied in sodium phosphate buffer.[23b] Native BPTI was dissolved in 0.1 M sodium phosphate buffer (pH 8.5) and then reacted

with performic acid reagent at 0°C for 10 minutes where a volume ratio of the buffer solution to the oxidizing reagent was 2 to 1 and the final solution pH was in the range of 1.0 to 2.0. Complete oxidation was expected to give a molecular weight of 6836 Da with a 326 mass increase (H_6O_{20}). However, the oxidation of native BPTI with performic acid resulted in a complex mixture of oxidized intermediates (**Figure II.2-19, Table III.2-9**). The peak which had eluted at the same elution time where native BPTI had eluted on HPLC, turned out to be an oxidized intermediate with a molecular weight of 6574 Da corresponding to a mass for native BPTI (6510 Da) plus four oxygen atoms. This compound was always present in the reaction mixture. Efforts to denature the native BPTI in the presence of 8 M urea at 0°C over a 10 minute period, failed to give fully oxidized BPTI as a relatively pure major product.

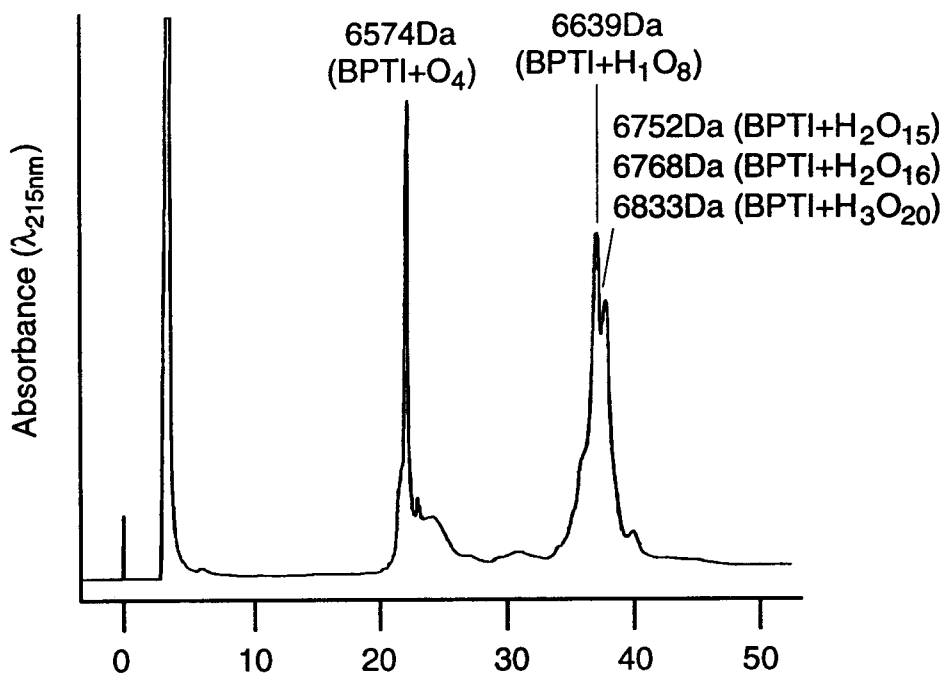

Figure II.2-19: Chromatographic Profile of Native BPTI Oxidized by Performic Acid in 0.1 M Sodium Phosphate Buffer (pH 1.2, 0°C, 10 min)

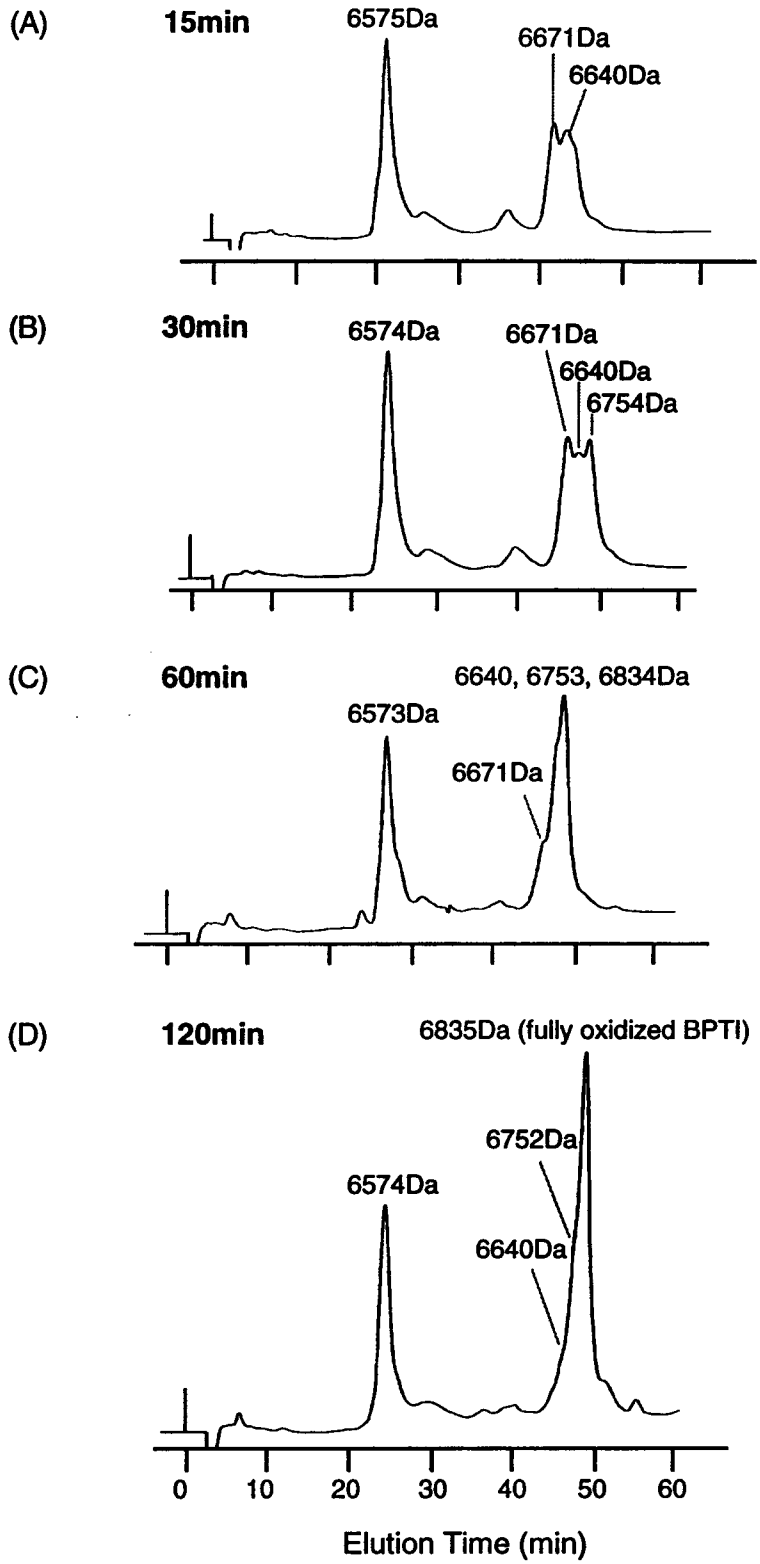

Figure II.2-20: Chromatographic Profile of Native BPTI Oxidized by Performic Acid in HCO_2H-NH_4OH/MeOH Buffer (pH 2.8, -20°C, up to 2 hours)

To try to overcome these problems, another buffer system consisting of formic acid-ammonium hydroxide, was used. The original performic acid oxidation condition[23] was mimicked for native BPTI by using formic acid as a buffer system. The solution was adjusted pH 2-3 with concentrated ammonium hydroxide solution. The reaction temperature was lowered to -20°C. Native BPTI was dissolved in a solution mixture consisting of five volumes of HCO_2H-NH_4OH buffer and one volume of MeOH, where MeOH was added as an anti-freeze. The final pH of this solution was 3. The BPTI solution was put in a cooling bath at -20°C and this mixture was allowed to react with a half volume of precooled performic acid reagent at -20°C., The final solution had pH 2.8. The reaction was allowed to continue at -20°C for up to 6 hours (**Figure II.2-20, Table III.2-10**). Completely oxidized BPTI started to be detected after an hour under these oxidation conditions. After 2 hours, relatively pure completely oxidized BPTI was observed as the major product with a molecular weight of 6834 Da as shown in the HPLC-ESI mass spectrum (**Figure II.2-21**). Other minor oxidized intermediates (6752 Da, 6640 Da) were also identified.

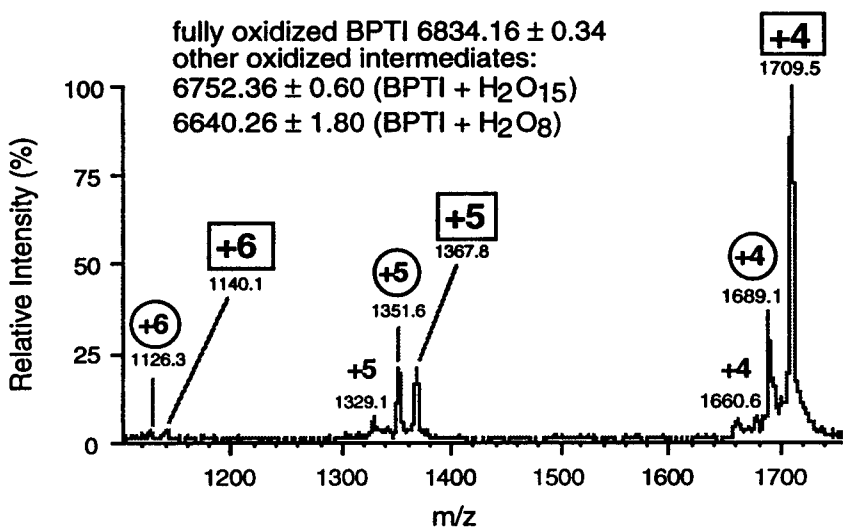

Figure II.2-21: Microbore HPLC-Ionspray Mass Spectrum of Oxidized BPTI

II.2-4-3 Pepsin Digestion of Oxidized BPTI

Proteolytic digestion of oxidized BPTI with immobilized pepsin was performed under slow H/D exchange conditions (E/S=5, pH 2.0, 0°C, 5 min) (**Figure II.2-22B**). As a control experiment, completely reduced BPTI in HCO_2H-NH_4OH/MeOH buffer was oxidized with the performic acid reagent under the same oxidation conditions (**Figure II. 2-22A**).

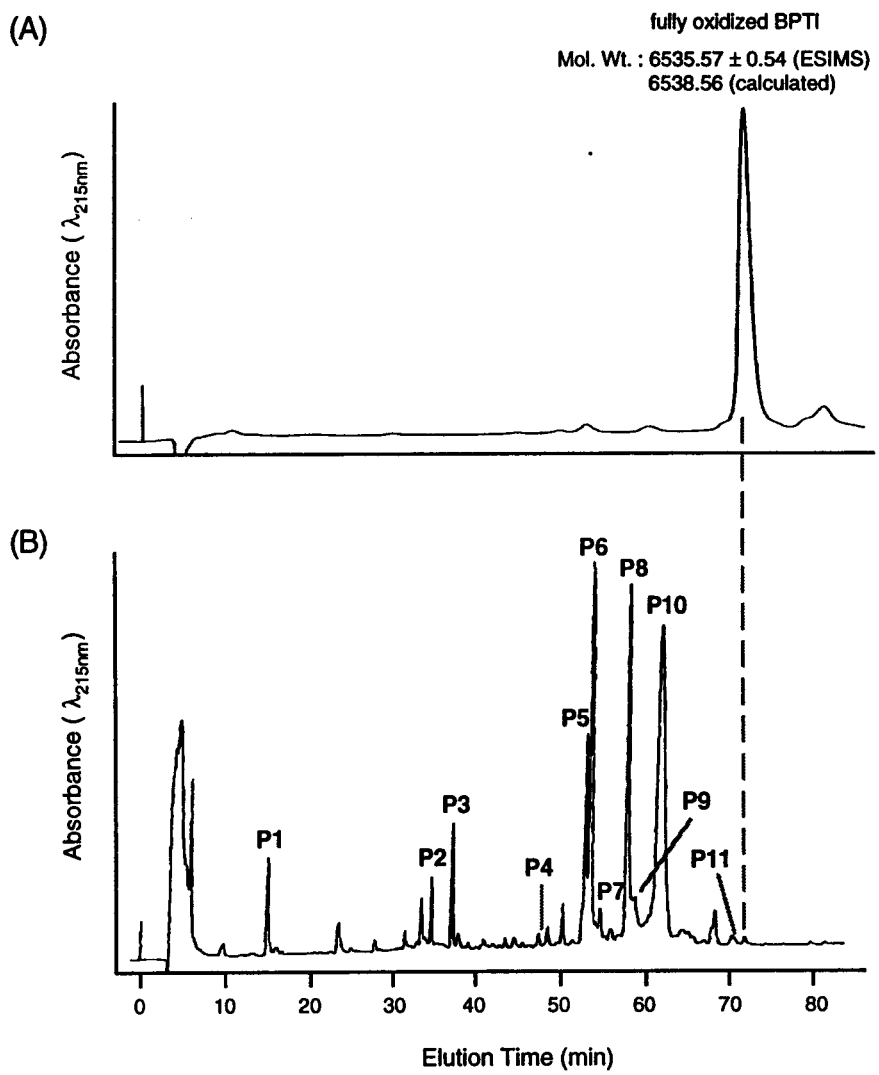

Figure II.2-22: Chromatographic Profile of (A) Oxidized BPTI Derived from Oxidation of Reduced BPTI (pD 2.8, -20 °C, 30 min) and of (B) Its Peptic Digest

The oxidation of BPTI that had been first been reduced, went much easier than native BPTI did. Fully oxidized BPTI was obtained in less than 30 minutes without the presence of the oxidized intermediate (BPTI+O_4) with a molecular weigh of 6575 Da (**Figure II.2-22A**). After lyophilization of the oxidation mixture, digestion was carried out with immobilized pepsin (E/S=5, pH 2.0, 0°C, 5 min). The digestion mixture was micro-filtered over a microcentrifuge tube and analyzed by HPLC (**Figure II.2-22B**). The immobilized pepsin completely digested the oxidized BPTI into eleven peptides with four of the peptides (P5, P6, P8 and P10) being the major products (**Table III.2-11**).

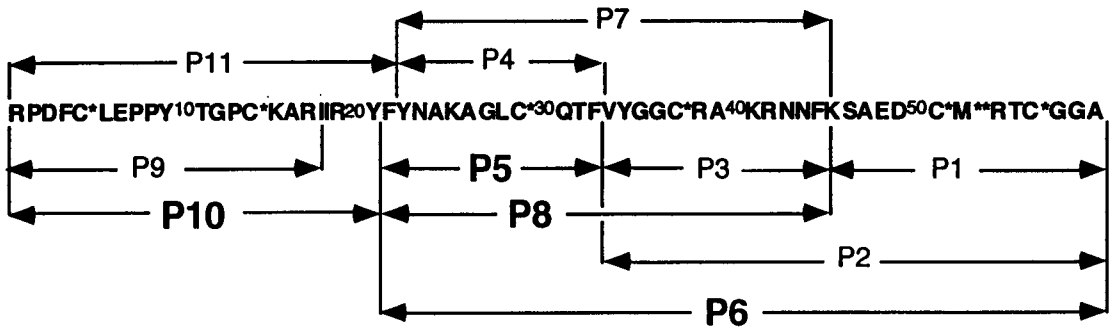

$$C^{*}: \text{Cys-SH} \xrightarrow{HCO_3H} \text{Cys-}SO_3H$$

$$M^{**}: \text{Met-}SCH_3 \xrightarrow{HCO_3H} \text{Met-}SO_2CH_3$$

Figure II.2-23: Peptide Map of Peptic Digest of Oxidized BPTI

All peptides were isolated and identified by ESIMS, ESIMS/MS, FABMS and MALDI-TOFMS (**Table III.2-11**). The peptide map of the oxidized BPTI is shown in **Figure II.2-23**. The oxidized BPTI provided fewer cleavage sites for

the immobilized pepsin than did the reduced BPTI which gave a total of 15 peptides under the same conditions (**Figure II.2-6, Figure II.2-9**). The peptic peptides obtained from oxidized BPTI were relatively larger in size and the number of peptides having overlapping sequences was much fewer than those obtained from reduced BPTI. Ten (P1-P8, P10, P11) out of eleven peptides were obtained from cleavages at the N- or C-terminal positions of phenylalanine residues (F22, F33, F45). None of the peptides were obtained from cleavages between F4 and C*5 or between C*51 and M**52 where C* an M** represent cysteic acid and methionine sulfone residues, respectively. These two positions were very labile for the pepsin digestion of reduced BPTI (**Figure II.2-9**). A16 and A40 were not cleaved probably because these residues are close in the sequence to C*14 and C*38. These results clearly show that the six cysteic acid residues strongly influence the pepsin-digestion of oxidized BPTI. Pepsin did not cleave the peptide bonds at or near these six cysteic acid residues. The structural difference between oxidized BPTI and reduced BPTI turned out to be very small as shown by H/D exchange behavior (**Figure II.2-30 ~ Figure II.2-31**) and CD spectra (**Figure II.2-32**). These two molecules have been shown by CD spectra to adopt very similar random coil structures and to follow very similar H/D exchange processes. Therefore, the structural factors cannot be an important factor in the different behavior to pepsin digestion.

Ionspray mass spectra of the 4 major peptides (P5, P6, P8 and P10) and their daughter-ion spectra produced by collisional activation of a selected molecular ion (parent ion) are shown in **Figure II.2-24** to **Figure III.2-27**. Mass values of these daughter ions observed are listed in **Table III.2-14** to **Table III.2-17**.

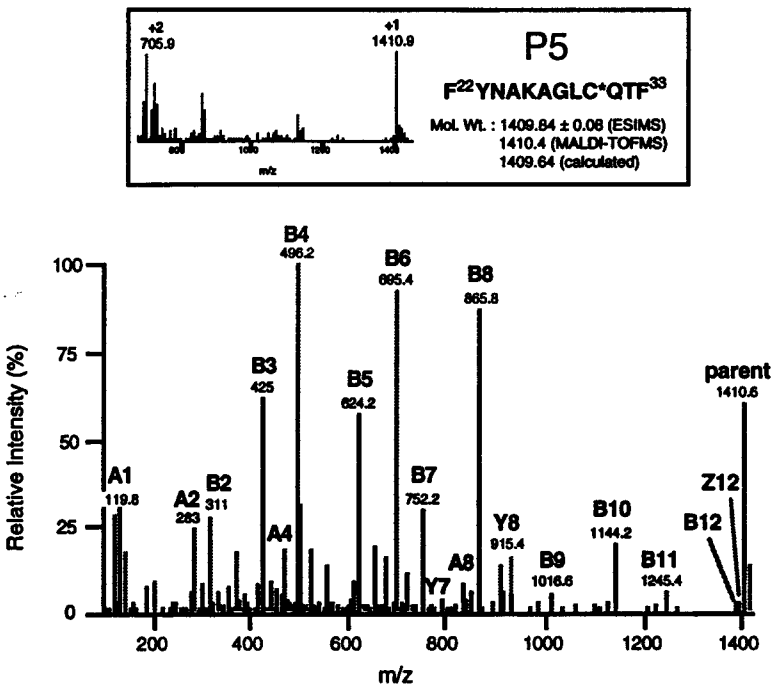

Figure II.2-24: Ionspray Mass Spectrum (Insert) and Daughter-Ion Spectrum (Parent Ion; m/z 1411) of Peptide 5

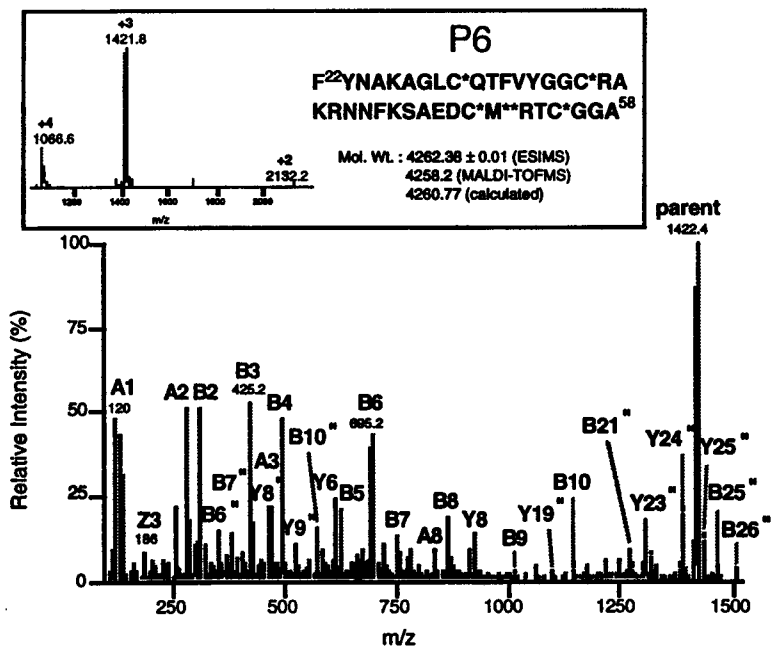

Figure II.2-25: Ionspray Mass Spectrum (Insert) and Daughter-Ion Spectrum (Parent Ion; m/z 1422) of Peptide 6

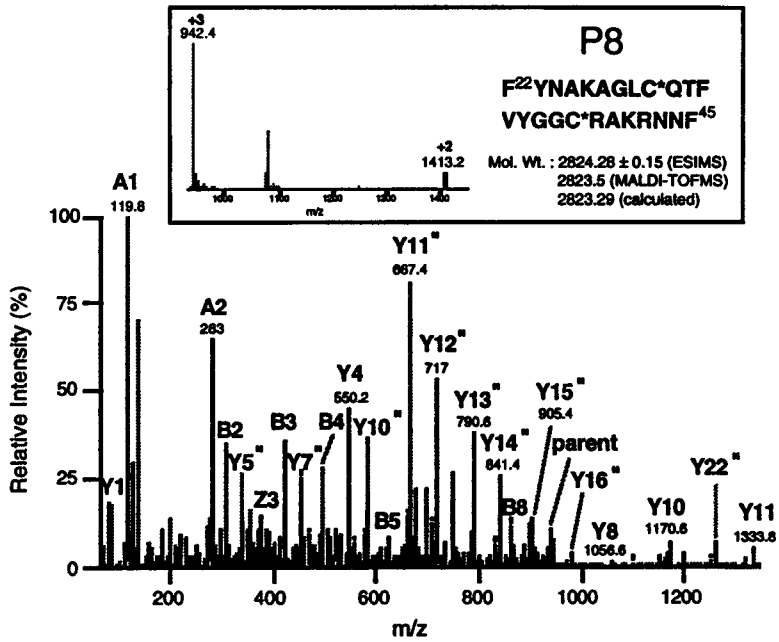

Figure II.2-26: Ionspray Mass Spectrum (Insert) and Daughter-Ion Spectrum (Parent Ion; m/z 942) of Peptide 8

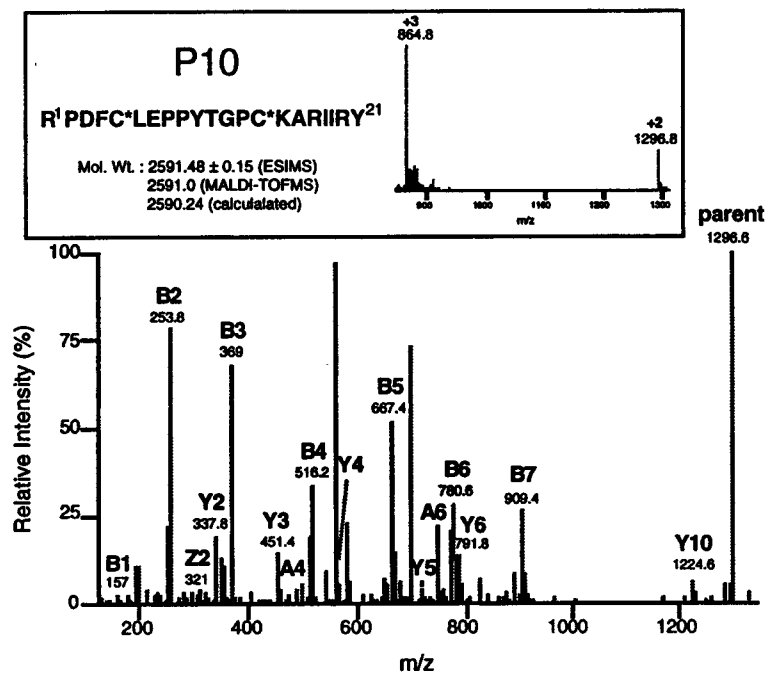

Figure II.2-27: Ionspray Mass Spectrum (Insert) and Daughter-Ion Spectrum (Parent Ion; m/z 1297) of Peptide 10

Peptic Digestion of oxidized BPTI derived from native BPTI was performed under the same conditions (E/S=5, pH 2.0, 0°C, 5 min) (**Figure II.2-28**).

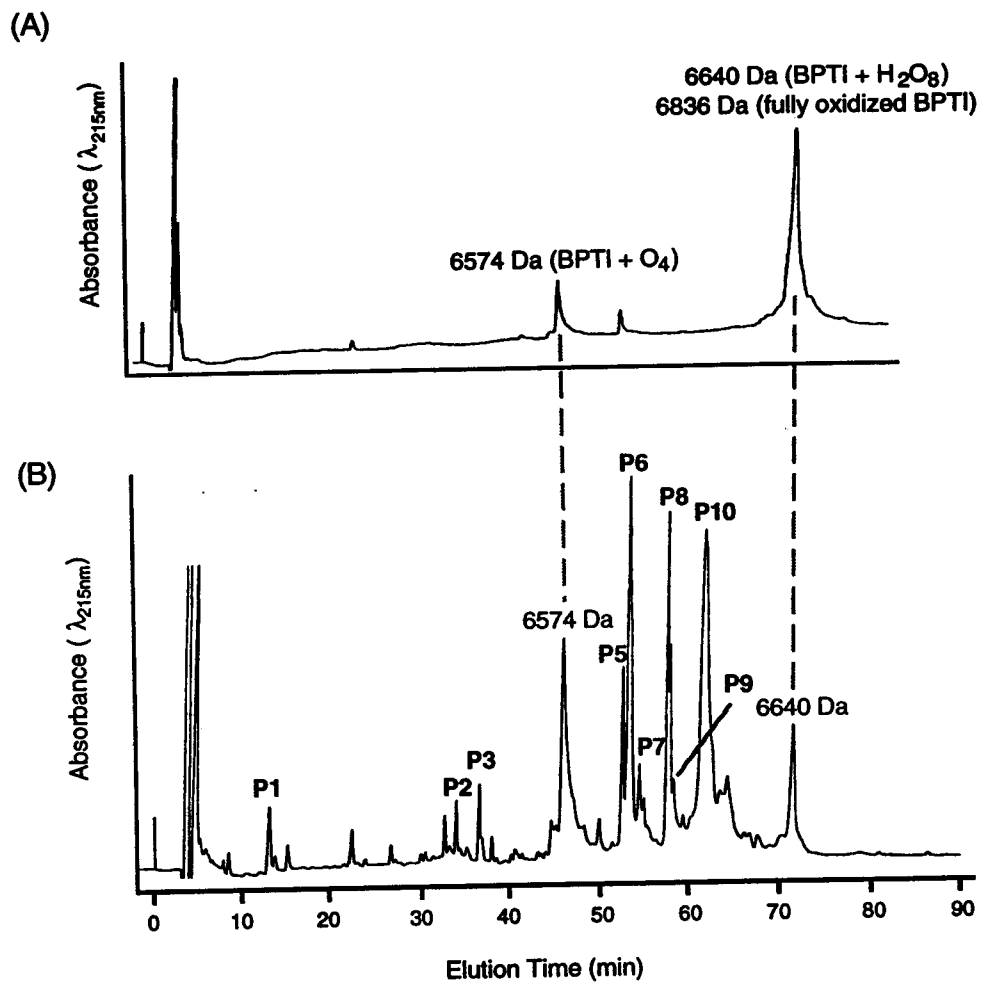

Figure II. 2-28: (A) Oxidized BPTI Derived from the Oxidation of Native BPTI with Performic Acid (pH 2.8, -20°C, 2 hr) and (B) Its Peptic Digest (E/S=5, pH 2.0, 0°C, 5 min)

Native BPTI was oxidized with the performic acid reagent in HCO_2H-NH_4OH/8.5% MeOH (pH 2.8, -20°C, 2 hr). The oxidized product mixture was analyzed by HPLC using a C-18 reverse-phase column (**Figure II.2-28A**).

Completely oxidized BPTI was obtained as the major product (6836 Da) and partially oxidized intermediates were obtained (6574 Da, 6640 Da) as minor products. This crude reaction mixture was subjected directly to immobilized pepsin for digestion (**Figure II.2-28B**). A total of nine peptides were determined to be present in the digestion mixture (P1 to P3, P5 to P10) using ESIMS and ESIMS/MS for the analysis (**Table III.2-13**). Only fully oxidized BPTI was digestible by pepsin, whereas the two partially oxidized BPTIs were indigestible under these conditions.

Microbore HPLC-ESIMS analysis of the digestion mixture was performed using a C-8 reverse-phase column at 0°C to separate the peptides (**Figure II.2-29**). Seven peptides were identified (P1, P3, P5, P6, P8, P9 and P10). Acetonitrile/0.1% TFA gradient was adjusted to elute all the peptides in less than 30 minutes with an acceptable resolution on microbore HPLC-ESIMS at low temperature (0°C). These peptides provided all the sequence-specific information when they were analyzed by microbore HPLC-ESIMS/MS.

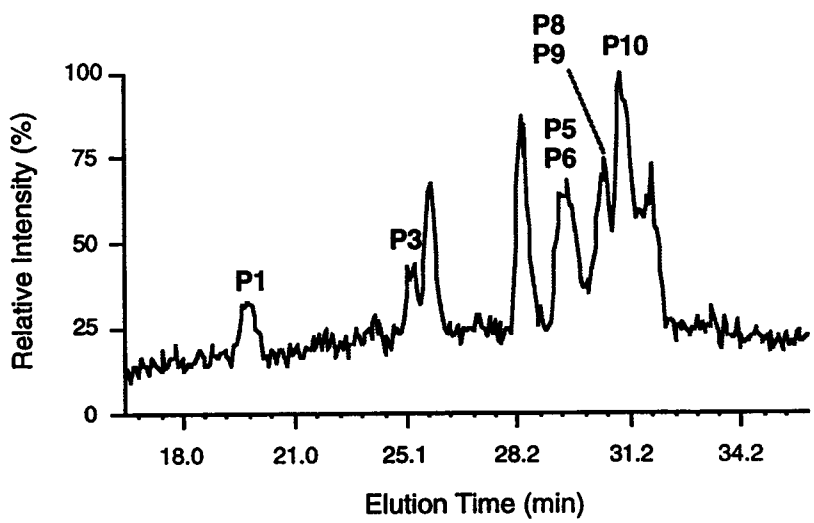

Figure II.2-29: Total Ion Chromatogram of Peptic Digest of Oxidized BPTI Derived from Native BPTI Oxidation Using Microbore HPLC-ESIMS Analysis (RP-C-8 Column, 0°C)

II.2-5 H/D Exchange of BPTI

II.2-5-1 Probing Tertiary Structure Changes of BPTI Using H/D Exchange-ESIMS Analysis

Deuterium exchange-in experiments were performed to study global structure changes of native BPTI, reduced BPTI, oxidized BPTI, and selectively reduced and carboxyamidomethylated BPTI at C14 and C38 (CAM(14,38)-BPTI) using the continuous flow infusion-ESIMS technique (CF-ESIMS) for the analysis (**Strategy VI (Scheme II.2-3)**). The deuterium exchange-in reactions were carried out in a deuterated solvent system consisting of AcOD and D_2O containing 8.5% MeOD at pD 2.8 and at 20°C. This solvent system was chosen to mimic the oxidation buffer system used for native BPTI and to make it compatible for ESI mass spectrometric analysis. The molecular weight increase was continuously monitored and the data were used to plot deuterium incorporation (%) as a function of exchange-in time (min) (**Figure II.2-30, Table III.2-18~Table III.2-21**). Native BPTI has a total of 108 exchangeable hydrogens consisting of 53 backbone amide hydrogens, 52 side-chain hydrogens and 3 terminal hydrogens. Among these, only 49% of the exchangeable hydrogens actually were exchanged for deuteriums in the first 30-minute period. The selectively alkylated BPTI (CAM(14,38)-BPTI) has a total of 112 exchangeable hydrogens consisting of 53 backbone amide hydrogens, 52 side-chain hydrogens, 3 terminal hydrogens and 4 additional hydrogens from the two carboxyamidomethyl groups. In the first 30-minute period, 55.5% of the exchangeable hydrogens were exchanged for deuteriums. After an hour, 50.7% hydrogens in native BPTI and 56.1% hydrogens in CAM(14,38)-BPTI had been replaced by deuteriums, respectively.

Strategy VI

Monitoring Global Structure Changes in BPTI Using H/D Exchange and Continuous Flow Infusion ESIMS

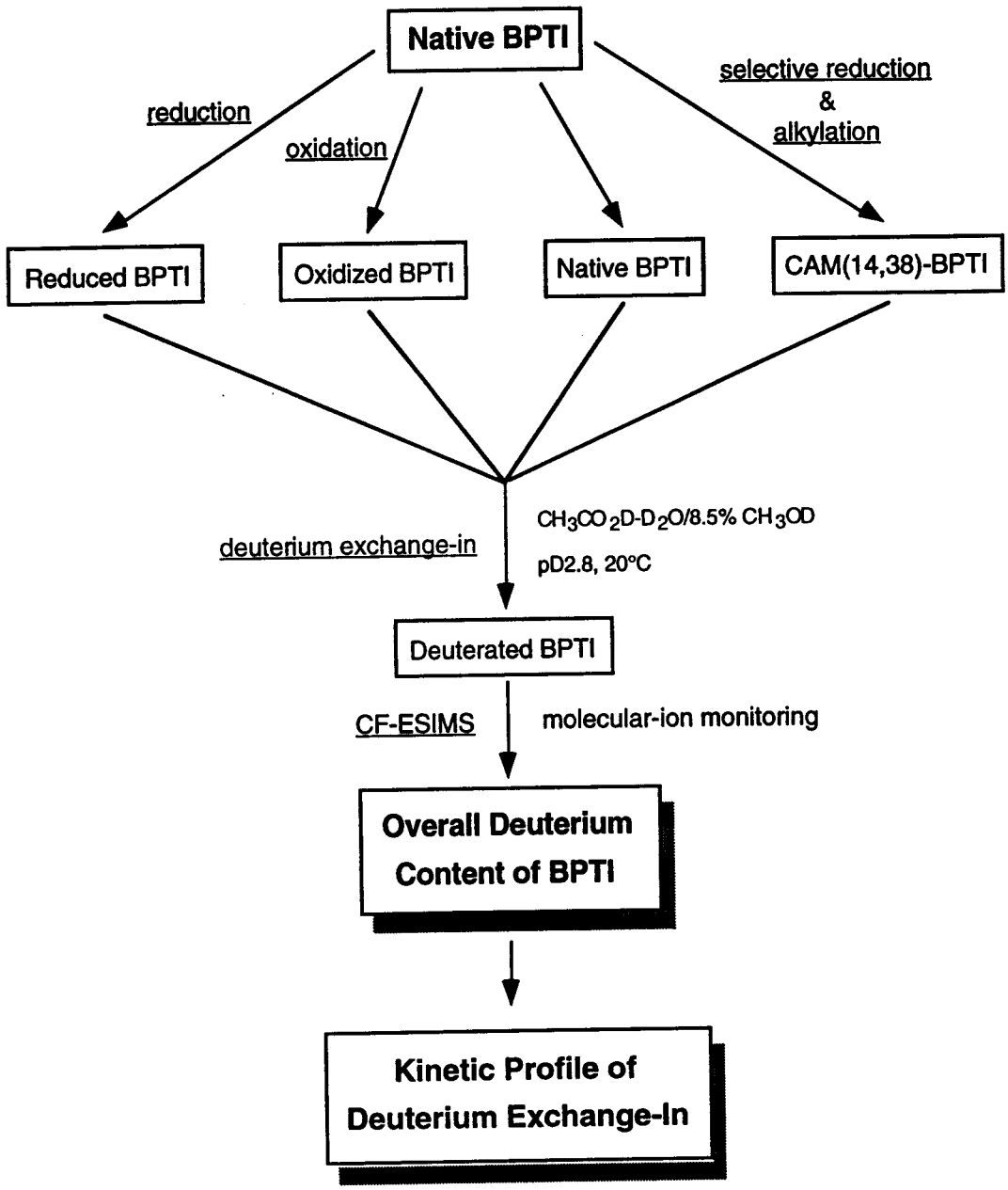

Scheme II.2-3: Strategy VI

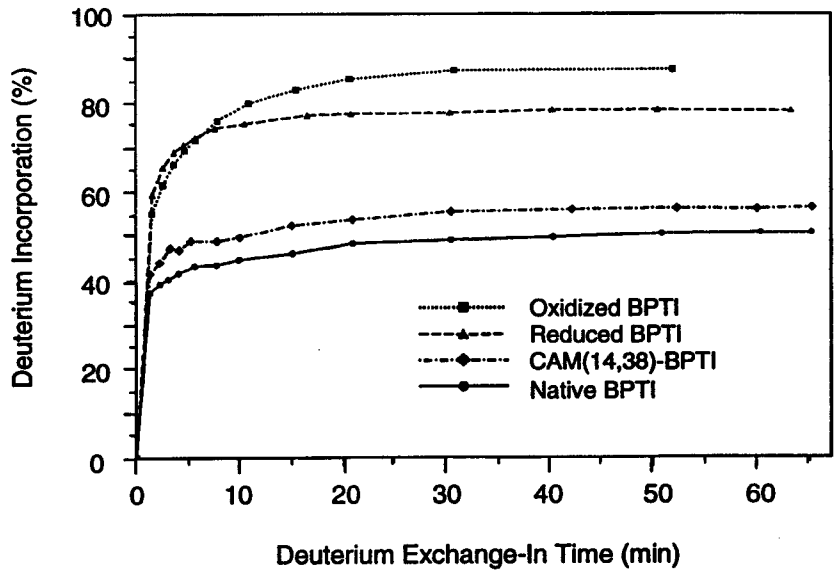

Figure II.2-30: Monitoring Deuterium Exchange-In into Native, CAM(14,38)-, Oxidized and Reduced BPTI in AcOD/D_2O/MeOD (pD 2.8, 20°C) by CF-ESIMS

The deuterium exchange-in processes between native BPTI and CAM(14,38)-BPTI were very similar. This similarity in the deuterium exchange-in reactions was confirmed by comparing the kinetic profiles for these H/D exchanges (**Figure II.2-31A**, **Figure II.2-31B**) and the CD spectra (**Figure II.2-32**) of these two molecules. In the plots of the number of exchangeable hydrogens remaining (H_t) versus exchange-in time (t), four different groups including a fastest-exchanging group of exchangeable hydrogens , were evident after about an hour of monitoring the exchange-in processes for native BPTI and CAM(14,38)-BPTI. Most of the fast-exchanging hydrogens at the two termini and the side chains were populated in the fastest-exchanging group and could not be analyzed in detail in the H/D exchange profile. The rest of the fast-exchanging hydrogens, 8.7 exchangeable hydrogens in group 1 and another 12 in group 2 exchanged to deuteriums in native BPTI with half-lives of 54 seconds and 12 minutes, respectively. In CAM(14,38)-BPTI, 9.4 exchangeable

hydrogens in group 1 and another 15 in group 2 exchanged with half-lives of 46 seconds and 9.7 minutes, respectively. All or most of 53 backbone amide hydrogens available in native BPTI and CAM(14,38)-BPTI were populated in group 3. Therefore, after the first hour of monitoring H/D exchange, detailed kinetics concerning backbone amide hydrogens for native BPTI and CAM(14,38)-BPTI were not available. The CD spectra of these two molecules showed similar proportions of secondary structural elements (**Figure II.2-32** and **Table II.2-1**). The CAM(14,38)-BPTI adopts a structure that is similar to native BPTI but with a lower proportion of α-helices and β-sheets.

Oxidized BPTI and reduced BPTI showed relatively rapid deuterium exchange-in profiles in comparison to native BPTI and CAM(14,38)-BPTI. Oxidized BPTI and reduced BPTI were very comparable to each other in deuterium exchange-in behavior (**Figure II.2-30**, **Figure II.2-31**) and in the contents of secondary structural elements (**Figure II.2-32** and **Table II.2-1**). Oxidized BPTI and reduced BPTI have a total of 114 exchangeable hydrogens (H_{total}) including 53 backbone amide hydrogens. Deuterium exchange-in into oxidized BPTI gave 71.5% deuterium incorporation in 5.7 min, 87% in 30 min, and 88% in 60 min. Deuterium exchange-in into reduced BPTI gave 72% deuterium incorporation in 5.7 min, 78% in 30 min, and 78% in 60 min. For about the first 6 minutes, reduced BPTI was deuterated faster than the oxidized BPTI. After 6 minutes, however, the reduced BPTI was deuterated slower than the oxidized BPTI. Kinetic profiles for the deuterium exchange-in into these two molecules clearly showed this interesting H/D exchange phenomenon (**Figure II.2-31C**, **Figure II.2-31D**). In the plots of the number of exchangeable hydrogens remaining (H_t) versus exchange-in time (t), four different groups including a fastest-exchanging group of exchangeable hydrogens, were determined for oxidized BPTI and reduced BPTI. In oxidized BPTI, 49 of the

relatively fast-exchanging hydrogens were populated in the fastest-exchanging group and could not be analyzed in detail in the H/D exchange profile. Another 12 exchangeable hydrogens and 7 backbone amide hydrogens in group 1 exchanged with a half-life of $t_{1/2}$=1.3 min. Among the rest of backbone amide hydrogens, 33 medium-exchanging ones with a half-life of 6 minutes in group 2, and 13 slowest-exchanging amide hydrogens in group 3 were determined. On the other hand, reduced BPTI had 48 and another 13 fast-exchanging hydrogens in the fastest-exchanging group and group 1, respectively. In group 1, 14 of relatively fast-exchanging backbone amide hydrogens ($t_{1/2}$=1.0 min) were included. Among the rest of backbone amide hydrogens, 14 medium-exchanging amide hydrogens with a half-life of 5 minutes in group 2, and 25 slowest-exchanging ones in group 3 were determined. Therefore, only the relatively slow-exchanging backbone amide hydrogens of oxidized BPTI were more rapidly exchanged to deuteriums than the corresponding amide hydrogens of reduced BPTI, whereas the fast-exchanging hydrogens in flexible regions of oxidized BPTI exchange relatively slowly compared to those of reduced BPTI. The CD spectra showed that these two molecules adopt similar random coil-like structures and reduced BPTI has less secondary structures than oxidized BPTI (**Figure II.2-32** and **Table II.2-1**). Based on these results, the difference in relative H/D exchange behavior between the hydrogens in flexible regions and the backbone amide hydrogens in structural regions might be explained by the six ionizable cysteic acid residues. The ionizable sulfonic acid groups of cysteic acid residues can influence the H/D exchange reactions of the backbone amide hydrogens through inductive or ionic effects. The sulfonic acid groups of cysteic acid residues, however, have less effect on the hydrogens in flexible regions. Therefore, H/D exchange of these hydrogens are determined mainly by the overall structural flexibility.

(A)

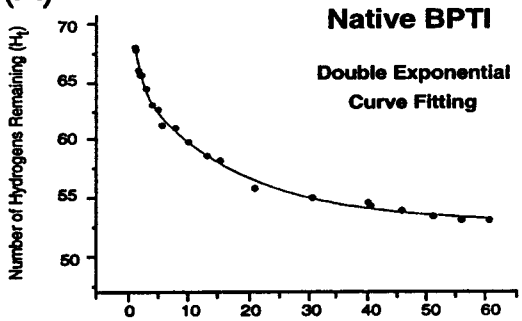

$H_t=53+8.7exp(-0.77t)+12exp(-0.059t)$
(χ^2=0.12)

H_{total}=108
Group 1 : H_1=8.7, k_1=-0.77 min^{-1}, $t_{1/2}$=54 sec
Group 2 : H_2=12, k_2=-0.059 min^{-1}, $t_{1/2}$=12 min
Group 3 : H_0=53 (too slow to be observed)

(B)

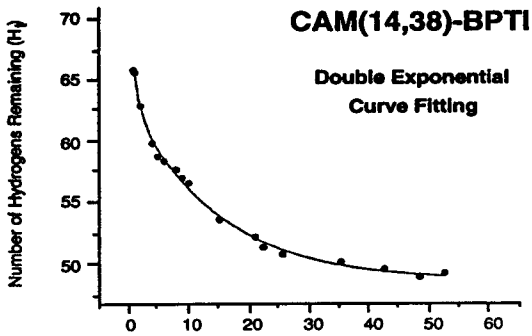

$H_t=48+9.4exp(-0.91t)+15exp(-0.071t)$
(χ^2=0.15)

H_{total}=112
Group 1 : H_1=9.4, k_1=-0.91 min^{-1}, $t_{1/2}$=46 sec
Group 2: H_2=15, k_2=-0.071 min^{-1}, $t_{1/2}$=9.7 min
Group 3 : H_0=48 (too slow to be observed)

(C)

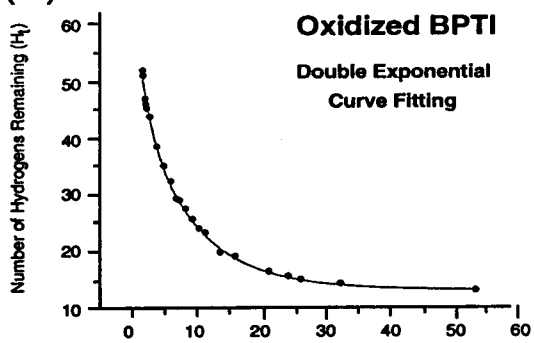

$H_t=13+19exp(-0.53t)+33exp(-0.12t)$
(χ^2=0.58)

H_{total}=114
Group 1 : H_1=19, k_1=-0.53 min^{-1}, $t_{1/2}$=1.3 min
Group 2: H_2=33, k_2=-0.12 min^{-1}, $t_{1/2}$=6.0 min
Group 3 : H_0=13 (too slow to be observed)

(D)

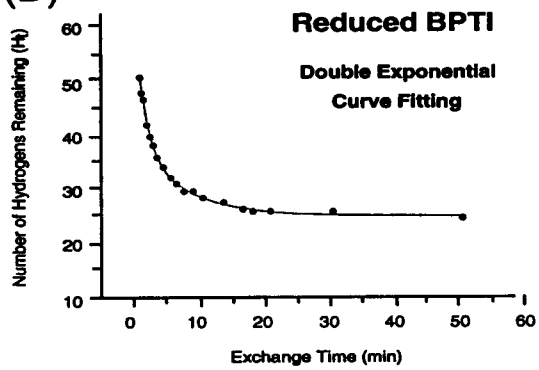

$H_t=25+27exp(-0.67t)+14exp(-0.14t)$
(χ^2=0.16)

H_{total}=114
Group 1 : H_1=27, k_1=-0.67 min^{-1}, $t_{1/2}$=1.0 min
Group 2 : H_2=14, k_2=-0.14 min^{-1}, $t_{1/2}$=5.0 min
Group 3 : H_0=25 (too slow to be observed)

Figure II.2-31: Kinetic Profiles for Deuterium Exchange-In into (A) Native BPTI, (B) CAM(14,38)-BPTI, (C) Oxidized BPTI and (D) Reduced BPTI at 20°C

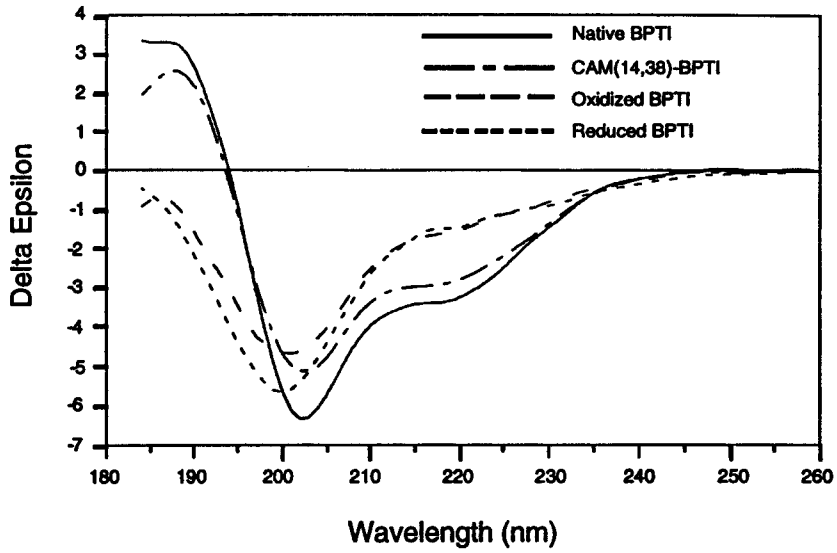

Figure II.2-32: CD Spectra of Native BPTI and Its Derivatives in 10 mM Sodium Phosphate Buffer Containing 8.5% MeOH (pH 2.8)

Table II.2-1: Comparison of Secondary Structural Elements in Native and Modified BPTI Molecules

	α-Helix	β-Sheet	β-Turn	Others
Native BPTI	19.2%	13.5%	28.8%	38.5%
CAM(14,38)-BPTI	16.3%	17.3%	26.9%	39.4%
Oxidized BPTI	8.6%	17.3%	30.8%	43.3%
Reduced BPTI	7.8%	13.7%	33.3%	45.1%

II.2-5-2 Locating Structural Regions of Native BPTI by Deuterium Exchange-Out and Protein Fragmentation-HPLC-ESIMS and HPLC-ESIMS/MS Analysis

To determine the structural changes during the course of folding of BPTI, deuterium exchange-out from the backbone amide groups of deuterated BPTI was monitored to probe for secondary elements. Protein digestion and directly coupled microbore HPLC-ESIMS and -ESIMS/MS under slow H/D exchange conditions were used for the analysis. Protein digestion was carried out using

pepsin and tandem mass spectrometric analysis (HPLC-ESIMS/MS) was used to give specific information on the deuterium content in different regions of the protein. The structural changes among the molecules can only be determined if chemical modifications of the disulfide bonds can be performed under slow H/D exchange conditions so that the deuterium labels can be largely preserved. The overall procedure for locating the structural regions of native BPTI is depicted in **Strategy VII (Scheme II.2-4)**.

Strategy VII

Determination of Structural Regions in Native BPTI by Deuterium Exchange-Out and Pepsin Digestion-HPLC-ESIMS and -ESIMS/MS via Performic Acid Oxidation of Disulfides

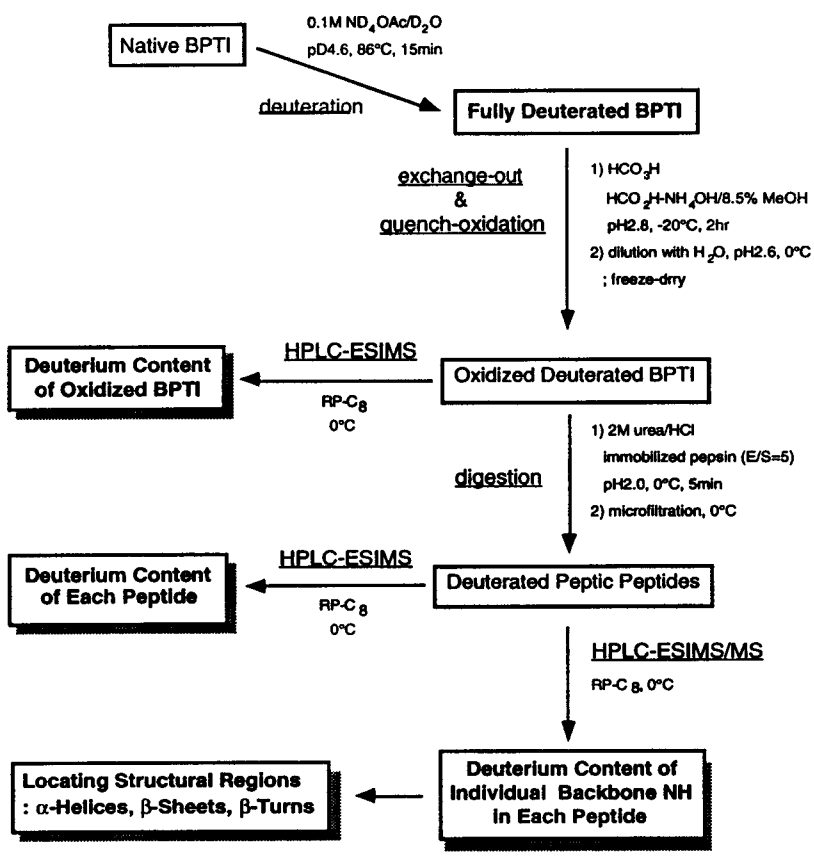

Scheme II.2-4: Strategy VII

Native BPTI is very stable against heat and towards extremes of pH and denaturants.[64] Fully deuterated BPTI was obtained under completely reversible thermal unfolding conditions as carried out in 40% deuterated n-propanol/D_2O (pD 2.2, 70°C, 15 min)[24a] or in 0.1 M ND_4OAc/D_2O (pD 4.6, 86°C, 15 min).[65] Under these deuteration conditions, BPTI is completely denatured by heat and completely loses its native structure, and all the exchangeable hydrogens including the very stable backbone amide hydrogens in the core structural regions, can be replaced with deuteriums. This thermally unfolded BPTI was refolded at 0°C and pH 3.6 where the H/D back-exchange rate on backbone amide groups is at a minimum. It has been known that after thermal denaturation, BPTI can be completely renatured and the refolded protein at low temperature is indistinguishable from the native structure as evidenced by NMR spectroscopy.[65] However, the heat-treated native BPTI gave two peaks in the chromatogram when analyzed by HPLC-ESIMS (**Figure II.2-33A**). The mass spectrum showed that one oxygen atom was incorporated into BPTI to give a compound with a molecular weight of 6526 Da as minor product (**Figure II.2-33B**). The position most easily oxidized within the sequence of native BPTI, is the methyl sulfide group of methionine 52 which oxidize to the sulfoxide. This residue was always present in the heat- treated BPTI, as an air-oxidation product. Complete deuteration under the thermal unfolding condition (0.1 M ND_4OAc/D_2O, pD 4.6, 86°C, 15 min) showed the same two peaks in the chromatogram when analyzed by HPLC-ESIMS at 0°C (**Figure II.2-34A**). The air-oxidized BPTI had a molecular weight of 6555 Da which represents a 29 mass-unit increase (**Figure II.2-34B**) and the fully deuterated BPTI had a molecular weight of 6542 Da which represents a 32 mass-unit increase (**Figure II.2-34C**). In the fully deuterated BPTI about 60% of the deuteriums (+31.8 mass increase) were preserved during microbore

HPLC-ESIMS analysis at 0°C and in the air-oxidized BPTI, 55% of them (+28.8 mass increase) were preserved.

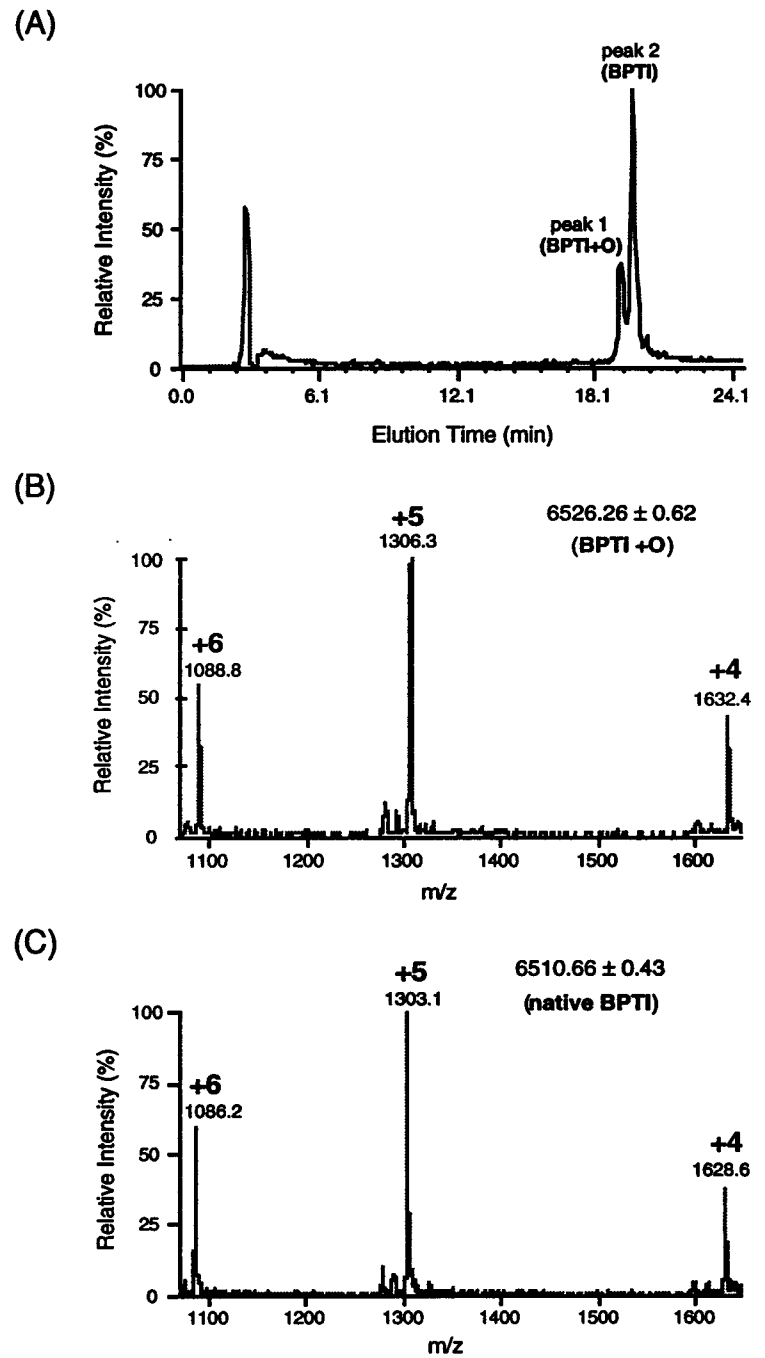

Figure II.2-33: (A) Total Ion Chromatogram of Native BPTI Treated with Heat (0.1 M NH_4OAc, pH 4.6, 86°C, 15 min) and Mass Spectra of (B) Peak 1 and (C) Peak 2

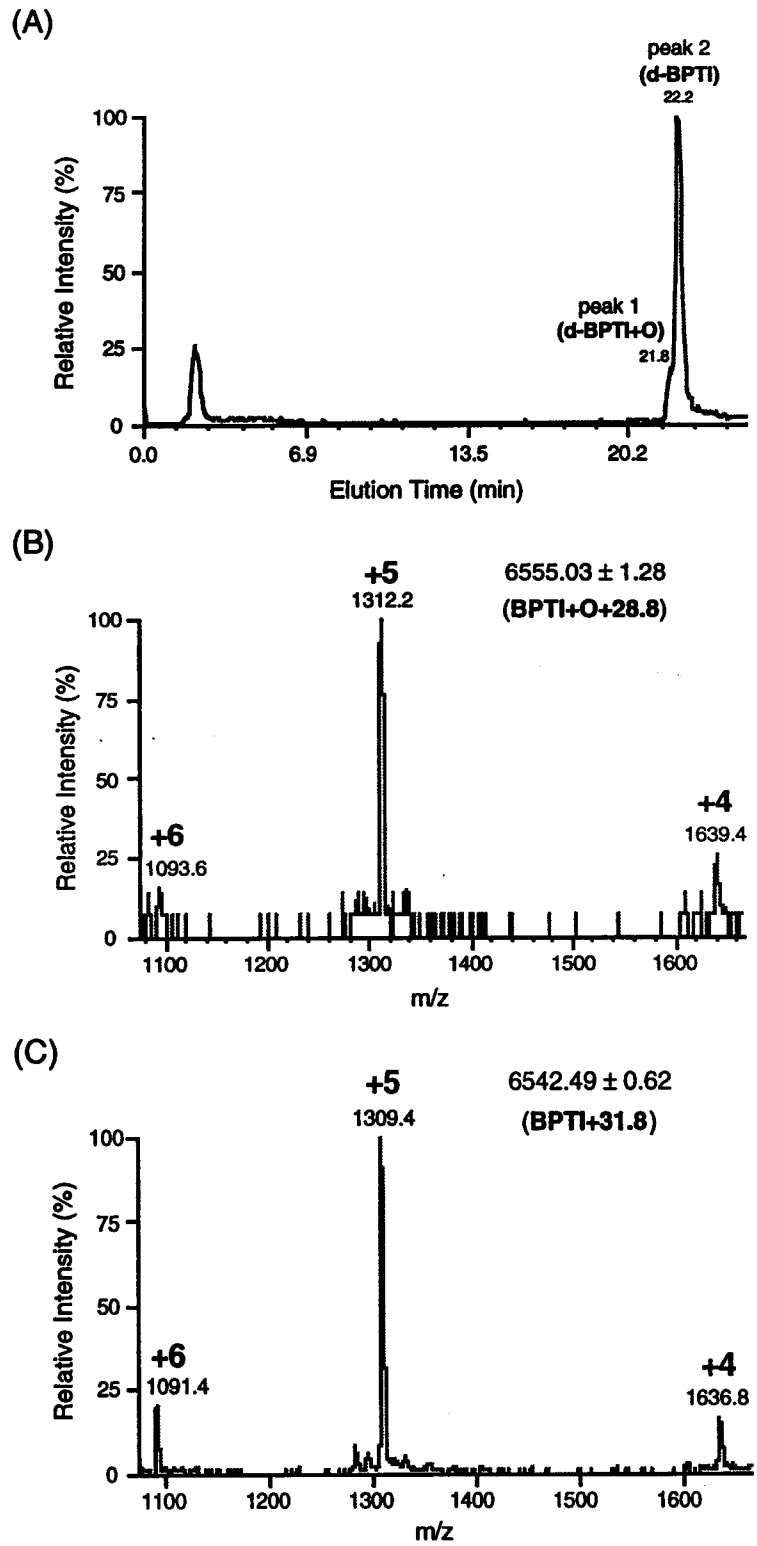

Figure II.2-34: (A) Total Ion Chromatogram of Deuterated BPTI Treated with heat (0.1 M ND_4OAc, pD 4.6, 86°C, 15 min) and Mass Spectra of (B) Peak 1 and (C) Peak 2

The effect of buffer systems on H/D exchange of fully deuterated native BPTI, was studied by a relatively fast and simple experiment using a micro-desalting method and CF-ESIMS analytical technique (**Scheme II.2-5**). Fully deuterated BPTI was dissolved in different buffer systems including dilute HCl , 0.1 M NH_4OAc, 0.1 M NH_4OAc/8 M urea, 10 mM sodium phosphate, 10 mM sodium phosphate/8.5% MeOH, and HCO_2H-NH_4OH/8.5% MeOH at pH 2.8 and 20°C. The deuterium exchange-out processes from fully deuterated native BPTI in these buffer solutions were monitored by ESIMS at 0°C where the time-sampled solutions were loaded onto a micro-desalting cartridge loop, prewashed with a cold 2.5% acetonitrile-water (pH 2.8, 0°C) solution, and injected into the ESI mass spectrometer (**Figure II.2-35**).

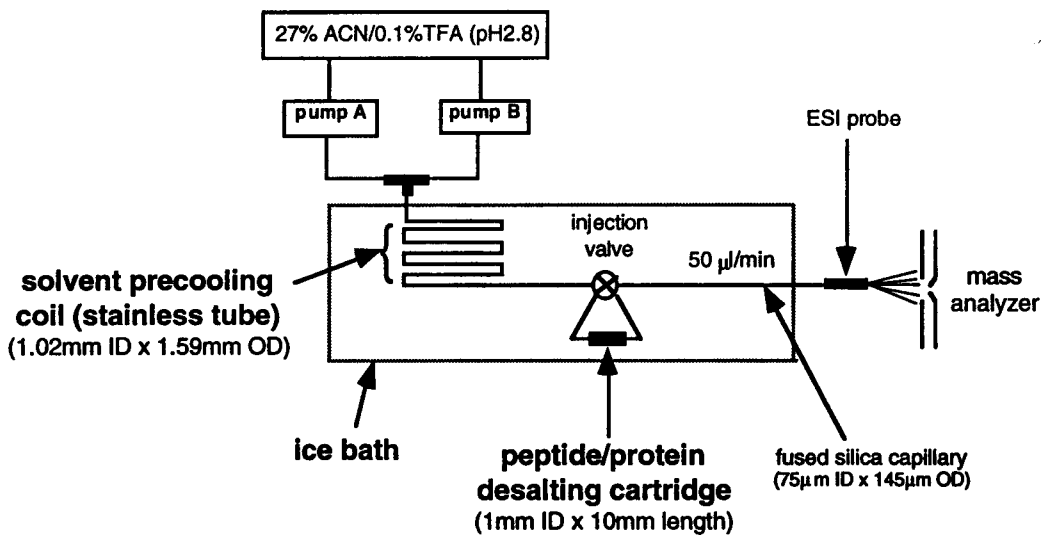

Figure II.2-35: Schematic Diagram of Micro-Desalting-ESIMS

The prewashing step before the injection of the sample solution into the mass spectrometer, is actually a desalting process that takes place in a tiny reverse phase cartridge inserted in the injection loop. Most of the salts existing

in the sample solution are washed away by cold 2.5% acetonitrile-water in this cartridge but protein is retained. By using this micro-desalting loop, ESIMS analysis can be carried out effectively even when the solutions contain high concentration of buffer salts.

Strategy VIII

Monitoring Deuterium Exchange-Out from Fully Deuterated BPTI in Different Buffers by Using Microdesalting-ESIMS at 0°C

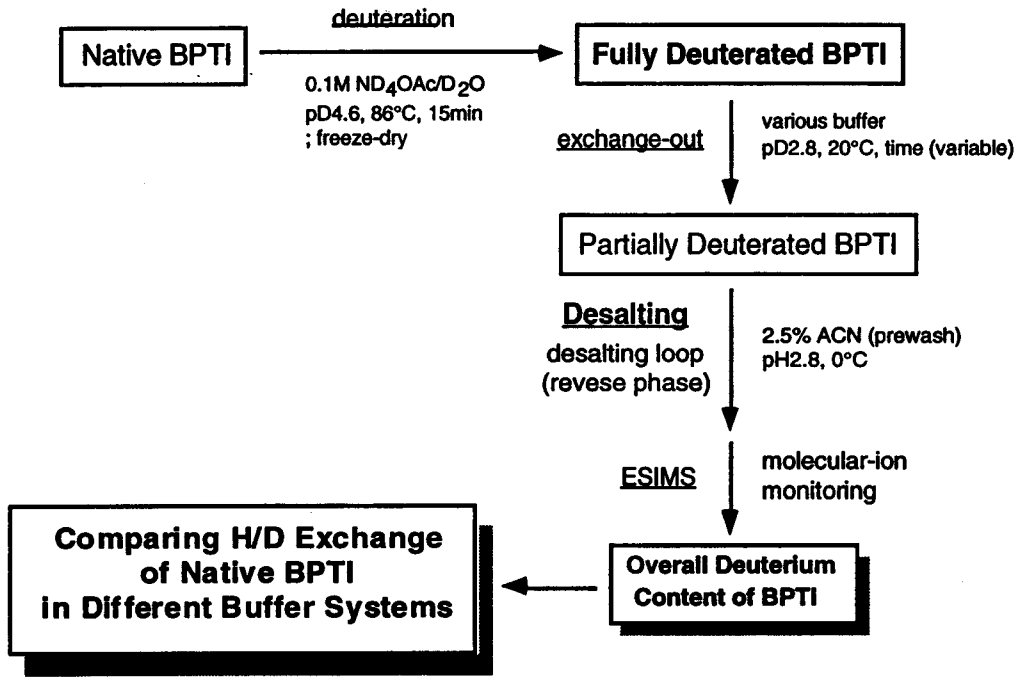

Scheme II.2-5: Strategy VIII

To mimic the microbore HPLC-ESIMS method for monitoring deuterium exchange-out, 27% acetonitrile with 0.1% TFA was forced into the ESI mass

spectrometer at a flow rate of 50 µl/min via the micro-desalting loop. To minimize deuterium loss during analysis, the eluting solvent was precooled to 0°C by using a sufficient length of stainless tube coil with larger ID, and all possible compartments including the injection port and outer tubing were immersed in an ice-bath. The overall strategy to determine the effect of different buffers on the deuterium exchange-out is depicted in **Scheme II.2-5.**

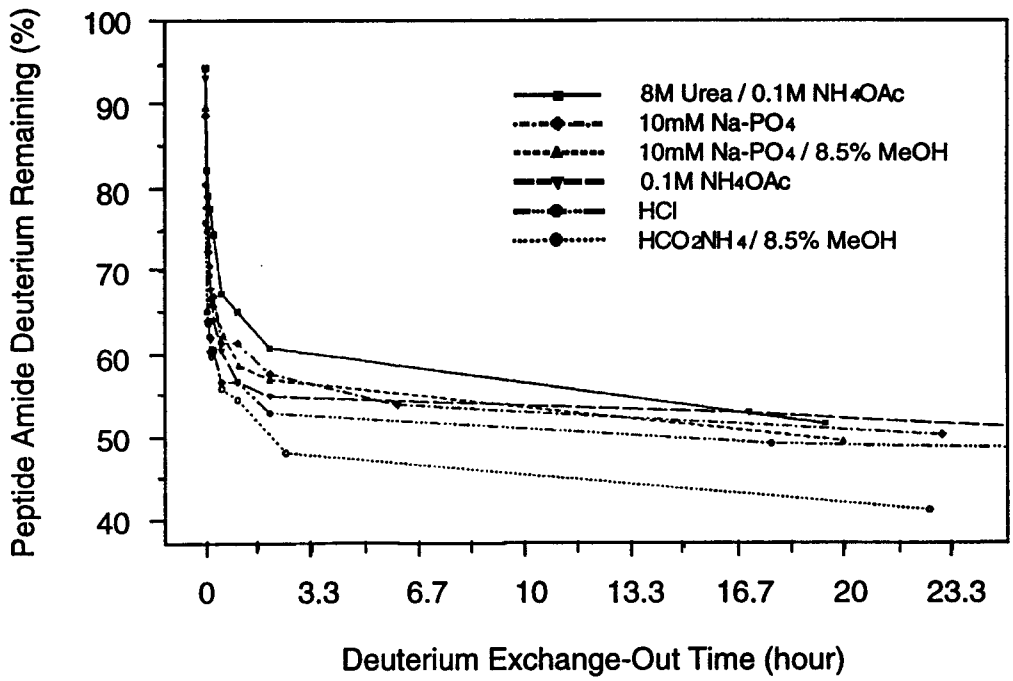

Figure II.2-36: Deuterium Exchange-Out of Fully Deuterated BPTI in Different Buffer Systems (pH 2.8, 20°C)

Deuterium exchange-out from fully deuterated BPTI was performed in six different buffer systems at pH 2.8 and 20°C. The results were plotted as a percentage of remaining peptide amide deuteriums versus exchange-out time (**Figure II.2-36** and **Table III.2-22~Table III.2-27**). Surprisingly, the slowest exchange of deuterium occurred in 8 M urea/0.1 M NH_4OAc buffer

system. This means that 8M urea is not a denaturing medium for native BPTI but rather a stabilizing medium for some peptide amide deuteriums. A similar retarding effect of 8 M urea on the H/D exchange rate of BPTI (30°C, pH 3.5) has been reported by Woodward and Kim.[66] Relatively fast exchange occurred in HCO_2H-NH_4OH/8.5% MeOH which is the buffer system used in the oxidation reactions. In this buffer, however 48% of the backbone amide deuteriums were still preserved after 2.5 hours incubation of the deuterated native BPTI at 20°C. After 22.6 hours under deuterium exchange-out conditions, 41% of the deuteriums remained. Other buffer systems showed relatively similar deuterium exchange-out behavior from the deuterated native BPTI.

Performic acid oxidation was performed on fully deuterated BPTI. The fully deuterated native BPTI was dissolved in HCO_2H-NH_4OH/8.5% MeOH and oxidized with the performic acid reagent (pH 2.8, -20°C, 2 hours). The product mixture was analyzed by microbore HPLC-ESIMS at 0°C (**Figure II.2-37**). Total ion chromatograms showed two peaks (**Figure II.2-37A**); the four oxygen atom-incorporated intermediate (BPTI+O_4) with a 17.8 mass unit increase (**Figure II.2-37B**) and the fully oxidized BPTI with 3.2 mass unit increase (**Figure II.2-37C**). Among 32 stabilized backbone amide deuteriums of fully deuterated native BPTI (**Figure II.2-34C**), only 10% of the amide deuteriums were preserved during performic acid oxidation whereas the oxidized intermediate (BPTI+O_4) preserved 56% of the amide deuteriums under the same conditions. This result clearly shows that even under slow H/D exchange condition (pH 2.8, -20°C), fully oxidized BPTI adopts a random coil structure and does not preserve it's deuterium labels on the backbone amide groups while the oxidized intermediate with a relatively compact structure retains it's deuteriums in the stabilized structural regions under the same condition.

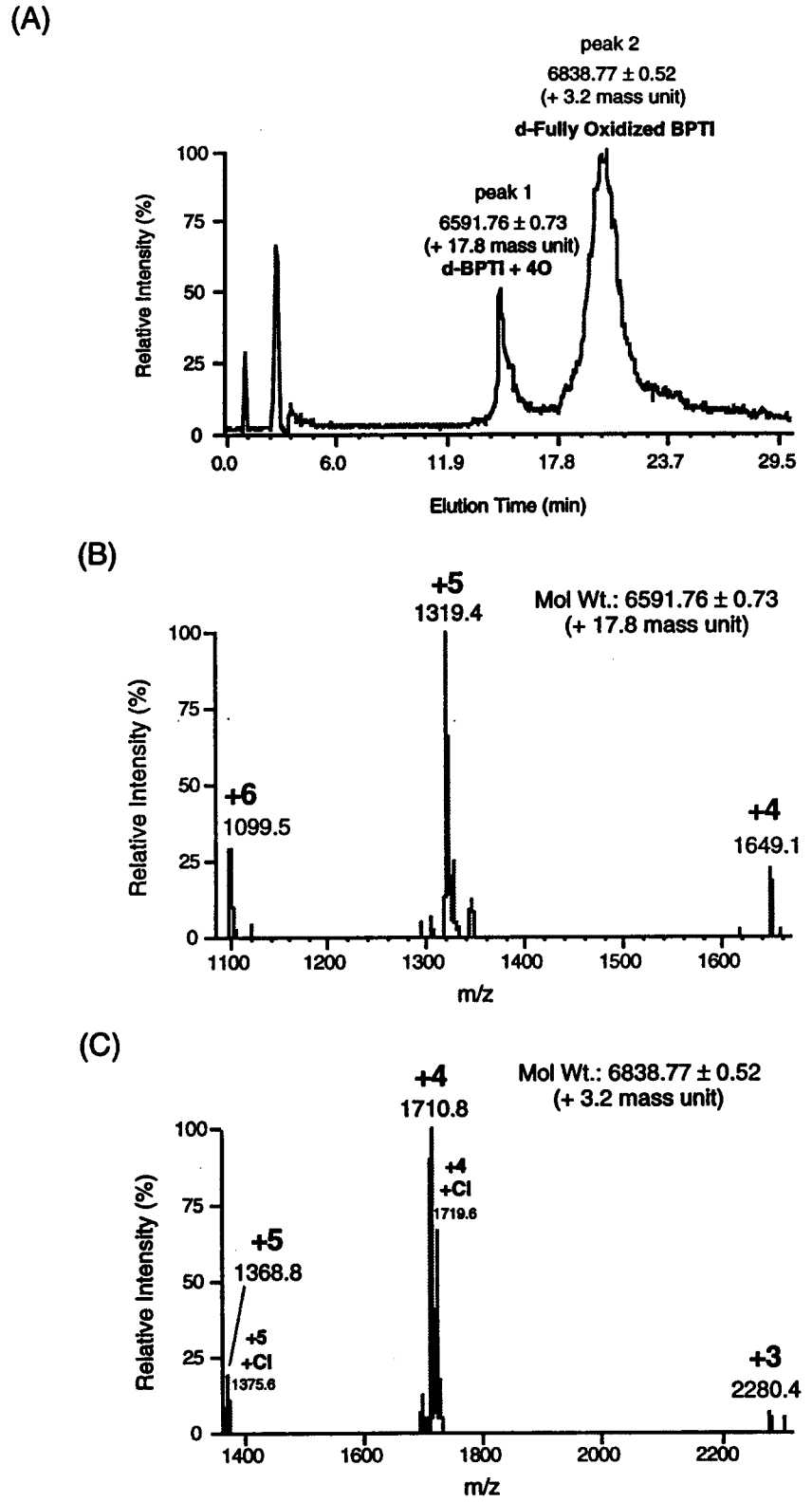

Figure II.2-37: (A) Total Ion Chromatogram of Deuterated Oxidized BPTI and Mass Spectra of (B) Peak 1 and (C) Peak 2

Pepsin digestion of the deuterated oxidized BPTI was performed directly after oxidation of fully deuterated BPTI, under the same digestion conditions (E//S=5, pH 2.0, 0°C, 5 min). As a control experiment, the normal oxidized BPTI which was derived from native BPTI treated with 0.1 M NH_4OAc at pH 4.6, 86°C and 15 min, was proteolyzed with immobilized pepsin (**Figure II.2-38**). A total of eight peptic peptides (P1-P3, P5, P6, P8 to P10), two oxidation intermediates (BPTI+O_4, BPTI+H_2O_8) and mono- and di-chlorinated peptides were identified.

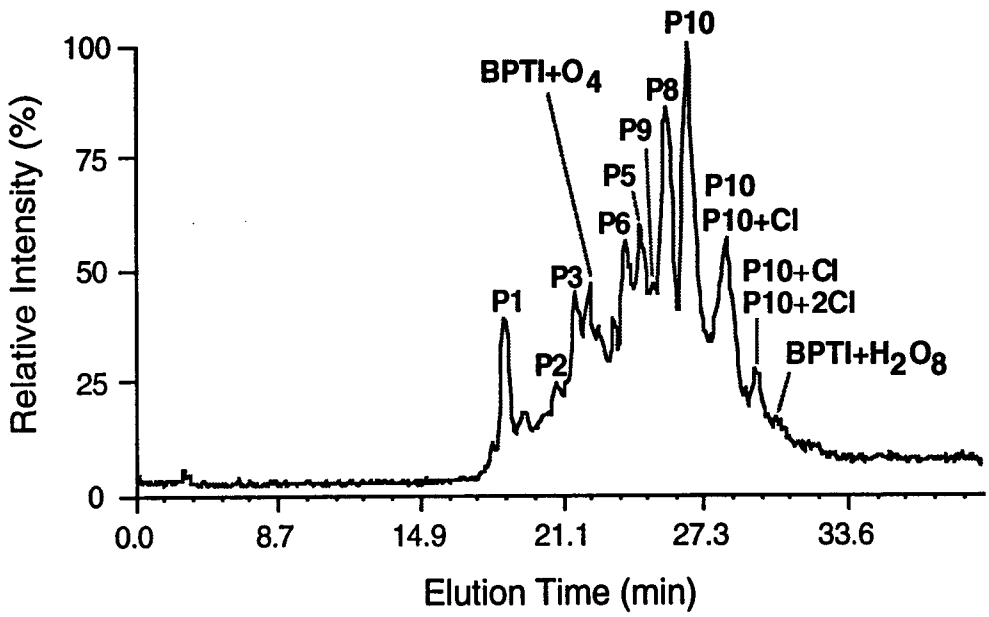

Figure II.2-38: Total Ion Chromatogram of Peptic Digest of Oxidized BPTI Derived from the Oxidation of Native BPTI with Performic Acid

The deuterated native BPTI was oxidized by performic acid and the oxidation product mixture was directly digested with immobilized pepsin (**Figure II.2-39**). The same peptic peptides were identified together with one of the oxidation intermediates (BPTI+O_4) which had 15.5 deuteriums retained after digestion. However, all eight peptic peptides showed mass spectra that were

identical to those of the corresponding controls. The peptic peptides showed no deuterium labels retained under these conditions.

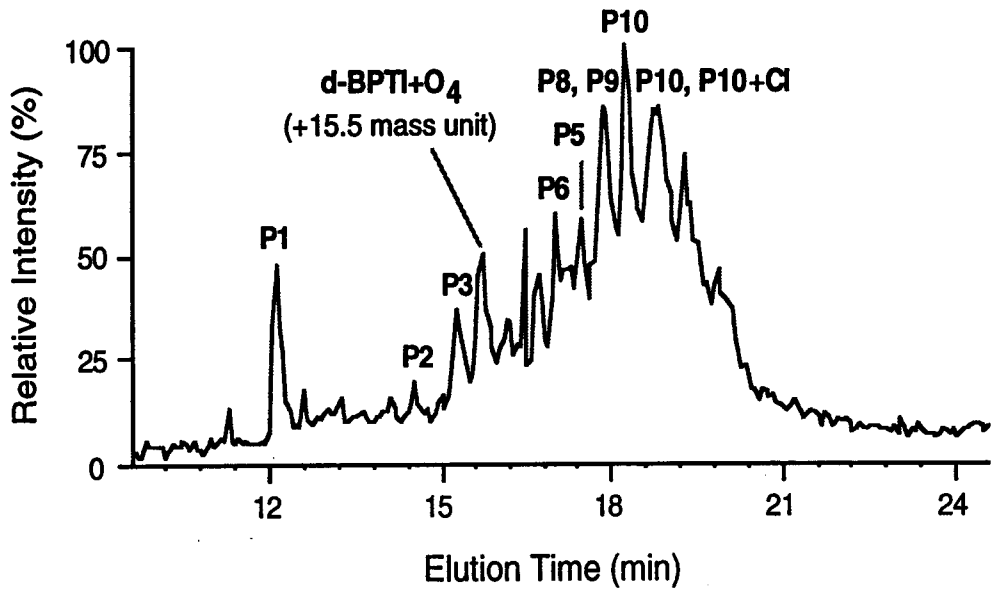

Figure II.2-39: Total Ion Chromatogram of Peptic Digest of Oxidized BPTI Derived from the Oxidation of Deuterated Native BPTI with Performic Acid

II.3 Conclusion

Electrospray Ionization Mass Spectrometry (ESIMS) has many inherent benefits over other analytical techniques. Thus, it is amenable to the analysis of biopolymers (~200 kDa of proteins) with exceptionally high sensitivity (pmol-fmol) and high mass accuracy (ppm). It is also fast (ms time scale) and can be used for continuous detection of analytes. Most importantly, it provides the only real method for introducing the effluents separated by high performance liquid chromatography (HPLC) or capillary electrophoresis directly into the mass spectrometer. The advent of the HPLC-MS system has made it possible to

study complex mixtures of peptides and proteins. Direct HPLC-MS analysis has been used for all aspects of protein structural features. Mass spectrometry has now been applied to solve the structural problems of peptides and proteins using hydrogen/deuterium (H/D) exchange as a structural probe and HPLC-MS as the important analytical tool for carrying out these measurements efficiently and with a high degree of accuracy.

Hydrogen/deuterium (H/D) exchange was monitored by continuous flow (CF)-ESIMS and by on-line microbore HPLC-ESIMS under slow exchange conditions (pH 2-3, 0°C, up to 10 min) to obtain structural information on a small peptide, melittin. H/D exchange and CF-ESIMS analysis of melittin was recently reported by Anderegg et. al (1994).[18] Our research goal for melittin analysis was to use H/D exchange result and the CF-ESIMS analytical method as a baseline information. The baseline data obtained were comparable to the previously reported results of Anderegg et. al.[18] Based on this baseline information for H/D exchange and CF-ESIMS analysis, H/D exchange experiments were performed on melittin using on-line microbore HPLC-ESIMS analysis. The structural data obtained, especially for monitoring deuterium exchange-out were almost identical to the baseline data obtained by monitoring deuterium exchange-in using CF-ESIMS. This provided confidence that the use of HPLC-ESIMS as a sample introduction and purification method would yield comparable results with H/D exchange and CF-ESIMS analysis.

To probe global structure fluctuations of melittin, H/D exchange was monitored at different solution pHs (pD 3.2 vs. pD 4.3), at different temperatures (0°C vs. 20°C vs. 60°C) and in different solvent systems (D_2O vs. 0.1% CD_3CO_2D/D_2O vs. $CD_3OD/D_2O/CD_3CO_2D$=80:20:2). H/D exchange coupled with ESIMS analysis is highly dependent on experimental parameters such as

pH, temperature and solvent composition similar to those required when using NMR spectroscopy and CD spectroscopy.[18,19]

The tandem mass spectrometric analysis of the +4-charge state molecular ion and the Y_{13}^{+2} fragment ion were carried out successfully to locate the two α-helical regions in melittin (Gly3-Leu13 and Ala15-Gln26). These result were comparable with the known data obtained by X-ray crystallography and NMR spectroscopy.[18,19]

H/D exchange coupled with ESIMS analysis was also applied to a model protein, i.e. bovine pancreatic trypsin inhibitor (BPTI). Global structure changes in native BPTI and modified BPTIs, were monitored using H/D exchange and ESIMS analysis using a continuous flow infusion mode for introducing the sample into the mass spectrometer. Native BPTI and selectively reduced BPTI which was carboxyamidomethylated at Cys14 and Cys38 (CAM(14,38)-BPTI) were subjected to H/D exchange conditions, i.e. in CH_3CO_2D/D_2O (pD 2.8, 20°C). During the first one-hour monitoring period, the kinetic profiles for the fast-exchanging hydrogens in both termini and side-chains of these molecules take place but the backbone amide hydrogens exchange too slowly to provide detailed kinetic information. Native BPTI and CAM(14,38)-BPTI in 10 mM sodium phosphate buffer showed very similar secondary structural elements in their CD spectra; 19.2% and 16.3% α-helix, 13.5% and 17.3% β-sheet, and 28.8% and 26.9% β-turn for native BPTI and CAM(14,38)-BPTI, respectively. This is also reflected in the kinetics of H/D exchange. Thus, it appears that the integrity of secondary structural elements are not dependent on the disulfide linkage between C14 and C38. On the other hand, oxidized BPTI and reduced BPTI showed characteristics of random-coil molecules and these two molecules showed very similar H/D exchange behavior. Most of the hydrogens were exchanged within the first hour. The CD spectra of these molecules showed

that oxidized and reduced BPTI adopted random coil-like structures; 8.6% and 7.8% α-helix, 17.3% and 13.7% β-sheet, and 30.8% and 33.3% β-turn, respectively. From these results, one might conclude either that certain disulfide bridges are necessary for BPTI to retain the secondary and tertiary structure of the native state, or that the consequence of chemical reactions cause modifications in the primary structure such that native-like behavior is no longer possible. If the oxidized and reduced BPTI kinetic profiles are compared, it appears that oxidation does indeed causes structure modifications that are related to the presence of oxidized amino acid residues, i.e. cysteic acids and methionine sulfone, while reduction of all the disulfide linkages leads to loss most of the native-like structure. Thus, it appears that the chemical modifications, as well as the loss of the disulfide linkages alters the native structure, but the way these structures are altered in the oxidized and reduced structures are different. Creighton has argued that disulfide linkages are necessary for BPTI to adopt the native structure. From these kinetic results however, only those disulfide bonds between Cys5 and Cys55, and Cys30 and Cys50 are necessary, but the disulfide bond between Cys14 and Cys38 is not.

The proteolytic digestion of the protein is essential because the intact BPTI molecule is relatively large and complete sequence information cannot be provided directly by ESIMS/MS. However, native BPTI is indigestible with pepsin under slow H/D exchange conditions (pH 2.0, 0°C, up to 30 min). Therefore, chemical reductions and oxidations experiments must be carried out to cleave the three disulfide bonds in native BPTI (C5-C55, C14-C38, C30-C50) prior to the digestion. Unfortunately, all reducing agents, such as tris-(2-carboxyethyl)-phosphine hydrochloride (TCEP·HCl; up to pH 4.0, 0°C, 10 min), Zn/HCl (pH 2.0, 0°C, up to 30 min), $NaCNBH_3$/AcOH (pH 2.0, 0°C, up to 30 min) with or without 8 M urea and organic solvents, failed to provide completely

reduced BPTI. Although native BPTI was indigestible with immobilized pepsin under the same slow exchange conditions, completely reduced BPTI obtained using TCEP·HCl (pH 3.0, 70°C, 10 min) or DTT (pH 8.5, 39°C, 30 min), was completely digested (E/S=5, pH 2.0, 0°C, 5 min) and gave 15 peptic peptides with high reproducibility. This allowed for complete sequence information to be obtained when analyzed by tandem mass spectrometry.

Native BPTI was successfully oxidized with performic acid in a buffer system consisting of HCO_2H-NH_4OH/8.5% MeOH (pH 2.8, -20°C, 2 hrs) and yielded completely oxidized BPTI as well as oxidation intermediates (BPTI+O_4, BPTI+H_2O_8). Oxidized BPTI could be completely digested with immobilized pepsin. A total of 11 peptic peptides were identified, which yielded the complete sequence when analyzed by ESIMS/MS. This is the first time success achieved with the pepsin-digestion of BPTI under conditions that would minimize exchange of amide hydrogens. From the experiments performed in these investigations it is clear that native BPTI is an extremely stable protein that is relatively impervious to protease, and even certain chemical reactions. The difficulty of reducing the disulfide linkages except under basic conditions, as well as more stringent requirements to oxidize the molecule testifies to its stability and compactness. The extraordinary stability of the protein may be the cause that leads to difficulties in the H/D exchange experiments.

H/D exchange experiments was performed on native BPTI. After oxidation and digestion of the deuterated native BPTI, no deuterium labels were retained in the peptic peptides. In the HCO_2H-NH_4OH/8.5% MeOH buffer alone, deuteriums were retained during the deuterium exchange-out from fully deuterated BPTI even at 20°C. In addition, the oxidation intermediate (BPTI+O_4) showed some remaining deuterium labels. Therefore, the HCO_2H-NH_4OH/8.5% MeOH buffer system used for performic acid oxidation was not

responsible for the global loss of deuteriums, but rather the loss of the labels occurred during the oxidation reaction. One contributing factor to the global loss of the deuterium labels may be the length of time it takes for the oxidation to go to completion. A relatively long reaction time (2 hrs) is required when performic acid oxidation is carried out at -20°C to obtain oxidized BPTI. Once oxidized, BPTI adopts a completely open structure, and under these conditions, amide deuteriums within the oxidized BPTI can be exchanged to hydrogens during the 2 hour-oxidation period.

But this may be only a partial explanation. The half-life for peptide amide hydrogen exchange in open structure is about 50 min at pH 2.5 and 0°C in water-based solvent system. The rate of exchange decreases about three fold per 10 degrees decrease in temperature. Therefore, under the oxidation conditions used (-20°C, 2 hr), the 10% of backbone amide deuteriums (3.2 ND) retained after oxidation of fully deuterated BPTI is surprisingly low. Even though the results obtained for open structured oxidized BPTI is inconsistent with the rate of exchange for open protein structures generally, it is clear from the experiments performed here, that the openness of the oxidized BPTI molecule is a major contribution to the high exchange rate. Thus, an oxidation intermediate (BPTI+O_4) showed 17.8 deuteriums (60%) retained after oxidation of deuterated BPTI and 15.5 (49%) after pepsin digestion. According to the HPLC profile and H/D exchange experiments, it is highly possible that this molecule adopts a native-like structure because of the intact disulfide bonds. Therefore, deuteriums in the native-like structural regions of the protein are not available for exchange, and these deuteriums are retained under the oxidation condition used.

Although oxidized BPTI retained only 10% of the backbone amide deuteriums (3.2 ND), this result clearly shows that it is possible for more

deuterium labels to be retained after oxidation. Most likely, the reaction period must be shorter. Therefore, it is worthwhile to apply the performic acid oxidation protocol to BPTI folding intermediates or other model proteins with relatively more open structures that can be easily oxidized during a shorter reaction period. Furthermore, in these relatively open structure proteins, there is the possibility that these proteins can be reduced sufficiently rapidly under the reduction conditions which were used for BPTI. The reduction method would be an advantage since it can give more simple and specific reaction products than performic acid oxidation and also yield a protein with more native-like character.

III. Experimental

Sequencing grade melittin, bovine pancreatic trypsin inhibitor (BPTI), dithiothreitol (DTT) and iodoacetamide were purchased from Sigma. Melittin was used without further purification, but BPTI was purified by semi-preparative HPLC. Tris-(2-carboxyethyl)-phosphine hydrochloride and an immobilized pepsin gel (50% weight) were purchased from Pierce. Formic acid (98%), urea, trifluoroacetic acid, sodium hydroxide (1N), ammonium hydroxide (1N), hydrochloric acid (1N), and acetic acid (> 99.5%) were purchased from Fluka Biochemika. Hydrogen peroxide solution (30%) and ammonium hydroxide (29.6%) were purchased from Mallinckrodt Chemical and Fisher Scientific, respectively. Microfilterfuge tubes with uncharged Nylon 66-membrane (0.45 μm pore size) from Rainin were used for microfiltration of pepsin digests. All deuterated solvents were purchased from Aldrich. All organic solvents were HPLC grade and water was purified by a Milli-Q water purification system. The performic acid reagent was prepared in a 5 ml Reacti vial from Pierce. Chemical reactions, pepsin-digestion and their HPLC fractionation were performed in 1.5 ml Eppendorf tubes. All liquid samples were evaporated on a Savant speed-vac concentrator or freeze-dried on Labconco freeze dry/shell freeze system. In the performic acid oxidation reaction, the Labconco shell freeze unit was used to maintain a cooling bath temperature of -20°C using 95% technical grade EtOH as cooling solvent. CD experiments were perform on a Jasco J720 Spectropolarimeter. The optical density (OD) was determined on a Cary 15 spectrophotometer. In both CD and OD experiments, a Hellma cylindrical cell with a 100 μm path length was used. For HPLC analysis, 0.1% TFA/H_2O was used as eluent A and 0.08% TFA/CH_3CN as eluent B. Vydac

protein/peptide reverse phase columns (C-4 and C-18) with 5 μm pore sizes and dimensions of 0.46 x 25 cm for analytical HPLC and of 1.0 x 25 cm for semi-preparative HPLC were used. The HPLC instrumentation consisted of a Beckman HPLC model 100A system, a model 421 controller and a Waters 486 tunable absorbance detector. For microbore HPLC analysis, an Applied Biosystems (ABI) 140B solvent delivery system equipped with a Rheodyne model 8125 injector and an ABI 759A absorbance detector was used. Flow rates were 40-50 μl/min. A Michrom BioResources peptide/protein concentration/desalting trap cartridge loop with cartridge dimensions of 1.0 x 10 mm was installed in the Rheodyne model 8125 injector. A Harvard Apparatus syringe pump was used to obtain a flow rate of 3-10 μl/min. An Aquapore reverse phase column (C-8) with 300 μm particle size, 7 μm pore size and dimensions of 1.0 x 10 mm was used for the microbore HPLC analysis of melittin. Vydac protein/peptide reverse phase columns (C-4, C-8) with 5 μm pore sizes and dimensions of 1.0 x 10 mm (C-4, C-8) and 1.0 x 250 mm (C-18) were used for microbore HPLC analysis of BPTI and pepsin digests. Fused silica capillary tubing with dimensions of 75 μm ID x 145 μm OD (Polymicro Technology), was used to couple the liquid effluent to the ESI mass spectrometer. A Perkin-Elmer Sciex API III Plus ionspray mass spectrometer equipped with a triple quadrupole mass analyzer was used in the positive ion mode. Air was used as the nebulizer gas and nitrogen as curtain gas. The collision gas was a mixture of nitrogen and argon in a volume ratio of 9 to 1. Fast atom bombardment (FAB) mass spectrometric analysis was performed on a Kratos MS50TC instrument. Matrix assisted laser desorption/ionization-time of flight mass spectrometric analysis (MALDI-TOFMS) was performed on a custom built instrument with a Nd:YAG laser from Spectra Physics (350 nm).

III.1 H/D Exchange of Melittin

III.1-1 Monitoring Deuterium Incorporation into Melittin by Continuous Flow Infusion-ESIMS and -ESIMS/MS

III.1-1-1 Temperature Dependence of Deuterium Exchange-In of Melittin

Melittin (5 μg) was dissolved in $CD_3OD/D_2O/CD_3CO_2D$=80:20:2 (350 μl, pD 3.2) at 0°C and 20°C, respectively and immediately analyzed by CF-ESIMS at 3.3 μl/min flow rate. The +3-, +4-, and +5-charge state molecular ions were monitored at 80 V orifice potential, m/z 560-970, 0.2 Da step size, 0.7 ms dwell time and 3.5 sec/scan speed. Deuterium incorporation (% H) and the number of hydrogens remaining as a function of H/D exchange time (t) were determined (**Table III.1-1**, **Table III.1-2**).

Table III.1-1: Monitoring Deuterium Incorporation into Melittin in $CD_3OD/D_2O/CD_3CO_2D$ (=80:20:2, pD 3.2) at 0°C by CF-ESIMS Analysis

Time t (min)	Molecular Weight (Da)	Deuterium Incorporation (% H)	H_t
0.0	2845.6	0.0	50
1.33	2871.1	51.0	24.6
4.17	2872.7	54.2	23.1
6.17	2873.5	55.8	22.3
8.15	2874.3	57.4	21.5
10.30	2875.9	60.6	19.9
13.92	2876.7	62.2	19.1
22.07	2876.7	62.2	19.1
32.80	2878.3	65.4	17.5
42.22	2878.3	65.4	17.5
51.08	2878.3	65.4	17.5
61.34	2879.1	67.0	16.7
92.45	2879.9	68.6	15.9
151.6	2881.5	72.6	14.3
330.0	2883.9	76.6	11.9
435.0	2883.9	76.6	11.9
1050	2886.3	81.4	9.54
1860	2886.3	81.4	9.54

Table III.1-2: Monitoring Deuterium Incorporation into Melittin in $CD_3OD/D_2O/CD_3CO_2D$ (=80:20:2, pD 3.2) at 20°C by CF-ESIMS Analysis

Time t (min)	Molecular Weight (Da)	Deuterium Incorporation (% H)	H_t
0.0	2845.6	0.0	50
3.2	2880.7	70.2	15.1
3.9	2880.7	70.2	15.1
4.6	2880.7	70.2	15.1
5.3	2881.5	71.8	14.3
6.0	2882.3	73.4	13.5
6.7	2883.1	75.0	12.7
7.3	2883.9	76.6	11.9
8.0	2884.7	77.2	11.1
8.7	2884.7	77.2	11.1
10.1	2885.5	79.8	10.3
10.8	2885.5	77.2	10.3
11.5	2886.3	81.4	9.5
13.2	2887.1	83.0	8.8
16.7	2887.9	84.6	8.0
18.4	2888.7	86.2	7.2
20.2	2888.7	86.2	7.2
21.9	2889.5	87.8	6.4
23.9	2889.5	87.8	6.4
27.0	2889.5	86.8	6.4
30.5	2890.3	89.4	5.6
32.2	2890.3	89.4	5.6
34.0	2890.3	89.4	5.6
37.5	2890.3	89.4	5.6
40.9	2890.3	89.4	5.6
44.4	2891.1	91.0	4.8
46.1	2891.1	91.0	4.8
∞	2895.6	100	0

III.1-1-2 pH and Solvent Dependence of Deuterium Exchange-In of Melittin

Melittin (16.6 μg) was dissolved in D_2O (330 μl, 17 μM, pD 4.3) at 20°C and immediately analyzed by CF-ESIMS at 5 μl/min flow rate. The +3-, +4-, and +5-charge state molecular ions were monitored at 80 V orifice potential, m/z 571-1000, 0.2 Da step size, 1.4 ms dwell time and 3.1 sec/scan speed (**Table III.1-3**). Melittin (17.4 μg) was dissolved in 0.1% CD_3CO_2D/D_2O (12.2 μM, pD 3.2) and immediately analyzed by CF-ESIMS at 20°C (**Table III.1-4**). The orifice potential 80 V, a mass range of m/z 560 to 1000, 0.2 Da step size, 1.4 ms

dwell time and 3.2 sec/scan speed were used. The molecular weight increases as a function of time in D_2O, 0.1% CD_3CO_2D/D_2O and $CD_3OD/D_2O/CD_3CO_2D$ (80:20:2) at 20°C were recorded and compared. Deuterium incorporation (% H) and the number of hydrogens remaining as a function of H/D exchange time (t) were determined.

Table III.1-3: Monitoring Deuterium Incorporation into Melittin in D_2O (pD 4.3) at 20°C by CF-ESIMS Analysis

Time t (min)	Molecular Weight (Da)	Deuterium Incorporation (% H)	H_t
0.0	2845.6	0.0	50
1.17	2893.0	94.8	3.0
2.0	2893.4	95.6	2.6
4.1	2893.8	96.4	2.2
8.0	2893.8	96.4	2.2
16.0	2894.2	97.2	1.8
30.0	2894.4	97.6	1.6
45.0	2894.8	98.4	1.2
60.1	2895.4	99.6	0.6
∞	2895.6	100	0

Table III.1-4: Monitoring Deuterium Incorporation into Melittin in 0.1% CD_3CO_2D/D_2O (pD 3.2) at 20°C by CF-ESIMS Analysis

Time t (min)	Molecular Weight (Da)	Deuterium Incorporation (% H)	H_t
0.0	2845.6	0.0	50
1.1	2879.7	68.2	16.4
2.1	2884.9	78.6	11.2
3.1	2887.3	83.4	8.8
4.1	2888.1	85.0	8.0
6.0	2889.2	87.2	6.9
10.1	2891.0	90.8	5.0
15.0	2892.0	92.8	4.0
19.4	2893.1	95.0	3.0
22.2	2893.2	95.2	2.9
25.5	2893.7	96.2	2.4
30.0	2894.0	96.8	2.1
45.0	2894.1	97.0	2.0
60.0	2894.2	97.2	1.9
∞	2895.6	100	0

III.1-1-3 CF-ESIMS/MS Analysis of +4-Charge State Molecular Ion

Melittin was dissolved in $CD_3OD/D_2O/CD_3CO_2D$=80:20:2 (10 μM, pD 3.2) at 20°C and immediately analyzed by CF-ESIMS/MS. The +4-charge state molecular ions at 3.3 μl/min flow rate (**Figure II.1-10**) were used as the precursor ion for collisional activation. At 80 V orifice potential, a mass range of m/z 50 to 1550, 0.2 Da step size and 0.7 ms dwell time were used. The mass increases from the fragment ions of the m/z 723 (+4) ion as the precursor ion were continuously monitored during the first 30 minute periods. To improve the sensitivity for fragment ion detection, the first quadrupole (MS 1) was scanned for the parent ion in a defocused mode. This encompassed the ions in the selected parent ion region by ± 5-10 mass units. The third quadrupole (MS 2) was scanned in the regular scan mode. Five to ten scans were averaged. The mass shifts in each fragment ions at 4 min-, 7 min-, 11 min- and 19 min-exchange, were determined (**Table II.1-1**).

III.1-1-4 CF-ESIMS/MS Analysis of Y_{13}^{+2} Fragment Ion

Melittin was dissolved in $CD_3OD/D_2O/CD_3CO_2D$=80:20:2 (20 μM, pD 3.2) at 20°C and immediately analyzed by CF-ESIMS/MS for the Y_{13}^{+2} fragment ions at 3.3 μl/min flow rate. An orifice potential of 120 V, a mass range of m/z 50 to 1550, 0.2 Da step size and 0.7 ms dwell time were used. The mass increases in the fragment ions from the m/z 825 (Y_{13}^{+2}) ion as parent ion were continuously monitored under the defocused mode of the first quadrupole (MS1) as a function of the deuterium exchange-in time (min) for 30 minutes. Five to ten scans were averaged. The mass shifts of each fragment ion after 4

min, 7 min, 11 min and 19 min of deuterium exchange-in, were determined (**Table II.1-2**).

III.1-1-5 Locating Secondary Structural Regions in Melittin

The mass shifts of the fragment ions observed by CF-ESIMS/MS analyses of the +4-charge state molecular ions and of the Y_{13}^{+2} fragment ion, were converted into the number of hydrogens remaining at each amino acid residue. The results were plotted for each residue of melittin at different deuterium exchange-in times (4 min, 7 min, 11 min and 19 min, **Table III.1-5**).

Table III.1-5: Number of Hydrogens Remaining in Each Amino Acid Residue of Melittin After a Period of Deuterium Exchange-In Time

Amino Acid Residue	4 min	7 min	11 min	19 min
G	-	-	-	-
I	-	-	-	-
G	0.4	0.2	0.2	0.2
A	0.3	0.3	0.1	0.1
V5	0.4	0.2	0.2	0.2
L	0.4	0.6	0.4	0.4
K	0.9	0.5	0.4	0.4
V	0.7	0.6	0.3	0.2
L	0.5	0.4	0.4	0.3
T10	0.7	0.5	0.3	0.5
T	0.7	0.6	0.7	0.4
G	0.2	0.2	0.4	0.4
L	0.2	0.2	0.2	0.2
P	0.1	0.2	0.1	0.0
A15	0.3	0.2	0.2	0.2
L	0.3	0.4	0.3	0.2
I	0.4	0.6	0.3	0.2
S	0.6	0.5	0.2	0.3
W	0.7	0.8	0.3	0.4
I20	1.0	0.8	0.7	0.4
K	0.9	0.9	0.6	0.2
R	1.0	1.0	0.9	0.4
K	1.0	0.9	0.7	0.4
R	0.9	1.0	0.7	0.1
Q25	-	-	-	-
Q	-	-	-	-

III.1-2 Monitoring Deuterium Incorporation into Melittin by HPLC-ESIMS and -ESIMS/MS

III.1-2-1 Temperature Dependence of Deuterium Exchange-In of Melittin

Melittin (57 μg) was dissolved in $CD_3OD/D_2O/CD_3CO_2D$=80:20:2 (500 μl, 40 μM, pD 3.2) at 20°C, 0°C and 60°C, respectively. Aliquots (5 μl, 200 pmole) were taken after a predetermined period of deuterium exchange-in time and immediately injected onto the microbore HPLC-ESIMS system with an Aquapore reverse phase column (C-8) in an ice-bath. Alternatively, aliquots (10 μl) were sampled according to their predetermined deuterium exchange-in times and frozen in liquid nitrogen for future analysis. These frozen samples were thawed in an ice-bath and aliquots (5 μl, 200 pmole) were quickly analyzed by microbore HPLC-ESIMS under slow H/D exchange conditions. The microbore HPLC conditions used, were; 0.1% TFA/H_2O as eluent A, 0.08% TFA/CH_3CN as eluent B, where 30% B was maintained for 1 min, and then raised from 30 to 95% gradient over a period of 20 min at 50 μl/min flow rate. The melittin peak was eluted within a retention time range of 8-10 min. The mass shifts in molecular ion peaks were monitored as a function of exchange-in time (t). Deuterium incorporation into peptide amide hydrogens (% ND) and the number of peptide amide hydrogens remaining (NH_t) after a predicted deuterium exchange-in time (t), were calculated (**Table III.1-6** to **Table III.1-8**).

Table III.1-6: Monitoring Deuterium Incorporation into Melittin in $CD_3OD/D_2O/CD_3CO_2D$ (=80:20:2, pD 3.2) at 20°C by HPLC-ESIMS Analysis

Time t (min)	Molecular Weight (Da)	Deuterium Incorporation (% ND)	NH_t
0	2845.6	0.0	24
1	2849.6	16.7	20.2
3	2850.4	20.0	19.2
5	2853.6	33.3	15.8
10	2856.8	46.7	13.4
30	2861.6	66.7	8.3
60	2864.0	76.7	5.6
120	2867.2	90.0	2.5
360	2868.0	93.0	1.8

Table III.1-7: Monitoring Deuterium Incorporation into Melittin in $CD_3OD/D_2O/CD_3CO_2D$ (=80:20:2, pD 3.2) at 0°C by HPLC-ESIMS Analysis

Time t (min)	Molecular Weight (Da)	Deuterium Incorporation (% ND)	NH_t
0	2845.6	0.0	24
1	2849.6	16.7	20.5
3	2849.6	16.7	20.5
6	2849.6	16.7	20.5
12	2850.4	20.0	19.8
30	2851.2	23.3	18.5
65	2852.8	30.0	17.1
120	2854.4	36.7	15.2
180	2856.8	46.7	13.1
374	2858.4	53.3	11.4
720	2861.6	66.7	5.9
1020	2864.0	76.7	4.9
1296	2864.0	76.7	4.9
2031	2864.0	76.7	4.9
3105	2864.8	80.0	4.5
4357	2865.6	83.3	3.5

Table III.1-8: Monitoring Deuterium Incorporation into Melittin in $CD_3OD/D_2O/CD_3CO_2D$ (80:20:2, pD 3.2) at 60°C by HPLC-ESIMS Analysis

Time t (min)	Molecular Weight (Da)	Deuterium Incorporation (% ND)	NH_t
0	2845.6	0.0	24
1	2867.2	90	2.5
5	2869.6	100	0
∞	2869.6	100	0

III.1-2-2 HPLC-ESIMS/MS Analysis of +4-Charge State Molecular Ion

Melittin (62 μg) was dissolved in $CD_3OD/D_2O/CD_3CO_2D$=80:20:2 (100 μl, 218 μM, pD 3.2) at 20°C. Aliquots (10 μl) were sampled after 4 min, 11 min and 19 min under deuterium exchange-in conditions and immediately frozen in liquid nitrogen. After thawing the frozen samples at 0°C, microbore HPLC-ESIMS/MS analysis of the 5 μl aliquot (1.1 nmole) was performed under slow H/D exchange conditions used previously. HPLC-ESIMS/MS was performed on the +4-charge state molecular ion (m/z 715) of deuterated melittin in the defocused mode (MS1) and at an 80 V orifice potential. The nebulizer gas pressure was 48 psi and the curtain gas flow rate was 1.2 l/min. The mass range of m/z 50-1300 was scanned with 0.2 Da step size and 1.0 ms dwell time. After averaging ten scans, the mass shifts of each fragment ions at 4 min-, 11 min- and 19 min-exchange, were determined (**Table II.1-3**).

III.1-2-3 HPLC-ESIMS/MS Analysis of Y_{13}^{+2} Fragment Ion

Melittin (400 μg) was dissolved in $CD_3OD/D_2O/CD_3CO_2D$=80:20:2 (100 μl, 1.4 mM, pD 3.2) at 20°C. Aliquots (5 μl, 7 nmole) were sampled after exposure of the sample to deuterium exchange-in conditions for 4 min, 11 min and 19 min. The aliquots were analyzed by microbore HPLC-ESIMS/MS at 120 V orifice potential under the same slow H/D exchange conditions used previously. After averaging 10 scans, the mass shifts of each fragment ion at 4 min-, 11 min- and 19 min-exchange were determined (**Table II.1-4**).

III.1-2-4 Locating Secondary Structural Regions in Melittin

The mass shifts in the fragment ions observed from the HPLC-ESIMS/MS analysis of the +4-charge state molecular ions and of the Y_{13}^{+2} fragment ion, were converted into the number of hydrogens remaining at each amino acid residue. The results were plotted for the melittin sequence at different deuterium exchange-in times (4 min, 11 min and 19 min, **Table III.1-9**).

Table III.1-9: Number of Hydrogens Remaining in Each Amino Acid Residue of Melittin After a Period of Deuterium Exchange-In Time

Amino Acid Residue	4 min	11 min	19 min
G	-	-	-
I	-	-	-
G	0.55	0.55	0.25
A	0.80	0.65	0.65
V5	0.62	0.65	0.76
L	0.68	0.60	0.48
K	1.00	1.00	0.80
V	0.90	0.30	0.40
L	1.10	1.20	0.98
T10	0.70	0.60	0.40
T	0.80	1.20	1.10
G	0.90	0.70	0.50
L	0.30	0.20	0.10
P	0.00	0.00	0.00
A15	0.85	0.85	1.00
L	1.00	0.90	0.85
I	0.50	0.50	0.10
S	0.70	1.00	1.20
W	0.90	0.40	0.00
I20	0.30	0.30	0.40
K	0.90	0.90	0.50
R	0.60	0.70	0.40
K	0.48	0.15	0.00
R	0.48	0.25	0.10
Q25	-	-	-
Q	-	-	-

III.1-3 Monitoring Hydrogen Incorporation into Fully Deuterated Melittin by HPLC-ESIMS and -ESIMS/MS

III.1-3-1 HPLC-ESIMS Analysis of Deuterium Exchange-Out from Fully Deuterated Melittin

Melittin (50 μg) was fully deuterated in D_2O (875 μl) at room temperature for 2 hr and subjected to lyophilization. The fully deuterated melittin (57 μg) was dissolved in MeOH/H_2O/AcOH=80:20:2 (500 μl, 40 μM, pH 3.2) at 20°C. Aliquots (5 μl, 200 pmole) were immediately analyzed by microbore HPLC-ESIMS under the slow H/D exchange conditions at 80 V orifice potential. The mass range of m/z 705-955 was scanned under the conditions of 0.1 Da step size, 1.0 ms dwell time and 2.63 sec/scan speed. The mass decreases in the molecular ions were determined and the hydrogen incorporation in peptide amide deuteriums (% NH) and the number of peptide amide deuterium remaining after a predicted deuterium exchange-out time t (ND_t) were calculated (**Table III.1-10**).

Table III.1-10: Monitoring Hydrogen Incorporation into Fully Deuterated Melittin in $CH_3OH/H_2O/CH_3CO_2H$ (=80:20:2, pH 3.2) at 20°C by HPLC-ESIMS

Time t (min)	Molecular Weight (Da)	Hydrogen Incorporation (% NH)	ND_t
0.0	2869.6	0.0	24
0.5	2863.1	24.6	18.0
1.0	2862.6	26.7	17.1
4.0	2858.4	44.2	13.1
11	2854.6	60.0	9.2
30	2850.6	76.7	5.4
60	2849.1	83.1	3.9
∞	2845.6	100	0

III.1-3-2 HPLC-ESIMS/MS Analysis of +4-Charge State Molecular Ion

To provide the results at time 0 min, the fully deuterated melittin (100 μg) was dissolved in $CD_3OD/D_2O/CD_3CO_2D$ (=80:20:2, 86 μl, 400 μM, pD 3.2) at 20°C and an aliquot (20 μl, 2 nmole) was analyzed by microbore HPLC-ESIMS/MS using m/z 718 as a parent ion and at 80 V orifice potential under slow H/D exchange conditions. Fully deuterated melittin (100 μg) was dissolved in $MeOH/H_2O/AcOH$=80:20:2 (86 μl, 400 μM, pH 3.2) at 20°C. Aliquots (20 μl, 2 nmole) were taken after 4 min, 11 min and 19 min under deuterium exchange-out conditions. The 4 min- and 11 min-exchange aliquots were analyzed using the m/z 715 parent ions. Microbore HPLC-ESIMS/MS at an orifice potential of 80 V in the defocused mode (MS1) under slow H/D exchange conditions was used. The 19 min-exchange aliquot was analyzed using the m/z 713 as a parent ion. The mass range of m/z 68 to 1550 was scanned with 0.2 Da step size and 0.7 ms dwell time. The mass shifts in each fragment ion at 0 min and after 4 min, 11 min and 19 min of deuterium exchange-out, were determined (**Table II.1-5**).

III.1-3-3 HPLC-ESIMS/MS Analysis of Y_{13}^{+2} Fragment Ion

Fully deuterated melittin (100 μg) was dissolved in $CD_3OD/D_2O/CD_3CO_2D$=80:20:2 (57.3 μl, 603 μM, pD 3.2) at 20°C, which provided the sample for the 0 min exchange-out time. Aliquots (5 μl, 3 nmole) were analyzed by microbore HPLC-ESIMS/MS using the m/z 818 parent ion and at an 120 V orifice potential under slow H/D exchange conditions. The fully deuterated melittin (100 μg) was dissolved in $MeOH/H_2O/AcOH$=80:20:2 (57.3 μl, 603 μM,

pH 3.2) at 20°C. Aliquots (5 μl, 3 nmole) were taken after 4 min, 11 min and 19 min deuterium exchange-out times. The 4 min-and the 11 min-exchange-out aliquots were analyzed by microbore HPLC-ESIMS/MS using the m/z 815 parent ions and at an 120 V orifice potential using the defocused mode (MS1) under slow H/D exchange conditions. The 19 min-exchange-out aliquot was analyzed using the m/z 813 parent ion. A mass range of 60 to 1350 was scanned at 0.2 Da step size and 0.7 ms dwell time. The mass shifts in each fragment ion at 0 min and after 4 min, 11 min and 19 min of deuterium exchange-out, were determined (**Table II.1-6**).

III.1-3-4 Locating Secondary Structural Regions of Fully Deuterated Melittin

The mass shifts in the fragment ions from the +4-charge state molecular ions and from the Y_{13}^{+2} fragment ion of the fully deuterated melittin were converted into the number of deuteriums remaining at each amino acid residue. The results were plotted for each amino acid residue in melittin at different deuterium exchange-out times (0 min, 4 min, 11 min and 19 min, **Table III.1-11**).

III.1-3-5 CD Spectra of Melittin in Different Solvent Systems

Melittin (100 μg) was dissolved in MeOH/H_2O/AcOH=80:20:2 (500 μl, pH 3.2) and in H_2O (500 μl, pH 4.3), respectively. CD spectra were taken in the wavelength range from 184 to 260 nm using a 100 μm path length cylindrical cell (**Figure II.1-6**).

Table III.1-11: Number of Deuteriums Remaining in Each Amino Acid Residue of Deuterated Melittin After a Period of Deuterium Exchange-Out Time

Amino Acid Residue	0 min	4 min	11 min	19 min
G	0.1	0.0	0.0	0.0
I	0.3	0.2	0.0	0.0
G	0.3	0.2	0.2	0.0
A	0.5	0.2	0.0	0.0
V5	0.4	0.3	0.1	0.0
L	0.5	0.2	0.1	0.2
K	1.0	0.6	0.6	0.1
V	0.9	0.7	0.7	0.1
L	0.8	0.6	0.4	0.3
T10	1.3	1.0	0.6	0.4
T	1.2	0.8	0.5	0.3
G	0.3	0.4	0.4	0.0
L	0.3	0.1	0.0	0.2
P	0.2	0.0	0.0	0.1
A15	0.4	0.1	0.0	0.1
L	0.3	0.1	0.1	0.0
I	0.5	0.2	0.1	0.0
S	0.5	0.2	0.2	0.2
W	0.5	0.2	0.2	0.1
I20	1.1	0.3	0.2	0.1
K	0.5	0.4	0.3	0.3
R	1.0	0.6	0.4	0.2
K	1.5	0.6	0.3	0.1
R	1.5	1.0	0.6	0.5
Q25	0.8	0.3	0.0	0.1
Q	0.6	0.2	0.0	0.1

III.2 H/D Exchange in Bovine Pancreatic Trypsin Inhibitor (BPTI)

III.2-1 Reduction of Disulfide Bonds in Native BPTI

III.2-1-1 Purification of Native BPTI

BPTI (14.4 mg) was dissolved in 200 µl of eluent A (0.1% TFA/H_2O) and purified on a semi-preparative reverse phase column (C-4, 1.0 x 25 cm) using an analytical HPLC system at a flow rate of 3 ml/min. Detection was achieved at

280 nm. The gradient was 10%B for 2 min, 10 to 20% B over 12 min and finally 20 to 35% B over 37 min.. The fraction eluted after a retention time of 18 min corresponding to an eluent strength of 23.3% B. It was pooled and lyophilized. The molecular weight of the purified BPTI was determined to be **6510.7 Da** (ESIMS; m/z 1086.2 (+6), m/z 1303.0 (+5), m/z 1628.6 (+4), m/z 2171.4 (+3)) or 6509.6 Da (MALDI-TOFMS) and the calculated value was 6511.6 Da (**Figure II.2-5A**).

III.2-1-2 Complete Reduction of Disulfide Bonds in Native BPTI

BPTI (50 μg) was dissolved in 0.2 M NH_4OAc buffer (76.8 μl, pH 3.0-3.3). To this solution, was added 10 mM tris-(2-carboxyethyl)-phosphine hydrochloride in 0.2 M NH_4OAc buffer (76.8 μl, pH 3.0). The reaction was carried out at 70°C for 10 min. The reaction mixture was then cooled in an ice-bath and analyzed by analytical HPLC using a Vydac C-18 column (0.46 x 25 cm) at a flow rate of 1 ml/min using a gradient of 10%B for 5 min and then 10 to 95% B over a period of 85 min. Detection was achieved at 215 nm. The completely reduced BPTI was pooled at 35 min retention time corresponding to an eluent strength of 40% B. Larger scale HPLC analysis of the fully reduced BPTI (500 μg - 3 mg) was carried out on a semi-preparative reverse phase column (C-4, 1.0 x 25 cm) at a 3 ml/min flow rate and maintained at 280 nm. After a 5 min at 10%B, the reduction mixture was eluted by gradient elution using 10 to 23% B over 10 min, followed by a gradient of 23 to 27% B over 13 min and then with a gradient of 27 to 45% over 30 min. The fraction eluted at 43.5 min retention time which corresponded to a solvent composition of 35.1% B. The eluents were pooled and lyophilized (**Figure II.2-4C**). The molecular

weight of the purified BPTI was determined to be **6517.0 Da** (ESIMS; m/z 815.8 (+8), m/z 932.2 (+7), m/z 1087.4 (+6), m/z 1304.2 (+5), m/z 1630.2 (+4), m/z 2173.0 (+3)) and the calculated value was 6517.6 Da (**Figure II.2-5B**). Completely reduced BPTI was also obtained using DTT as a reducing reagent. BPTI (100 µg) was dissolved in 50 mM NH_4HCO_3 buffer (142.5 µl, pH 8.6) containing dithiothreitol (DTT) at 2 mg/ml concentration. The reduction was performed at 39°C for 30 min and quenched by adding 142.5 µl of 1 N HCl at 0°C to give a solution pH< 2.0. The reaction mixture was directly analyzed by HPLC using a Vydac C-18 reverse phase column (0.46 x 25 cm) with a flow rate of 1 ml/min and a wavelength set to 215 nm. The gradient of 10%B for 5 min, followed by 10 to 95% B over a period of 85 min was used. Completely reduced BPTI was eluted at 35 min (40% B) and partially reduced BPTI with C14-C38 disulfide cleaved, was also observed at 34 min retention time (39% B) (**Figure II.2-4D**).

III.2-1-3 Partial Reduction of Disulfide Bonds in Native BPTI

BPTI (50 µg) was dissolved in 0.2 M NH_4OAc buffer (76.8 µl, pH 3.1). To this solution, was added 20 mM tris-(2-carboxyethyl)-phosphine hydrochloride in 0.2 M NH_4OAc buffer (76.8 µl, pH 3.1). The reaction was carried out at 0°C for 10 min. The reaction mixture was directly analyzed by HPLC using a Vydac C-18 column (0.46 x 25 cm) at a flow rate of 1 ml/min. The gradient was 10%B for 5 min followed by a gradient of 10 to 95% B over 85 min. Partially reduced BPTI was observed as a minor product at 34 min (39% B) and native BPTI as a major peak at 23.5 min (28.5% B) (**Figure II.2-4B**). An aliquot (46 µl, 15 µg) was analyzed by microbore HPLC-ESIMS using a Vydac C-8 column (1.0 x 150 mm) at a flow rate of 50 µl/min.

III.2-1-4 Selective Reduction and Alkylation of C14-C38 Disulfide

DTT was dissolved in 0.1 M Tris-HCl buffer containing 2 mM EDTA (pH 8.2) to give 0.61 μg/μl final concentration. BPTI (102 μg) was reacted with DTT (25 times molar excess, 100 μl, pH 8.2) for 2 min at room temperature. An aliquot (25 μl) was taken and acidified with 25 μl of 1 N HCl to quench the reduction (pH 1.4). This reaction mixture was directly analyzed by microbore HPLC-ESIMS using a Vydac C-8 column. To another aliquot (76 μl) from the DTT reduction mixture, iodoacetamide (285 μg, 5 times excess over DTT) was added and the solution was adjusted to pH 7.3. The reaction was continued for 10 min at room temperature and quenched by adding 1 N HCl to give pH 1.8. An aliquot was analyzed by microbore HPLC-ESIMS using a Vydac C-8 column at a flow rate of 50 μl,/min. The molecular weight of BPTI with C14-C38 disulfide bond cleaved and with C14 and C38 carboxyamidomethylated (CAM(14,38)-BPTI) was found to be **6626.6 Da** [ESIMS; m/z 1105.7 (+6), m/z 1326.2 (+5), m/z 1657.4 (+4)], the calculated value was 6627.7 Da (**Figure II.2-5C**).

III.2-1-5 Pepsin Digestion of Completely Reduced BPTI

Completely reduced BPTI (217 μg) was dissolved in 0.1% TFA/H_2O (100 μl) and cooled down to 0°C. A aqueous slurry (745 μl) containing 50% immobilized pepsin gel (E/S=5) in 0.1 M NaOAc/50% glycerol/0.05% NaN_3 (pH 4.5) was washed three times with dilute HCl solution (3 x 745 μl, pH 2.0) and cooled to 0°C. The reduced BPTI solution was added to precooled immobilized pepsin gel solution. The reaction was continued for 5 min at 0°C and then

quenched by filtering the digest in microfilterfuge tube. The filtrate was analyzed by analytical HPLC using a Vydac C-18 column at a flow rate of 1 ml/min using a wavelength 215 nm to monitor the elution. A gradient of 5%B for 2 min and then 5 to 45% B over 200 min was used to elute the product (**Figure II.2-6**). The digestion mixture was also analyzed by microbore HPLC-ESIMS using a C-8 column at 0°C (**Figure II.2-7**). A total of 15 peptides were pooled and identified by peptide mapping. ESIMS and ESIMS/MS analyses of these peptide were carried out using loop-injection mode in 50% CH_3CN/0.1% AcOH at a flow rate of 5 µl/min. FABMS analyses were carried out at glycerol and 3-nitrobenzyl alcohol mixture (1:1) in the presence of p-toluene sulfonic acid. MALDI-TOFMS was carried out at a volume ratio of sample solution to α-cyano-4-hydroxcinnamic acid (HCCA) (1:10) (**Table III.2-1**).

III.2-1-6 ESIMS/MS Analysis of the Peptic Peptides of Reduced BPTI

Daughter-ion spectra for seven major peptides are shown in **Figure II.2-1-10** to **Figure II.2-16**. The observed fragment ions in these spectra are shown below (**Table III.2-2** to **Table III.2-8**). Other minor peptides were also analyzed by ESIMS/MS.

Table III.2-2: Observed Fragment Ions in Daughter-Ion Spectrum of Peptide 6 [$\mathbf{R^{17}IIRY^{21}}$, parent ion=m/z 720 (+1)]

Observed Mass (Type of Ion)	355.2 (A3), 157.2 (B1), 270.0 (B2), 383.2 (B3), 539.2 (B4), 338.0 (Y2), 451.2 (Y3), 321.2 (Z2), 703.2 (Z5)

Table III.2-1: Peptic Peptides of Completely Reduced BPTI

Peptide	ESIMS	MALDI-TOFMS	FABMS	Calculated
P 1 M^{52}-A^{58}	694.61 ± 0.52 Da 695.2(+1),348.5(+2)	696.1(+1)	695.4(+1)	694.3 Da
P 2 R^{39}-E^{49}	1319.98 ± 0.52 Da 1320.8(+1) 660.8(+2), 441.2(+3)	-	1320.9(+1)	1319.71 Da
P 3 N^{24}-T^{32}	905.18 ± 0.69 Da 905.8(+1) 453.4(+2), 303.0(+3)	-	453.6(+2) 905.6(+1)	904.45 Da
P 4 R^{39}-C^{51}	1537.78 ± 0.71 Da 1538.0(+1) 770.0(+2), 513.8(+3)	-	1538.6(+1)	1537.75 Da
P 5 Y^{23}-L^{29}	735.59 ± 0.56 Da 736.2(+1), 369.0(+2)	-	736.4(+1)	735.40 Da
P 6 R^{17}-Y^{21}	719.69 ± 0.42 Da 720.4(+1), 361.0(+2)	720.3(+1)	720.4(+1)	719.45 Da
P 7 F^{33}-A^{40}	871.7 ± 0.30 Da 872.4(+1), 437.0(+2)	872.3(+1)	871.9(+1)	871.41 Da
P 8 F^{33}-E^{49}	1946.58 ± 0.36 Da 1947.2(+1) 974.4(+2), 650.0(+3)	1947.3(+1)	1946.0(+1)	1945.97 Da
P 9 F^{22}-L^{29}	882.5 Da 883.5(+1)	883(+1)	883.6(+1)	882.5 Da
P 1 0 F^{33}-C^{51}	2165 ± 0.64 Da 1083.2(+2) 722.8(+3), 542.4(+4)	2164.7(+1)	2163.7(+1)	2164.0 Da
P 1 1 C^{5}-A^{16}	1277.04 ± 0.20 Da 1277.7(+1), 639.6(+2)	1277.9(+1)	1278.2(+1)	1277.6 Da
P 1 2 F^{33}-F^{45}	1531.58± 0.19 Da 1532.4(+1) 766.8(+2), 511.6(+3)	1531.8(+1)	1531.3(+1)	1530.8 Da
P 1 3 C^{5}-I^{18}	1545.18 ± 0.20 Da 1546.2(+1) 773.7(+2), 516.0(+3)	-	1547.6(+1)	1546.77 Da
P 1 4 R^{17}-F^{22}	866.84 ± 0.49 Da 867.5(+1), 434.6(+2)	-	867.4(+1)	866.52 Da
P 1 5 R^{1}-A^{16}	1793.08 ± 0.35 Da 1793.7(+1) 897.6(+2), 598.8(+3)	1793.4(+1)	1793.9(+1)	1792.8 Da

Table III.2-3: Observed Fragment Ions in Daughter-Ion Spectrum of Peptide 8 [F^{33}**VYGGCRAKRNNFKSAE**^{49}, parent ion=m/z 650(+3)]

Observed Mass (Type of Ion)	119.8 (A1), 218.8 (A2), 851.5 ($A15^{+2}$), 200.8 ($A6^{+3}$), 257.8 ($A8^{+3}$), 634.3 ($A17^{+3}$), 148.0 (B1), 247.0 (B2), 643.3 ($B17^{+3}$), 148.0 (Y1), 218.8 (Y2), 434.2 (Y4), 809.5 (Y7), 769.9 ($Y14^{+2}$), 851.5 ($Y15^{+2}$), 103.0 ($Y3^{+3}$), 634.3 ($Y17^{+3}$), 131.2 (Z1), 102.1 ($Z2^{+2}$), 339.1($Z6^{+2}$), 44.2 ($Z1^{+3}$)

Table III.2-4: Observed Fragment Ions in Daughter-Ion Spectrum of Peptide 9 [F^{22}**YNAKAGL**^{29}, parent ion=m/z 884(+1)]

Observed Mass (Type of Ion)	120.1 (A1), 283.0 (A2), 468.1 (A4), 310.9 (B2), 425.2 (B3), 496.0 (B4), 624.1 (B5), 695.2 (B6), 752.5 (B7), 865.6 (B8), 388.0 (Y4), 459.1 (Y5), 573.1 (Y6)

Table III.2-5: Observed Fragment Ions in Daughter-Ion Spectrum of Peptide 10 [F^{33}**VYGGCRAKRNNFKSAEDC**^{51}, parent ion=m/z 723(+3)]

Observed Mass (Type of Ion)	120.2 (A1), 218.9 (A2), 220.1 ($A4^{+2}$), 247.1 (B2), 900.8 ($B16^{+2}$), 716.4 ($B19^{+3}$), 218.9 ($Y4^{+2}$), 960.2 ($Y17^{+2}$), 220.1 (Z2), 951.5 ($Z17^{+2}$), 716.4 ($Z19^{+3}$)

Table III.2-6: Observed Fragment Ions in Daughter-Ion Spectrum of Peptide 11 [C^{5}**LEPPYTGPCKA**^{16}, parent ion=m/z 1279(+1)]

Observed Mass (Type of Ion)	189.0 (A2), 218.2 (Y2), 418.2 (Y4), 475.0 (Y5), 576.2 (Y6), 836.6 (Y8), 933.4 (Y9)

Table III.2-7: Observed Fragment Ions in Daughter-Ion Spectrum of Peptide 12 [F^{33}**VYGGCRAKRNNF**^{45}, parent ion=m/z 767(+2)]

Observed Mass (Type of Ion)	120.0 (A1), 218.8 (A2), 382.4 (A3), 496.0 (A5), 826.8 (A8), 300.0 ($A6^{+2}$), 377.6 ($A7^{+2}$), 246.8 (B2), 410.4 (B3), 466.8 (B4), 524.4 (B5), 626.8 (B6), 782.8 (B7), 262.8 ($B5^{+2}$), 428.0 ($B8^{+2}$), 570.0 ($B10^{+2}$), 626.8 ($B11^{+2}$), 280.0 (Y2), 678.4 (Y5), 749.6 (Y6), 1122.4 (Y10), 339.2 ($Y5^{+2}$), 453.6 ($Y7^{+2}$), 533.2 ($Y9^{+2}$), 561.6 ($Y10^{+2}$), 643.2 ($Y11^{+2}$), 692.8 ($Y12^{+2}$), 262.8 (Z2), 377.6 (Z3), 533.2 (Z4), 661.2 (Z5), 1105.6 (Z10),1268.4 (Z11), 524.4 ($Z9^{+2}$), 552.8 ($Z10^{+2}$), 635.2 ($Z11^{+2}$), 684.4 ($Z12^{+2}$), 758.0 ($Z13^{+2}$)

Table III.2-8: Observed Fragment Ions in Daughter-Ion Spectrum of Peptide 15 [R^{1}**PDFCLEPPYTGPCKA**^{16}, parent ion=m/z 898(+2)]

Observed Mass (Type of Ion)	129.2 (A1), 254.0 (B2,) 369.2 (B3), 861.6 (B7), 218.0 (Y2), 418.0 (Y4), 933.6 (Y9), 888.8 ($Z16^{+2}$)

III.2-2 Oxidation of BPTI

III.2-2-1 Performic Acid Oxidation of Native BPTI in Sodium Phosphate Buffer

The performic acid reagent was made up by mixing 30% H_2O_2 (200 µl) in formic acid (1.8 ml). The oxidation reaction was carried out at room temperature for 2.5 hrs and then the reaction mixture was cooled to -20°C. Native BPTI (100 µg) was dissolved in 100 µl of 0.1 M sodium phosphate buffer (pH 8.2) and cooled to 0°C. To this solution, 46 µl of the precooled performic acid reagent was added at 0°C, which provided a solution pH 1.2-1.3. The reaction was

continued for 10 min at 0°C. After dilution with ice-cold water, the reaction mixture was subjected to lyophilization. The dried sample was redissolved in 100 µl of 0.1% TFA/H_2O and analyzed by analytical HPLC using a Vydac C-4 column at a flow rate of 1 ml/min and monitoring at 220 nm. The gradient was 10% B for 2 min, then 10 to 25% B over 25 min, and finally 25 to 45% B over 50 min. The fractions were pooled and freeze-dried. These fractions were analyzed by ESIMS (**Table III.2-9**).

Table III.2-9: Oxidation Intermediates Observed During the Reaction of Native BPTI with Performic Acid in Sodium Phosphate Buffer (pH 1.2, 0°C, 10 min)

Molecule	Mol. Wt. (Da)	Observed Mass (Charge State)
BPTI+O_4	6574.36 ± 1.02	1096.9 (+6), 1315.6 (+5), 1644.7 (+4)
BPTI+H_1O_8	6639.16 ± 0.75	1107.7 (+6), 1328.8 (+5), 1660.6 (+4)
BPTI+H_2O_{15}	6751.52 ± 0.87	965.3 (+7), 1126.4 (+6), 1351.4 (+5), 1688.9 (+4)
BPTI+H_2O_{16}	6768.48 ± 1.64	968.3 (+7), 1129.1 (+6), 1354.4 (+5), 1692.8 (+4)
BPTI+H_3O_{20}	6833.42 ± 0.41	977.3 (+7), 1139.9 (+6), 1367.6 (+5), 1709.3 (+4)

III.2-2-2 Performic Acid Oxidation of Native BPTI in HCO_2H-NH_4OH/MeOH

The HCO_2H-NH_4OH/MeOH buffer was made by adding concentrated ammonium hydroxide to formic acid at 0°C to obtain pH 3.0 and then adding MeOH at a volume ratio of MeOH to the buffer (1:5). The HCO_2H-NH_4OH/MeOH buffer solution was cooled at -20°C. Native BPTI (44 µg) was dissolved in the HCO_2H-NH_4OH/MeOH buffer (44 µl, pH 3.0, -20°C) and then reacted with precooled performic acid reagent (22 µl) at -20°C. The reaction mixture solution was at pH 2.8. Aliquots (10 µl) was taken after 15 min, 30 min, 60 min, 2 hr and 4 hr reaction periods. Each aliquot were diluted with ice-cold

water (100 µl), and then subjected to lyophilization. The freeze-dried samples were redissolved in 20 µl of 1% i-PrOH/2% AcOH. Each sample (15 µl) was loaded to the desalting trap cartridge loop, prewashed with 2% CH_3CN-H_2O (200 µl) and then analyzed by microbore HPLC-ESIMS using a C-4 column. The gradient was 10% B for 5 min , 10 to 15% B over 5 min, 15 to 25% B over 20 min, 25 to 31% B over 20 min and finally 31 to 41% B over 20 min. A mass range of 1060 to 1800 was scanned (**Figure II.2-20, Table III.2-10**).

Table III.2-10: Reaction Profile of Native BPTI with Performic Acid in HCO_2H-NH_4OH/8.5% MeOH Buffer (pH 2.8, -20°C)

Reaction Time	Product Mol. Wt. (Da)	Observed Mass (Charge State)
15 min	6574.80 ± 0.86 6640.27 ± 0.38 6671.20 ± 0.80	1097.0 (+6), 1315.8 (+5), 1644.6 (+4) 1107.8 (+6), 1329.0 (+5), 1661.0 (+4) 1335.4 (+5), 1668.6 (+4)
30 min	6574.20 ± 0.45 6640.27 ± 0.38 6671.25 ± 0.75 6754.50 ± 0.86	1096.6 (+6), 1315.8 (+5), 1644.6 (+4), 2192.6(+3) 1107.8 (+6), 1329.0 (+5), 1661.0 (+4) 1335.1 (+5), 1669.0 (+4) 1126.9 (+6), 1351.9 (+5), 1689.4 (+4)
1 hr	6573.36 ± 0.86 6640.16 ± 0.86 6671.16 ± 0.86 6754.50 ± 0.73 6834.0	1096.6 (+6), 1315.6 (+5), 1644.4 (+4) 1108.0 (+6), 1328.8 (+5), 1660.9 (+4) 1112.8 (+6), 1335.4 (+5), 1668.7 (+4) 1126.9 (+6), 1351.3 (+5), 1689.1 (+4) 1367.8 (+5), 1709.5 (+4)
2 hr	6573.780± 0.75 6640.30 ± 1.48 6752.40 ± 0.49 6834.56± 0.49	1096.6 (+6), 1315.6 (+5), 1644.7 (+4) 1108.0 (+6), 1329.1 (+5), 1660.6 (+4) 1126.3 (+6), 1351.6 (+5), 1689.1 (+4) 1140.1 (+6), 1367.8 (+5), 1709.8 (+4)
4 hr	6573.80 ± 1.40 6834.56 ± 0.49	1097.0 (+6), 1315.8 (+5), 1644.2 (+4), 2191.8 (+3) 1140.1 (+6), 1367.8 (+5) ,1709.8 (+4)

III.2-2-3 Pepsin Digestion of Oxidized BPTI Derived from the Oxidation of Native BPTI with Performic Acid

Native BPTI (100 µg) was dissolved in 100 µl of the HCO_2H-NH_4OH/MeOH buffer (pH 3.0) at -20°C and was reacted with the precooled

performic acid reagent (50 µl) at -20°C and pH 2.8 for 2 hr. After 2 hr oxidation, the reaction mixture was diluted with ice-cold water (850 µl) and subjected to lyophilization. The freeze-dried sample was redissolved in 45 µl of 8 M urea-HCl (pH 2.0), diluted with 0.04% HCl (pH 2.0) to give a total of 180 µl solution containing 2 M urea. This solution was put in an ice-bath. Immobilized pepsin gel (50%, 337 µl) was washed three times with 0.04% HCl (3 x 337 µl, pH 2.0) and put in an ice-bath. The oxidized BPTI solution was added to the precooled immobilized pepsin gel solution. The digestion was continued for 5 min at 0°C and quenched by microfiltration in a microfilterfuge tube followed by washing of the gel two times with 0.04% HCl (pH 2.0, 2 x 100 µl) at 0°C. Half of the final solution (250 µl) was analyzed on the analytical HPLC system with Vydac C-18 column at 1 ml/min flow rate and 220 nm wavelength; 2 min isocratic (5%B), a 5 to 45% B gradient in 100 min (**Figure II.2-28**). A total of nine peptic peptides (P1, P2, P3, P5, P6, P7, P8, P9, P10) as well as the two undigested oxidation intermediates of BPTI (BPTI+O_4, BPTI+H_2O_8), were determined (**Table III.2-11**).

III.2-2-4 Performic Acid Oxidation of Reduced BPTI in HCO_2H-NH_4OH/MeOH

The reduced BPTI (251 µg) in 251 µl of the HCO_2H-NH_4OH/MeOH buffer was oxidized with 125 µl of the performic acid reagent at -20°C and pH 2.8 up to for 2 hours. Aliquots (15 µl) were taken after 30 min-, 60 min-, 2 hr-oxidation reaction, diluted with 150 µl of ice-cold water and freeze-dried. Microbore HPLC-ESIMS was performed on a C-4 column; 10% B isocratic for 5 min, 10 to 15% B gradient in 5 min, 15% to 25% B gradient in 20 min, 25% to 31% B gradient in 20 min and 31 to 41% B gradient in 20 min at 40 µl/min flow rate

(**Figure II.2-22A, Table III.2-12**). The calculated molecular weight of the completely oxidized BPTI was 6538.56 Da.

Table III.2-11: Peptic Peptides of Oxidized BPTI Derived from the Reaction of Native BPTI with Performic Acid (pH 2.8, -20°C, 2 hr)

Molecule	ESIMS	MALDI-TOFMS	Calculated
P 1 K^{46}-A^{58}	1456.20 ± 0.43 Da 1456.8(+1) 729.0(+2), 486.6(+3)	-	1455.50 Da
P 2 V^{34}-A^{58}	2869.65 ± 0.15 Da 1435.9(+2), 957.5(+3)	-	2869.16 Da
P 3 V^{34}-F^{45}	1431.85 ± 0.15 Da 1432.7(+1), 717.0(+2)	-	1431.68 Da
P 5 F^{22}-F^{33}	1409.8 4 ± 0.08 Da 1410.9(+1), 705.9(+2)	1410.4(+1),	1409.64 Da
P 6 F^{22}-A^{58}	4262.40 Da 2132.2(+2) 1421.8(+3),1066.6(+4)	4259.2(+1)	4260.77 Da
P 7 Y^{23}-F^{33}	2677.50 ± 0.30 Da 1339.6(+2), 893.6(+3)	-	2676.22 Da
P 8 F22-F45	2824.30 ± 0.10 Da 1413.2(+2), 942.4(+3)	2824.5(+1),	2823.29 Da
P 9 R^{1}-I^{18}	2158.70 ± 0.10 Da 2159.6(+1), 1080.4(+2)	2158.4(+1)	2157.99 Da
P 10 R^{1}-Y^{21}	2590.95 ± 0.15 Da 1296.4(+2), 864.7(+3)	2591.0(+1)	2590.24 Da
BPTI+O_4	6574.00 Da 1315.8(+5)	6576.2(+1)	6574.66 Da
BPTI+H_2O_8	6640.66 ± 0.94 Da 1661.0(+4) 1329.0(+5), 1108.0(+6)	2164.7(+1)	6540.66 Da

Table III.2-12: Reaction Profile of Reduced BPTI with Performic Acid in HCO_2H-NH_4OH/8.5% MeOH Buffer (pH 2.8, -20°C)

Time	Mol. Wt. (Da)	Observed Mass (Charge State)
30 min	6536.67 ± 0.47	1368.4 (+5), 1710.0 (+4), 2280.0 (+3)
1 hr	6836.00 ± 0.82	1368.0 (+5), 1710.0 (+4), 2280.0 (+3)
2 hr	6836.60± 0.42	1140.4 (+6), 1368.4 (+5), 1710.0 (+4), 2280.0 (+3)

III.2-2-5 Pepsin Digestion of Oxidized BPTI Derived from the Oxidation of Reduced BPTI with Performic Acid

Reduced BPTI (200 μg) in 200 μl of HCO_2H-NH_4OH/MeOH buffer was oxidized with 100 μl of performic acid reagent (pH 2.8, -20°C, 2 hr) and then freeze-dried after dilution with ice-cold water. The lyophilized oxidation mixture was redissolved in 90 μl of 8 M urea-HCl (pH 2.0), diluted with 0.04% HCl (pH 2.0) to give a total of 360 μl solution containing 2 M urea and put in an ice-bath. A 50% immobilized pepsin gel solution (674 μl) was washed three times with 700 μl of 0.04% HCl (pH 2.0) and put in an ice-bath. The oxidized BPTI solution was added to precooled immobilized pepsin gel solution. The digestion was continued for 5 min at 0°C and then quenched by microfiltration in a microfilterfuge tube followed by washing of the gel twice with 0.04% HCl at 0°C. The filtrate solution was analyzed by an analytical HPLC system using a Vydac C-18 column at a flow rate of 1 ml/min and monitored at 220 nm. After the first 2 min elution with 5% B, a gradient of 5 to 45% B over 100 min was used (**Figure II.2-22B**). A total of 11 peptic peptides were determined (**Table III.2-13**).

III.2-2-6 ESIMS/MS Analysis of the Peptic Peptides from Oxidized BPTI

Tandem mass spectrometry of the peptic peptide fractions pooled from HPLC separation, was performed in 10% i-PrOH-2% AcOH at 5 μl/min flow rate. Daughter-ion spectra for the four major peptides are shown in **Figures II.2-24** to **II.2-27**. The observed fragment ions from these spectra are shown in **Tables III.2-14** to **III.2-17**). Other minor peptides were also analyzed in a similar way by ESIMS/MS.

Table III.2-13: Peptic Peptides of Oxidized BPTI Derived from the Reaction of Reduced BPTI with Performic Acid (pH 2.8, -20°C, 2 hr)

Molecule	ESIMS	MALDI-TOFMS	Calculated
P 1 K^{46}-A^{58}	1455.74 ± 0.22 Da 1456.9(+1), 728.8(+2)	-	1455.50 Da
P 2 V^{34}-A^{58}	2869.70 ± 0.96 Da 1435.8(+2) 957.9(+3), 718.2(+4)	-	2869.16 Da
P 3 V^{34}-F^{45}	1431.88 ± 0.26 Da 1432.7(+1) 716.9(+2), 478.4(+3)	-	1431.68 Da
P 4 Y^{23}-F^{33}	1263.0 Da 1264.0(+1)	-	1262.57 Da
P 5 F^{22}-F^{33}	1409.84 ± 0.08 Da 1410.9(+1), 705.9(+2)	1410.4(+1)	1409.64 Da
P 6 F^{22}-A^{58}	4262.98 ± 0.19 Da 2132.2(+2) 1421.8(+3), 1066.6(+4)	4259.2(+1)	4260.77 Da
P 7 Y^{23}-F^{33}	2677.50 ± 0.30 Da 1339.6(+2), 893.6(+3)	-	2676.22 Da
P 8 F22-F45	2824.71 ± 0.75 Da 1413.2(+2) 942.4(+3), 707.4(+4)	2824.5(+1)	2823.29 Da
P 9 R^{1}-I^{18}	2159.6 Da 1080.8(+2)	2158.4(+1)	2157.99 Da
P 10 R^{1}-Y^{21}	2591.43 ± 0.35 Da 1296.6(+2), 864.9(+3)	2591.0(+1)	2590.24 Da
P 11 R^{1}-F^{22}	6574.00 Da 1370.4(+2), 914.0(+3)	-	2737.31 Da

Table III.2-14: Observed Fragment Ions in Daughter-Ion Spectrum of Peptide 5 [**F^{22}YNAKAGLC*QTF^{33}**, parent ion=m/z 1411(+1)]

Observed Mass (Type of Ion)	119.8 (A1), 283.0 (A2), 468.2 (A4), 837.4 (A8), 311.0 (B2), 425.0 (B3), 495.8 (B4), 624.2 (B5), 695.4 (B6), 752.2 (B7), 865.8 (B8), 1016.6 (B9), 1144.4 (B10), 1245.4 (B11), 1392.6 (B12), 915.4 (Y8), 1100 (Y10), 1246.6 (Z11), 1393.8 (Z12)

Table III.2-15: Observed Fragment Ions in Daughter-Ion Spectrum of Peptide 6 [**F^{22}YNAKAGLC*QTFVYGGC*RAKRNNFKS AEDC*M**RTC*GGA^{58}**, parent ion=m/z 1422(+3)]

Observed Mass (Type of Ion)	120.0 (A1), 283.2 (A2), 468.0 (A4), 724.4 (A7), 837.6 (A8), 1059.6 ($A19^{+2}$), 310.8 (B2), 425.2 (B3), 496.0 (B4), 624.4 (B5), 695.2 (B6), 752.4 (B7), 865.6 (B8), 1016.4 (B9), 1145.2 (B10), 348.8 ($B6^{+2}$), 376.8 ($B7^{+2}$), 572.0 ($B10^{+2}$), 1216.8 ($B21^{+2}$), 1273.6 ($B22^{+2}$), 1331.2 ($B23^{+2}$), 1468.8 ($B25^{+2}$), 1511.2 ($B26^{+2}$), 1270.0 ($B32^{+3}$), 1416.4 ($B37^{+3}$), 612.0 (Y6), 775.6(Y7) 926.4(Y8) 464.0($Y8^{+2}$) 521.2($Y9^{+2}$) 585.2($Y10^{+2}$) 995.0 ($Y17^{+2}$), 1059.6 ($Y18^{+2}$), 1094.4 ($Y19^{+2}$), 1173.2 ($Y20^{+2}$), 1248.8 ($Y21^{+2}$), 1276.4 ($Y22^{+2}$), 1305.2 ($Y23^{+2}$), 1387.2 ($Y24^{+2}$), 1436.8 ($Y25^{+2}$), 1318.8 ($Y35^{+3}$), 186.0 (Z3), 720.4 ($Z13^{+2}$), 908.4 ($Z16^{+2}$), 1378.0 ($Z24^{+2}$)

Table III.2-16: Observed Fragment Ions in Daughter-Ion Spectrum of Peptide 8 [**F^{22}YNAKAGLC*QTFVYGGC*R AKRNNF^{45}**, parent ion=m/z 942(+3)]

Observed Mass (Type of Ion)	119.8 (A1), 283.0 (A2), 467.8 (A4), 311.0 (B2), 425.0 (B3), 495.8 (B4), 624.2 (B5), 695.4 (B6), 752.2 (B7), 865.4 (B8), 165.8 (Y1), 279.8 (Y2), 393.8 (Y3), 550.2 (Y4), 678.2 (Y5), 749.4 (Y6), 905.4 (Y7), 1056.6 (Y8), 1170.6 (Y10), 1333.4 (Y11), 83.8 ($Y1^{+2}$), 339.8 ($Y5^{+2}$), 453.4 ($Y7^{+2}$), 538.6 ($Y8^{+2}$), 557.0 ($Y9^{+2}$), 585.8 ($Y10^{+2}$), 667.4 ($Y11^{+2}$), 717.0 ($Y12^{+2}$), 790.6 ($Y13^{+2}$), 841.4 ($Y14^{+2}$), 905.4 ($Y15^{+2}$), 980.6 ($Y16^{+2}$), 1101.8 ($Y19^{+2}$), 1165.4 ($Y20^{+2}$), 1200.6 ($Y21^{+2}$), 1257.8 ($Y22^{+2}$), 263 (Z2), 377.0 (Z3), 533.0 (Z4), 661.0 (Z5), 732.2 (Z6), 888.2 (Z7), 577.4 ($Z10^{+2}$), 659.0 ($Z11^{+2}$), 708.6 ($Z12^{+2}$), 782.2 ($Z13^{+2}$), 832.6 ($Z14^{+2}$), 896.6 ($Z15^{+2}$), 1249.8 ($Z22^{+2}$)

Table III.2-17: Observed Fragment Ions in Daughter-Ion Spectrum of Peptide 10 [**R^1PDFC*LEPPYTGPC*KARIIRY^{21}**, parent ion=m/z 1297(+2)]

Observed Mass (Type of Ion)	488.2 (A4), 752.2 (A6), 157.0 (B1), 253.8 (B2), 369.0 (B3), 516.2 (B4), 667.4 (B5), 780.6 (B6), 909.4 (B7), 337.8 (Y2), 451.4 (Y3), 564.2 (Y4), 720.2 (Y5), 791.4 (Y6), 1224.6 (Y10), 321.0 (Z2), 703.8 (Z5), 774.6 (Z6)

III.2-3 H/D Exchange of BPTI

III.2-3-1 Global Structure Changes in BPTI

The purified native BPTI (130 μg) was dissolved in CH_3CO_2D/D_2O (1 ml, pD 2.8, 20 μM) and immediately analyzed by CF-ESIMS at 20°C (**Table III.2-18**). Molecular weights observed, the percentage of deuterium incorporation and the H_t value where H_t is the number of remaining hydrogens at time t, were calculated. CAM(14,38)-BPTI (102.4 μg) was dissolved in CH_3CO_2D/D_2O (1 ml, pD 2.8, 15.45 μM) and immediately analyzed by CF-ESIMS at 20°C (**Table III.2-19**). A mass range of 920-1400 was continuously scanned at 0.2 Da step size, 1.4 dwell time and 3.48 sec/scan speed for one hour. Completely oxidized BPTI (139 μg) was dissolved in CH_3CO_2D/D_2O (1 ml, pD 2.8, 20 μM) and immediately analyzed by CF-ESIMS at 20°C (**Table III.2-20**). A mass range of 920-1740 was continuously scanned at 0.3 step size, 1.2 ms dwell time and 3.42 sec/scan speed for one hour. Completely reduced BPTI (133 μg) was dissolved in CH_3CO_2D/D_2O (1 ml, pD 2.8, 20.4 μM) and immediately analyzed by CF-ESIMS at 20°C (**Table III.2-21**).

Table III.2-18: Deuterium Exchange-In into Native BPTI

Time t (min)	Molecular Weight (Da)	Deuterium Incorporation (%)	H_t
0.00	6510.66	0.0	108
1.17	6549.93	37.0	68.1
1.22	6549.93	37.0	68.1
1.28	6550.13	37.2	67.9
1.72	6551.93	38.8	66.1
2.00	6552.27	39.1	65.7
2.23	6552.27	39.1	65.7
3.06	6553.47	40.2	64.5
4.06	6554.93	41.6	63.1
5.01	6555.33	42.0	62.7
5.62	6556.67	43.2	61.3
7.82	6556.93	43.4	61.1
10.00	6558.13	44.6	59.9
13.03	6559.33	45.7	58.7
15.18	6559.67	46.0	58.3
20.97	6562.07	48.2	55.9
30.55	6562.93	49.0	55.1
39.99	6563.27	49.3	54.7
40.41	6563.60	49.6	54.4
45.62	6564.00	54.0	54.0
50.89	6564.47	50.4	53.5
55.65	6564.80	50.7	53.2
60.35	6564.80	50.7	53.2

Table III.2-19: Deuterium Exchange-In into CAM(14,38)-BPTI

Time t (min)	Molecular Weight (Da)	Deuterium Incorporation (%)	H_t
0.00	6626.56	0.0	112
1.06	6672.30	41.3	65.7
1.30	6672.50	41.5	65.5
2.22	6675.30	44.0	62.7
4.10	6678.40	47.2	59.6
5.01	6679.50	47.8	58.5
6.04	6679.90	47.8	58.1
7.87	6680.60	48.8	57.4
8.04	6680.60	48.8	57.4
9.01	6681.30	49.4	56.7
10.07	6681.70	49.7	56.3
15.10	6684.70	52.4	53.3
20.95	6686.13	53.7	51.9
22.26	6686.87	54.3	51.1
25.46	6687.47	54.9	50.5
35.17	6688.13	55.5	49.9
42.26	6688.67	56.0	49.3
48.13	6689.27	56.5	48.7
52.36	6689.00	56.2	49.
∞	6738.56	100	0

Table III.2-20: Deuterium Exchange-In into Oxidized BPTI

Time t (min)	Molecular Weight (Da)	Deuterium Incorporation (%)	H_t
0.00	6835.66	0.0	114
1.46	6898.05	54.4	52.0
1.51	6898.88	55.2	51.1
1.80	6903.00	58.8	47.0
1.91	6903.90	59.6	46.1
2.04	6904.70	60.3	45.3
2.52	6906.22	61.6	43.8
3.60	6911.48	66.2	38.5
4.63	6914.92	69.2	35.1
5.72	6917.55	71.5	32.4
6.52	6920.70	74.3	29.3
7.03	6921.00	74.6	29.0
7.95	6922.55	75.9	27.5
8.98	6924.30	77.4	25.7
9.95	6925.90	78.8	24.1
10.92	6926.62	80.0	23.4
13.20	6930.00	82.4	20.0
15.52	6930.68	83.0	19.3
20.67	6933.30	85.4	16.7
23.66	6934.10	86.0	15.9
25.57	6934.70	86.6	15.3
31.69	6935.40	87.2	14.6
52.70	6936.50	88.2	13.5
∞	6949.66	100	0

Table III.2-21: Deuterium Exchange-In into Reduced BPTI

Time t (min)	Molecular Weight (Da)	Deuterium Incorporation (%)	H_t
0.00	6516.58	0.0	114
1.05	6579.45	50.6	50.4
1.26	6582.28	58.1	47.5
1.52	6583.70	59.4	46.3
2.06	6588.40	63.5	41.6
2.55	6590.65	65.5	39.4
3.04	6592.15	66.8	37.8
3.59	6594.45	68.8	35.6
4.57	6596.25	70.4	33.8
5.66	6598.10	72.0	31.9
6.53	6599.20	73.0	30.8
7.67	6600.60	74.2	29.4
9.08	6600.60	74.2	29.4
10.55	6601.75	75.2	28.2
13.76	6602.56	75.9	27.4
16.62	6603.85	77.1	26.2
18.12	6604.25	77.4	25.8
20.81	6604.24	77.4	25.8
30.45	6604.60	77.7	25.4
50.48	6605.44	78.4	24.6
∞	6630.58	100	0

III.2-3-2 CD Spectra of BPTI

The native BPTI, the CAM(14,38)-BPTI, the oxidized BPTI and the reduced BPTI were dissolved in 10 mM sodium phosphate buffer containing 8.5% MeOH (pH 2.8) and compared with each other by CD spectroscopy. The wavelength range from 184 to 260 nm was scanned. The variable selection program was used to determine the percentages of the secondary structures in these molecules (**Figure II.2-31**, **Table II.2-1**).

III.2-3-3 Complete Deuteration of Native BPTI

Native BPTI (88 μg) was fully deuterated in 88 μl of 0.1 M ND_4OAc/D_2O (pD 4.6) at 86°C for 15 min. The reaction mixture was put in an ice-bath. Microbore HPLC-ESIMS analysis at 0°C and a flow rate of 50 μl/min, was carried out using a Vydac C-4 column. The gradient was 30% B for 2 min followed by a gradient of 30 to 95% B over 30 min. At 21.8 min retention time, peak 1 was eluted (**d-BPTI+O**: 6555.03 Da) (**Figure II.2-34B**). At 22.2 min retention time, peak 2 was eluted (**d-BPTI**: 6542.49 Da) (**Figure II.2-34C**).

III.2-3-4 Deuterium Exchange-out of Fully Deuterated Native BPTI in Different Buffer Systems

Fully deuterated BPTI (28 μg) was dissolved in 2.8 μl of $DCl\text{-}D_2O$ solution (pD 2.8). To this solution, 25.2 μl of HCl/H_2O solution (pH 2.8) was added. After a predetermined H/D exchange time, an aliquot (5 μl) was loaded onto the preequilibriated desalting trap cartridge loop at 0°C and analyzed by ESIMS

(**Figure II.2-35, Table III.2-22**). In a similar way, deuterium exchange-out of the fully deuterated BPTI was performed in 10 mM sodium phosphate buffer, 10 mM sodium phosphate/8.5% MeOH, 0.1 M NH_4OAc, 8 M urea/0.1M NH_4OAc and HCO_2H-NH_4OH/8.5% MeOH, respectively (**Tables III.2-23~III.2-27**).

Table III.2-22: Deuterium Exchange-Out of Fully Deuterated BPTI in HCl (pH 2.8) at 20°C

Time (min)	Molecular Weight (Da)	Amide Deuterium Remaining (% ND)
0.5	6552.6	80.4
3.5	6543.9	64.0
5.5	6543.9	64.0
8	6541.9	60.3
10	6542.8	62.0
15	6541.9	60.3
30	6540.0	56.6
60	6540.0	56.6
120	6538.0	52.9
1062	6536.1	49.2
2535	6535.2	47.5

Table III.2-23: Deuterium Exchange-Out of Fully Deuterated BPTI in 0.1 M NH_4OAc (pH 2.8) at 20°C

Time (min)	Molecular Weight (Da)	Amide Deuterium Remaining (% ND)
0.5	6559.3	93.1
3.5	6551.7	78.7
5.5	6549.7	75.0
8	6546.7	69.3
10	6545.8	67.6
15	6543.9	64.0
30	6541.9	60.3
60	6540.0	56.6
120	6539.1	54.9
1020	6538.0	52.9
2512.2	6535.2	47.5

Table III.2-24: Deuterium Exchange-Out of Fully Deuterated BPTI in 10 mM Sodium Phosphate (pH 2.8) at 20°C

Time (min)	Molecular Weight (Da)	Amide Deuterium Remaining (% ND)
0.5	6556.5	88.7
3.0	6550.6	77.7
5.78	6547.8	72.3
8.0	6546.9	70.6
10.33	6544.8	66.7
15	6544.9	66.9
30	6541.9	61.3
60	6541.9	61.3
120	6540.0	57.6
360	6538.0	53.9
1380	6536.1	50.2

Table III.2-25: Deuterium Exchange-Out of Fully Deuterated BPTI in 10 mM Sodium Phosphate/8.5% MeOH (pH 2.8) at 20°C

Time (min)	Molecular Weight (Da)	Amide Deuterium Remaining (% ND)
0.25	6556.5	89.7
3.0	6548.7	75.0
5.58	6547.8	73.3
8.33	6545.8	69.6
11.16	6543.9	66.0
15.5	6543.9	66.0
33	6542.0	62.3
62	6540.0	58.6
120	6539.1	56.9
1195.2	6535.2	49.5

Table III.2-26: Deuterium Exchange-Out of Fully Deuterated BPTI in HCO_2H-NH_4OH/8.5% MeOH (pH 2.8) at 20°C

Time (min)	Molecular Weight (Da)	Amide Deuterium Remaining (% ND)
0.5	6549.2	75.8
3	6543.5	65.1
5	6542.8	63.7
8	6541.9	62.1
11	6540.7	59.7
15	6541.1	60.6
30	6538.6	55.8
60	6537.9	54.5
150	6534.5	48.1
1356	6530.8	41.2

Table III.2-27: Deuterium Exchange-Out of Fully Deuterated BPTI in 8 M Urea/0.1M NH_4OAc (pH 2.8) at 20°C

Time (min)	Molecular Weight (Da)	Amide Deuterium Remaining (% ND)
0.17	6559.0	94.4
3	6552.5	82.1
5.5	6550.9	79.0
8.67	6550.1	77.5
15	6548.5	74.4
30	6544.6	67.2
60	6543.5	65.1
120	6541.2	60.7
1161	6536.4	51.6

III.2-3-5 Performic Acid Oxidation of Fully Deuterated Native BPTI

Fully deuterated BPTI was oxidized with performic acid reagent (pH 2.8, -20°C. 2 hr). An aliquot was taken and directly analyzed by microbore HPLC-ESIMS using a Vydac C-4 column at 0°C and at a flow rate of 50 µl/min. The HPLC conditions were 15% B for 5 min, 15 to 40% B over 12.5 min and finally 40 to 95% B over 7.5 min (**Figure II.2-37**).

III.2-3-6 Pepsin Digestion of Deuterated Oxidized BPTI

In the cold room (4°C), the oxidation mixture obtained from fully deuterated BPTI (90 µg) was redissolved in ice-cold 8 M urea/HCl (pH 2.0) and diluted with an ice-cold HCl solution (180 µl). Digestion of the deuterated oxidized BPTI with immobilized pepsin gel (180 µl) was carried out (E/S=5, 0°C, 5 min). After microfiltration of the digest, an aliquot was immediately analyzed on a microbore HPLC-ESIMS (C-8) at 0°C. After prewashing the loaded sample with the precooled 2% CH_3CN-H_2O (pH 2.0) on the desalting trap

cartridge loop, an elution condition of 10 to 30% B over 10 min followed by 30 to 44% B over 28 min, was used at 0°C. Peptides of P1, P2, P3, P5, P6, P8, P9 and P10 were detected as well as a mono-chlorinated peptide-10 (**2626.48 Da**; 876.4(+3) 1314.4(+2)). All peptides showed complete loss of their deuterium labels. The deuterated molecule, BPTI+O4, showed 15.9 deuteriums retained (**6590.55 Da**; 1099.6(+6) 1318.9(+5)).

References

1. (a) Creighton, T.E. *Proteins: Structures and Molecular Properties* **1993**, Freeman, W.H. and Co., New York. (b) Creighton, T.E. *Biochem. J.* **1990**, *270*, 1.

2. (a) Havel, H.A. *Spectroscopic Methods for Determining Protein Structure in Solution* **1996**, VCH Publishers Inc., New York. (b) Clore, G.H.; Gronenborn, A.M. *Annu. Rev. Biophys. Chem.* **1991**, *20*, 29. (c) Braun, W. *Quart. Rev. Biophys.* **1987**, *19*, 115.

3. (a) Johnson, W.C., Jr. *Annu. Rev. Biophys. Chem.* **1988**, *17*, 145. (b) Johnson, W.C., Jr. *Proteins: Struct. Funct. Genet.* **1990**, *7*, 205. (c) Manning, M.C.; Woody, R.W. *Biochemistry* **1989**, *28*, 8609.

4. Zhang, Z.; Smith, D.L. *Proterin Sci.* **1993**, *2*, 522.

5. (a) Katta, V.; Chait, B.T. *J. Amer. Chem. Soc* **1993**, *115*, 6317. (b) Stevenson, C.L.; Anderegg, R.J.; Borchardt, R.T. *J. Amer. Soc. Mass Spectrom.* **1993**, *4*, 646.

6. Linderstrøm-Lang, K. *Chem. Soc. Spec. Publ.* **1955**, *2*, 1.

7. (a) Wagner, G.; Wüthrich, K. *J. Mol. Biol.* **1982**, *160*, 343. (b) Jeng, M.F.; Englander, S.W.; Elove, G.A.; Wand, A.J.; Roder, H. *Biochemistry* **1990**, *29*, 10433. (c) Englander, S.W.; Mayne, L. *Annu. Rev. Biophys. Biomol. Struct.* **1992**, *21*, 43.

8. (a) Rosa, J.J.; Richards, F.M. *J. Mol. Biol.* **1979**, *133*, 399. (b) Rohl, C.A.; Scholtz, J.M.; York, E.J.; Stewart, J.M; Baldwin, R.L. *Biochemistry* **1990**, *31*, 1263.

9. (a) Dobson, C.M.; Evans, P.A *Nature* **1988**, *335*, 666. (b) Bycroft, M.; Matouschek, A.; Kellis, J.T.; Serrano, L.; Fersht, A.R. *Nature* **1990**, *346*, 488.

10. (a) Brandt, P.; Woodward, C. *Biochemistry* **1987**, *26*, 3156. (b) Paterson, Y.; Englander, S.W.; Roder, H. *Science* **1990**, *249*, 755. (c) Mayne, L.; Paterson, Y.; Cerasoli, D.; Englander, S.W. *Biochemistry* **1992**, *31*, 10678.

11. (a) Englander, S.W.; Kallenbach, N.R. *Quart. Rev. Biophys.* **1984**, *16*, 521. (b) Eriksson, M-A.L.; Hard, T.; Nilsson, L. *Biophys. J.* **1995**, *69*, 329.

12. Scholtz, J.M.; Robertson, A.D. *Methods Mol. Biol.* **1995**, *40*, 291.

13. Suckau, D.; Shi, Y.; Beu, S.C.; Senko, M.W.; Quinn, J.P.; Wampler, F.M.; McLafferty, S.W. *Proc. Nat'l. Acad. Sci. USA* **1993**, *262*, 790.

14. (a) Miranker, A.; Robinson, C.V.; Radford, S.E.; Aplin, R.T.; Dobson, C.M. *Science* **1993**, *262*, 896. (b) Hooke, S.D.; Eyles, S.j.; Miranker, A.; Radford, S.E.; Robinson, C.V.; Dobson, C.M. *J. Am. Chem. Soc.* **1995**, *117*, 7548.

15. Englander, J.J.; Rogero, J.R.; Englander, S.W. *Anal. Biochem.* **1985**, *147*, 234.

16. Wagner, D.S.; Anderegg, R.J. *Anal. chem.* **1994**, *66*, 706.

17. Johnson, R.S.; Walsh, K.A. *Protein Sci.* **1994**, *3*, 2411.

18. Anderegg, R.J.; Wagner, D.S.; Stevenson, C.L. *J. Amer. Soc. Mass Spectrom.* **1994**, *5*, 425.

19. (a) Bazzo, R,; Tappin, M.J.; Pastore, A.; Harvey, T.S.; Carver, J.A.; Campbell, I.D. *Eur. J. Biochem.* **1988**, *173*, 139. (b) Dempsey, C.E. *Biochemistry* **1988**, *27*, 6893.

20. (a) Wlodawer, A.; Nachman, J.; Gilliland, G.L.; Gallagher, W.; Woodward, C. *J. Mol. Biol.* **1987**, *198*, 469. (b) Berndt, K.D.; Günter, P.; Orbons, L.P.M.; Wüthrich, K. *J. Mol. Biol.* **1992**, *227*, 757.

21. (a) Creighton, T.E. *Proc. Nat'l. Acad. Sci. USA* **1988**, *85*, 5032.
(b) Creighton, T.E. *Science* **1992**, *256*, 111.
(c) Weissman, J.S.; Kim, P.S. *Science* **1992**, *256* , 112.

22. (a) Rüegg, U.T.; Rudinger, J. *Methods Enzymol.* **1987**, *143*, 111.
(b) Burns, J.A.; Butler, J.C.; Moran, J.; Whitesides, G.M. *J. Org. Chem.* **1991**, *56*, 2648 (c) Gray, W.R. *Protein Sci.* **1993**, *2*, 1732.

23. (a) Hirs, C.H.W. *Methods Enzymol.* **1967**, *11*, 197. (b) Chowdhury, S.K.; Eshraghi, J.; Wolfe, H.; Forde, D.; Hlavac, A.G.; Johnson, D. *Anal. chem.* **1995**, *67*, 390.

24. (a) Wüthrich, K.; Roder, H. *Proteins: Struct. Funct. Genet.* **1986**, *1*, 34.
(b) Kim, K-S,; Fuchs, J.A.; Woodward, C.K. *Biochemistry* **1993**, *32*, 9600.

25. Hvidt, A. *Dynamic Aspects of Comformation Changes in Biological Systems* **1973**, 103, Reidel, Dordrecht, Holland.

26. (a) Molday, R.S.; Englander, S.W.; Kallen, R.G. *Biochemistry* **1972**, *11*, 150. (b) Molday, R.S.; Kallen, R.G. *J. Am. Chem. Soc.* **1972**, *94*, 6739.

27. Woodward, C.K.; Hilton, B.D. *Biophys. J.* **1980**, *32*, 561.

28. Leichtling, B.M.; Klotz, I.M. *Biochemistry* **1966**, *5*, 4026.

29. Perrin, C.L. *Acc. Chem. Res.* **1989**, *22*, 268.

30. Fersht, A.R.; Jencks, W.P. *J. Am. Chem. Soc.* **1970**, *92*, 5432.

31. Pletcher, T.C.; Koehler, S.; Cordes, E.H. *J. Am. Chem. Soc.* **1968**, *90*, 7072.

32. Perrin, C.L., Arrhenius, G.M. *J. Am. Chem. Soc.* **1982**, *104*, 6693.

33. Tüchsen, E., Woodward, C.K. *J. Mol. Biol.* **1985**, *185*, 405.

34. (a) Woodward, C.K.; Rosenberg, A. *J. Biol. Chem.* **1971**, *246*, 4105. (b) Ellis, L.M.; Bloomfield, V.A.; Woodward, C.K. *Biochemistry* **1975**, *14*, 3413.

35. Wagner, G.; Wüthrich, K. *J. Mol. Biol.* **1979**, *134*, 75.

36. Greory, R.B.; Crabo, L.; Percy, A.J.; Rosenberg, A. *Biochemistry* **1083**, *22*, 910.

37. (a) Fenn, J.B.; Mann, M.; Meng, C.K.; Wong, S.F.; Whitesides, C.M. *Mass Spectrom. Rev.* **1990**, *9*, 377. (b)Smith, R.D.; Loo, .J.A.; Ogorzalek-Loo, R.R.; Busman, M.; Udseth, H.R. *Mass Spectrom. Rev.* **1991**, *10*, 359.

38. (a) Chait, B.T.; Katta, V. *J. Am. Chem. Soc.* **1991**, *113*, 8534. (b) Ganem, B.;Heinion, J.D.; Li, Y.T.; Hsieh, Y.L. *J. Am. Soc. Mass Spectrom.* **1993**, *4*, 631.

39. Chowdhury, S.K.; Katta, V.; Chait, B.T. *J. Am. Chem. Soc.* **1990**, *112*, 9012.

40. Schnier, P.D.; Gross, D.S.; Williams, E.R. *J. Am. Chem. Soc.* **1995**, *117*, 6747.

41. Smith, R.D.; Light-Wahl, K.J. *Biol. Mass Spectrom.* **1993**, *22*, 493.

42. Fenn, J.B. *J. Am. Soc. Mass Spectrom.* **1993**, *4*, 524.

43. Röllgen, F.W.; Lüttgens, U.; Dülcks, T.; Giessmann, U. *Proc. 41st Conf. Am. Soc. Mass Spectrom. Allied Topics* **1993**, 1.

44. Iribarne, J.V.;Thomson, B.A. *J. Chem. Phys.* **1976**, *64*, 2287.

45. (a) Hsieh, Y.L.; Cai, J.; Li, Y.T.; Heinion, J.D.; Ganem, B. *J. Am. Soc. Mass Spectrom.* **1995**, *6*, 85. (b) Ganem, B.; Heinion, J.D.; Li, Y.T. *J. Am. Chem. Soc.* **1991**, *113*, 7818. (c) Griffey, R.H.; Greig, M.J.; Gaus, H.; Cummins, L.L. *J. Am. Chem. Soc.* **1995**, *117*, (d).Ganguly, A.k.; Pramanik, B.N.; Tsarbopoulos, A.; Covey, T.R.; Haung, E.; Fubrman, S.A. *J. Am. Chem. Soc.* **1992**, *114*, 6559. (e) Kent, B.H.; Baca, M. *J. Am. Chem. Soc.* **1993**, *115*, 6317. (f) Smith, R.D.; Light-Wahl, K.J.; Winger, B.E. *J. Am. Chem. Soc.* **1993**, *115*, 5869.

46. Thomson, B. *PE Sciex Ion-Spray Technical Note* No 15288 and No 15789.

47. Feng, R.; Konishi, Y. *Anal. Chem.* **1992**, *64*, 2090.

48. Bergmeyer, H.U. *Methods Enzymol.* **1984**, *107*, 232.

49. Konigsberg, R.W.; Goldstein, J.; Hill, R.J. *J. Biol. Chem.* **1963**, *238*, 2028.

50. (a) Biemann, K.; Martin, S.A. *Mass Spectrom. Rev.* **1987**, *6*, 1.
(b) Biemann, K. *Biomed. Environ. Mass spectrom.* **1988**, *16*, 99.
(c) Roepstrorff, P.; Fohlman, J. *Biomed. Mass Spectrom.* **1984**, *11*, 601.

51. Thévenon-Emeric, G.; Kozlowski, J.; Zhang, Z.; Smith, D.L. *Anal. Chem.* **1992**, *64*, 2456.

52. (a) Creighton, T.E. *Biochem J.* **1990**, *270*, 1. (b) Creighton, T.E. *Methods Enzymol.* **1984**, *107*, 305.

53. Creighton, T.E. *Methods Enzymol.* **1986**, *131*, 83.

54. Gilbert, H.F. *Adv. Enzymol.* **1990**, *47*, 1309.

55. Houk, J.; Whitesides, G.M. *J. Am. Chem. Soc.* **1987**, *109*, 6825.

56. Jocelyn, P.C. *Methods Enzymol.* **1987**, *143* 246.

57. (a) Creighton, T.E. *J. Mol. Biol.* **1975**, *96*, 167. (b) Creighton, T.E. *J. Mol. Biol.* **1975**, *96*, 767.

58. (a) Katta, V.; Chait, B.T. *Rapid Commun. Mass Spectrom.* **1991**, *5*, 214.
(b) Guevremont, R.; Siu, K.W.; Le Blanc, J.C.Y.; Berman, S.S. *J. Am. Soc. Mass Spectrom.* **1992**, *3*, 216. (c) Loo, J.A.; Loo, R.R.O.; Udseth, H.R.; Edmonds, C.G.; Smith, R.D. *Rapid Commun. Mass Spectrom.* **1991**, *5*, 101.

59. Woodward, G.E.; Fry, E.G. *J. Biol. Chem.* **1932**, *97*, 465.

60. Hase, S.; Hara, S.; Matsushima, Y. *J. Biochem.* **1979**, *85*, 217.

61. Ryle, A.P. *Methods Enzymol.* **1970**, *Vol XIX*, 246.

62. Sanger, F. *Nature* **1947**, *160*, 295.

63. (a) Savige, W.E.; Maclaren, J.A. *The Chemistry of Organic Sulfur Compounds* **1966**, *Vol.2*, 367; Kharasch, N.; Meyers, C.Y. eds., Pergamon Oxford. (b) Torchinskii, Y.M.; Dixon, H.B.F. *Sulfhydryl and Disulfide Groups of Proteins* **1974**, *Chapter2*, 94; Consultants Bureau, New York and London.

64. Makhatadze, G.I.; Kim, K-S., Woodward, C.; Privalov, P.L. *Ptotein Sci.* **1993**, *2*, 2028. and references therein.

65. Richarz, R.; Sehr, P.; Wagner, G.; Wüthrich, K. *J. Mol. Biol.* **1979**, *130*, 19.

66. Kim, K-S., Woodward, C. *Biochemistry* **1993**, *32*, 9609.